Feasibility Study on Hybrid Energy Harvesting Solution in Rail Transportation System

Kalamkas Akmurzina, B. Eng

Submitted in fulfillment of the requirements

for the degree of Master of Science

in Electrical and Computer Engineering

School of Engineering and Digital Science

Department of Electrical and Computer Engineering

Nazarbayev University

53 Kabanbay batyr avenue

Astana, Kazakhstan, 010000

Supervisor: Mehdi Bagheri

Co-supervisor: Prashant Jamwal

Date of completion: April, 2024

Abstract

Currently, it is important to investigate environmentally friendly and sustainable energy sources due to ecological issues, such as greenhouse gas emissions and climate change. This thesis represents the feasibility study on hybrid energy harvesting solutions within rail transportation systems, especially the application of solar and wind energy systems. The hybrid energy source is defined as the combination of various types of energy generation equipment. To be more exact, this master's thesis examines the significance of using solar panels, micro-hydro turbines, and a battery energy storage system (BESS) to supply the energy needs of railway systems in Kazakhstan. It is important to note that the selected train is the Talgo Tulpar passenger train, moving from Astana to Almaty cities. However, the application of small-scale solar and wind energy systems cannot fully support the railway energy network. Therefore, this master's thesis also considers the integration of solar panels on the sleepers over the railway track. This helps to support the energy network of the railway system. One of the first steps in designing the hybrid energy system is to construct a mathematical model of the system for the rail transportation system. A mathematical model of the proposed hybrid energy system, including analytical calculations and MATLAB simulations, is investigated to assess the performance and energy generation capabilities. To achieve the simulation results, data was collected individually for each energy generation source, also the train's speed and energy demand profiles were created based on the literature review. Furthermore, the strategic plan for the working principles of the system has been proposed in this master's thesis. To investigate more accurately the energy network of the proposed system, it has considered three different study cases. By considering one randomly selected day in each season, this master's thesis demonstrates a seasonal analysis for each study case.

Acknowledgements

Firstly, I would like to express my deepest gratitude to my supervisor, Professor Mehdi Bagheri, for his encouragement and patience, and for supporting me throughout my master's degree education period. His experience and guidance have been pivotal in my academic development and in the successful completion of this thesis.

Secondly, I would also like to thank my co-supervisor, Professor Prashant Jamwal, who inspired and directed me to achieve the goal of my thesis paper. His wise inquires and words of support enabled me to develop this master's thesis work.

My deepest gratitude is extended to my lovely family, especially to my parents. Their constant moral encouragement and support have been the strength during my master's degree education. Their support and encouragement have always come from their faith in me and my goals.

Lastly, I would like to thank my friends for their support and companionship, especially Aiym, Diana, Kamilya, Abdul Moeed, Samat, and my classmates. During the most challenging times, they were there to listen to my complaints, offer their encouragement, and stay by my side. The journey has been easier and more pleasant because of their influence and understanding.

Your support has meant the world to me, to everyone who has shared in this adventure. My sincerest gratitude to you for everything.

Table of Contents

List of Abbreviations & Symbols

BESS	Battery Energy Storage System
DEMU	Diesel Electrical Multiple Unit
DGS	Distributed Generation System
DER	Distributed Energy Resources
DOD	Depth of Discharge
EMS	Energy Management System
ESS	Energy Storage Systems
GOST	State Standard (Russia and CIS countries)
HAWT	Horizontal Axis Wind Turbines
VAWT	Vertical Axis Wind Turbines
IEA	International Energy Agency
NOCT	Nominal Operating Cell Temperature
PV	Photovoltaic
RES	Renewable Energy Sources
SOC	State of Charge
UUG	Upstream Utility Grid
DOD	Depth of Discharge
MGs	Microgrids

List of Tables

List of Figure

Chapter 1 - Introduction

1.1. Background information

Nowadays fossil fuels play an important role that can be seen from their application in various fields, such as transportation, industry, and energy production fields. Consequently, these actions lead to significant environmental issues, such as air pollution and climate change, due to their carbon dioxide emissions. Therefore, one of the main factors influencing carbon dioxide emissions is the daily application of transport networks. Figure 1.1 indicates that the highest contribution of greenhouse gas emissions corresponds to transportation and energy supply sections, which are about 28.3% and 25.3% of the total amount, respectively [1]. Additionally, according to the International Energy Agency (IEA), the transportation industry is responsible for 29% of the world's total energy consumption, which has increased dramatically over the previous several decades [2]. Therefore, the need for energy is constantly increasing, and the state of the environment is getting worse along with the world economy's fast expansion. This requires investigating the transition from traditional energy resources to green energy resources.

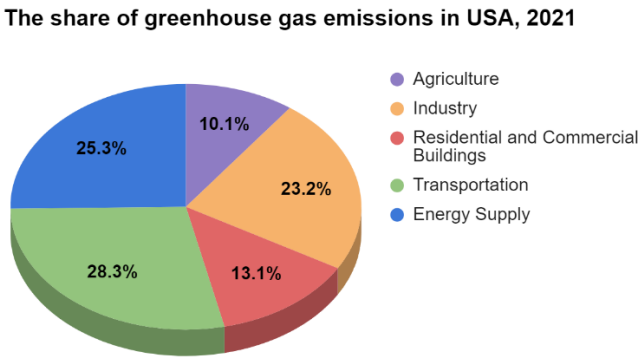

Figure 1. 1: The contribution of various sectors to greenhouse emissions, data taken from [3]

Hybrid energy systems have been expanding widely in recent years to make the driving systems of the transportation sector, including railway vehicles, more adaptable and ecologically

friendly. These hybrid energy systems consist of several types of energy generation equipment, including electrical energy generators, electrical energy storage systems, and renewable energy sources (RESs) [4]. Hybrid energy systems, which combine various types of RES, provide an optimal solution for developing sustainable energy [5, 6]. This implies that the energy system can include both solar power plants and wind turbines. Similarly, this master's thesis utilizes solar and wind energy resources for the rail transportation system.

The use of clean energy in larger vehicles (such as buses, trains, and airplanes) is quite an innovative approach, even though electric and hybrid automobiles are now commonplace for transportation. Compared to other renewable energy resources, wind and solar energy dominate annually at 623 GW and 586 GW, respectively, making up 48% of the total amount of renewable energy sources [2]. Accordingly, wind and solar energy systems are some of the major components of renewable energy resources. Therefore, the use of wind and solar energy to power trains, buses, and trucks is the subject of numerous studies.

1.2. Thesis outline

This thesis aims to investigate the implementation of renewable energy resources, especially solar and wind energy, in the rail transportation system. It focuses on strategies for generating energy from hybrid energy resources and implementing them in the rail transportation system. The solar panels will be installed on top of the moving train. Additionally, the micro-hydro turbines will be placed on the roof of the moving train between the solar power plants. The solar energy and wind energy systems are considered hybrid energy harvesting solutions located on top of the train. It is important to inform that renewable energy resources demonstrate stochastic energy characterization, which can influence the safety and stability of the energy supply. Thus, the battery energy storage system (BESS) will be applied to the system to observe the excess

energy from renewable energy resources. However, this might not be sufficient to fully meet the energy requirements of the train. Therefore, additional solar panels are considered over the sleepers of the railway truck. This master's thesis aims to decrease the energy coming from the main grid and increase the usage of renewable energy resources. To achieve the goal, the strategy plan for optimizing the condition of battery storage system in the hybrid energy system is proposed in this master's thesis. In addition, it demonstrates a mathematical model of the proposed system with its analytical calculations. The simulation of power generation will be performed in MATLAB software. The required data for the simulation and analysis in this thesis were created due to the lack of information and available data from the Internet. Therefore, the data for each considered energy resources and train's load were examined and demonstrated in the first order. This master's thesis considered three study cases for each season. By choosing one randomly selected day in a season, this master's thesis demonstrated a seasonal analysis of the hybrid energy harvesting solutions in rail transportation system.

1.3. Thesis overview

The master's thesis is structured in the following manner. Chapter 2 demonstrates the literature review about the integration of renewable energy resources in the rail transportation system. Chapter 3 gives a general overview of the system as well as the methodology, where the strategic plan of the system is presented. Chapter 4 illustrates the mathematical modeling of each renewable energy resource, and the objective function of the system is also given. The simulation details and analytical calculations are demonstrated in Chapter 5. The simulation results for each case study are investigated in Chapter 6. Finally, Chapter 7 concludes the achieved results and works.

Chapter 2 - Literature Review

2.1. Integration of renewable energy in transportation systems

The integration of renewable energy into transportation systems is one of the significant directions in the search for effective and sustainable mobility solutions. This is an essential method for decreasing the use of fossil fuels and reducing the negative environmental consequences that electric vehicles have on public transportation networks. According to Jia and Ma [2], electrified railways are considered the most energy-efficient, least polluting, and automated transport modes. Also, Teng et al. [7] agree that the railway, among the numerous modes of transportation, is frequently propelled by electric energy; as a result, it is usually recognized as a low-carbon transportation option. Therefore, the construction of electric railways plays an important role in the sustainable growth of the country. The electrified rail transportation systems help to minimize the energy from the major grid and become less dependent on the network. This can be achieved by maximizing the use of renewable energy resources. According to [5, 8 - 11], the maximal use of RESs in transportation systems will be significant in decreasing energy drawn from the upstream utility grid (UUG), which is also called the main grid. In these studies [8 - 11], the authors investigated the power management plan consisting photovoltaic arrays, diesel generators, energy storage systems, and wind turbines to charge the plug-in hybrid electric vehicle in the microgrids (MGs). Consequently, the RESs will support the rail transportation system by feeding it with energy. However, it is impossible to fully support the energy network of the railway with RESs. Any application of renewable energy will certainly be supported by the careful use of fossil fuels, particularly natural gas, which is a low-carbon source [12]. Therefore, it is necessary to investigate the application structure and methods of RESs in our energy network.

There is an increasing demand for finding appropriate energy solutions in energy usage due to the negative influence of fossil fuels on the environment. Current technological achievements facilitate the transition period from fossil fuels to renewable energy resources in transportation networks.

2.2. Hybrid energy systems in rail transportation

There are many feasibility studies that investigated the application of hybrid energy systems in railway and electric vehicles. However, not many studies have been conducted on the implementation of hybrid energy harvesting solutions on a moving train. This thesis aims to investigate this sphere.

2.2.1. Solar energy systems

The search for sustainable transportation solutions leads to the investigation of renewable energy sources in the transportation field. In addition, the integration of solar energy systems into the railway system might be an appropriate solution for reducing carbon emissions and obtaining efficient energy. There are various research projects investigating the possibilities of their integration. Historically, small-scale trials using solar energy to power station facilities and signal systems were the first step in solar power application in trains. One of the first solar-powered cars in history is named "Sunmobile," which is a tiny 38-cm General Motors car created by William Cobb in 1955 [13]. This solar-powered vehicle was built using a modest electric powertrain and twelve photovoltaic cells. However, it was not accessible for driving. The solar vehicle of the proper size was created later in 1962 [13]. An outdated Baker electric automobile was converted into a solar-powered vehicle by the International Rectifier Company. Figure 2.1 represents the image of the Baker solar-powered car, where 10,640 solar cells were crammed inside it [13].

Figure 2. 1: The first solar-powered car, taken directly from [13]

Furthermore, there have also been solar-powered trains in the history of solar energy system development. One of the first solar-powered diesel electrical multiple unit (DEMU) trains was introduced in India, where the train consisted of 16 solar panels fitted in six coaches [14]. Each of the PV panels produced 300 W, which is equivalent to demonstrating the electricity for fans and lights in the carriage. However, it is important to increase the efficiency of solar panels placed on top of the train. Currently, Indian Railways has put solar panels on the roofs of 250 local trains after realizing the possibility of using the rail corridor to produce solar energy [15]. As time passed, these programs grew to include more ambitious endeavors, such as installing photovoltaic (PV) panels on station buildings and trains powered by the sun. Generally, there are approximately 50 stations in India that are based on solar energy systems [16]. In Australia, rooftop solar panels were connected with solar farms situated next to or along the railway [14]. The diesel-electric train's batteries store all the energy that is produced. The train's rooftops provide 8% of the 0.015 GW of power required to run it, the solar farm provides 58%, and the solar railway panels provide 34% [14]. It can be seen that the energy generated from solar farms is significantly higher than the solar panels on the roof of the train. Following the positive results of the experimental trials conducted in Australia and India, train operators began to install solar panels on the tunnels above

trains, like the tunnel in Belgium. The first tunnel in Europe was this solar tunnel that connected Brasschaat and Schoten cities, which can be seen in Figure 2.2 [17]. It generates roughly 3.6 GWh, has 16,000 PV panels, and lowers yearly CO2 emissions by about 2500 tons [14].

Figure 2. 2: The first solar-powered railway tunnel in Belgium, taken from [17]

There are various feasibility studies that consider the solar panels not only on top of the train but also how they can be applied at train and metro stations. Jia et al. [2] considered in their paper the possibilities of solar energy generation in road and rail transportation in China. The authors have analyzed the amount of energy that can be generated from solar panels integrated into the road and rail transportation of China. Also, Hayashiya et al. [18] investigated the application of solar panels on the roof of the railway station in Tokyo. The authors have considered the shadow effect of the surrounding buildings for the solar panels with 453 kW of power installed on the roof of the station. They stated that one of the consequences of this shadow effect is the mismatch between energy consumption and demand. Therefore, this Hiraizumi station implemented a combined system comprising a 78 kW solar production system and 240 kWh lithium-ion batteries for local stations to supply all electric power with solar power in order to overcome the temporal mismatch problem [18]. The application of storage systems is essential to supporting renewable

energy resources. In addition, the distributed generation that consisted of solar energy systems and ESS was deeply characterized in these research articles [2, 6, 15, 18 - 20]. Based on the literature, there is an increasing interest in the application of solar energy in the railway industry.

An innovative approach to producing electricity directly from the railway infrastructure is provided by solar sleepers, which integrate photovoltaic panels within the sleepers themselves. Currently, the German Deutsche Bahn and the British Bankset Energy Group have been implementing photovoltaic panels on sleepers on the German railway track [16]. According to the company's calculations, the proposed design can generate 0.1 MW of electricity per kilometer [16]. Preliminary implementations in Germany illustrate the viability and efficiency of this technology, suggesting promising results for expanding renewable energy sources within the railway network. In addition, the Italian company Greenrail is proposing the integration of solar panels that transform railroad infrastructure into a photovoltaic field [16]. It can be seen that the integration of renewable energy resources is expanding significantly. To support the energy network, it is not required to depend on only one source of renewable energy. In India, approximately 300 stations are dependent on solar and wind energy systems [16]. It can be combined with other sources of renewable energy, which helps to make the system more efficient and reliable.

2.2.2. Wind energy systems

The application of wind turbine systems is one of the important steps in the direction of achieving sustainable energy solutions. Similar to solar energy systems, these devices provide a clean and renewable energy source that can drastically lower greenhouse gas emissions. Currently, the use of wind energy systems in various industries, as well as solar energy systems, is increasing

significantly. In the railway system, one of the most efficient ways to use wind energy to power electric trains is through wind farms. As an example, it is stated that Dutch state-owned railway operator Nederlandse Spoorwegen's (NS) trains, which is a passenger railway operator in Netherlands, are totally powered by wind energy systems starting in 2017 [16]. It means that the energy produced from wind farms is enough to support the Dutch rail system. Another example of the application of green energy systems is the railway system in Austria, where most of the electricity used to operate the traction system comes from hydropower plants as well as solar power plants. There is essentially no need for additional electrical lines because the generated energy is fed straight to the train overhead line [16]. Furthermore, there are significantly fewer energy losses because the trains are directly powered by wind energy [16].

As mentioned above, the solar panel and wind turbine systems are planned to be put on top of the train. The use of renewable energy on a moving train is an extremely creative strategy in this situation. It appears that the electricity produced by the available renewable resources is insufficient when taking into account the train's overall fuel usage. As a result, a lot of studies are conducted to investigate potential scenarios that can maximize the use of alternative energy on trains. The first step in designing the wind energy system is to investigate the overall technical characteristics and their applied type. There are two main types of wind turbines: horizontal-axis wind turbines (HAWT) and vertical-axis wind turbines (VAWT). Generally, the VAWT has Savonius and Darrius types of wind turbines [21]. Both differ in terms of their functions and technical characteristics. According to Bulbul et al. [21], the HAWT has advantages in producing a high efficiency of energy, but it is impractical to apply it on trains due to the occurrence of high drag. Consequently, this might increase fuel consumption. Because of the following reasons, this master's thesis applies the horizontally aligned Savonius type VAWT.

- HAWT consists of parallel blades that attach to the ground and extract wind energy on a horizontal axis [22]. On the other hand, the VAWT is defined as having blades rotated perpendicularly to the ground and around the vertical axis.
- Application of HAWT on the roof of the train prevents its movement by producing a force against its acceleration [23].
- The overall power output efficiency of the HAWT is higher than that of the VAWT; however, the average output efficiency of the VAWT is preferable due to its limitations [21].
- Compared to the HAWT, the VAWT has a preferable design because the gearbox and other equipment are well fitted to its structure [22, 24].
- The efficiency of the HAWT depends on its constant wind existence, which is not appropriate for unpredictable conditions. According to Johari et al. [22], an additional mechanism must be implemented to ensure that the blades are facing the direction of the wind, which results in obtaining a higher power output. On the other hand, the VAWT can operate in various windy conditions and can still be used for the entire running period [21, 22, 23]. This means that it is not required for VAWT to have constant regulations.

Based on these aforementioned reasons, this master's thesis considers micro-wind turbines, or more exactly, the horizontally aligned Savonius type of the vertical axis wind turbine. There are not many studies conducted on the application of wind energy systems on a moving train. However, Nurmanova et al. examined the viability of mounting a wind harvester on a wagon roof [24]. In addition, Nurmanova et al. [24, 25] proposed the design of the horizontally aligned VAWT that can be installed on the train's roof. Furthermore, the authors [24, 25] have addressed the mechanical challenges that can occur due to the specific design of the micro wind turbine, which

is not the scope of this master's thesis. According to the simulation results demonstrated in [24, 25], the wind power system's ability can overcome excessive air drag and provide a specified amount of electricity to the load. In addition, the economic and ecological aspects are discussed in their work [24, 25]. This master's thesis investigates the integration of small wind turbines, whose design is proposed in [24, 25], in addition with other hybrid energy solutions in the rail transportation system.

2.2.3. Energy storage systems (ESS)

One of the drawbacks of using renewable energy resources is their inability to be stored for future use. Therefore, it is crucial to extract as much energy as possible from them while they are still available. Furthermore, because they frequently rely on the site's climate, it is impossible to guarantee that they will always be concentrated and consistent. This means that the generation of renewable energy sources is unpredictable due to their reliance on environmental conditions. The distributed generation system (DGS) can be improved by applying energy storage devices, and this can balance the power flow of the whole network. Fathima and Palanisamy [26] have reviewed various types of energy storage systems. Battery Energy Storage System (BESS), which is one of the most widely used storage devices, will be useful to stabilize the energy network. The problem of stochastic behavior between the supply and demand sides is addressed in various articles [8 - 11]. The authors from [8 - 11] suggested a smart charging system for PHEVs that can provide MGs with optimal performance. The goal of the suggested power management plan is to reduce MG's reliance on the main grid and charge PHEVs by using RERs to their fullest potential. This master's thesis has taken into account the proposed mathematical model in these articles [8 - 11]. According to [27], a distribution system's power quality can be raised by using battery storage devices. Additionally, the voltage and distribution system loss can be controlled by carefully

positioning the battery within the distribution network [27]. In the context of power system applications, the study [27] offers a likely future perspective for electric hybrid vehicles and battery technology. Furthermore, Li et al. [28] have investigated the application of BESS for generating energy from solar panels and wind turbines. In their paper [28], the authors have presented power system simulation analysis for improving the unbalanced performance of the hybrid generation system. Bakhtvar et al. [29] have investigated the operation of the hybrid renewable energy system with BESS in the electricity market during the daytime. The authors in [29] have proposed optimized operating strategies by testing them in a sample study case. Therefore, the crucial role of BESS requires advanced planning and technology solutions to ensure smooth operation. It is important to apply the strategic integration of the BESS with other renewable energy resources.

Chapter 3 - Methodology

3.1. System overview

This master's thesis work aims to investigate the application of renewable energy sources on a moving electric train. Designing a hybrid energy system in the rail transportation system consists of several main steps. Firstly, the train characteristics and specifications were identified, such as the technical parameters of the train and their trip schedule and the length of the route. This thesis work considers the "Talgo Tulpar" train moving from Astana to Almaty cities in Kazakhstan. The technical parameters of the train are essential for identifying the available roof space to implement the solar panels and wind turbines on top of the train.

Secondly, it is important to construct the mathematical model of the system, which helps to understand the system components. This master's thesis considers not only the solar panels and wind turbines on top of the train but also the battery energy storage system (BESS) and the solar sleepers on the selected route. Then the appropriate type of solar panels and wind turbine has been selected. Both the selected solar panels for the train and the sleepers are monocrystalline, and the wind turbine is selected as a horizontally aligned small VAWT. The mathematical model is constructed based on the objection of the master's thesis work, which is aimed at minimizing the energy coming from the upstream utility grid (main energy network). Therefore, the contribution of renewable energy sources should be increased to fulfill the energy demand of the train.

It is significant to identify the total number of solar panels and micro-wind turbines that can be located on the available roof space of the train. Also, the required number of solar panel sleepers that can be implemented on the route is determined. This helps identify the total power generation from each energy source. This step requires investigating the main equations of each

component's power values. Consequently, it is necessary to identify the power demand of the train and the availability of power from each energy source. The solar energy system is influenced by solar radiation and air temperature parameters, while the main parameter for wind turbines is the speed of the train.

One of the main steps before the simulation process starts is to identify the train energy load, which means the energy consumption of the train during the trip. However, there were not any available sources that were able to provide the energy consumption profile of the selected train. Therefore, this master's thesis created the energy profile of the train based on the modeling in various articles. Finally, after collecting the required data, it is necessary to apply for the simulation process. Based on the proposed strategic plan, it aims to minimize the energy coming from the grid.

3.2. Energy management system

An essential technology framework used in many industries, including transportation, to optimize energy use, improve operational efficiency, and reduce environmental effects is called an Energy Management System (EMS). By lowering imports of fossil fuels, the benefits of RES enable countries to improve their energy security while maintaining their standard of living without negatively impacting the environment. Recently, the idea of a microgrid (MG) has been used to benefit the environment by lowering generation costs and lowering pollution levels by utilizing a variety of renewable resources, such as solar and wind energy, in addition to other energy generators, like micro turbines and fuel cells [30]. A microgrid consists of RES and ESS, also known as distributed energy resources (DER), as well as loads and other controllable loads that can operate locally in grid-connected and islanded modes [31]. This master's thesis considers

distributed energy resources in the railway energy system. The diagram or structure of the hybrid energy system considered in this master's thesis can be seen in Figure 3.1. It can be seen that wind turbines, solar panels, BESS, and solar sleepers are applied in the form of distributed energy resources. The energy management system is based on the strategic plan, which aims to improve the energy network of the railway system. This will be discussed more in the next section.

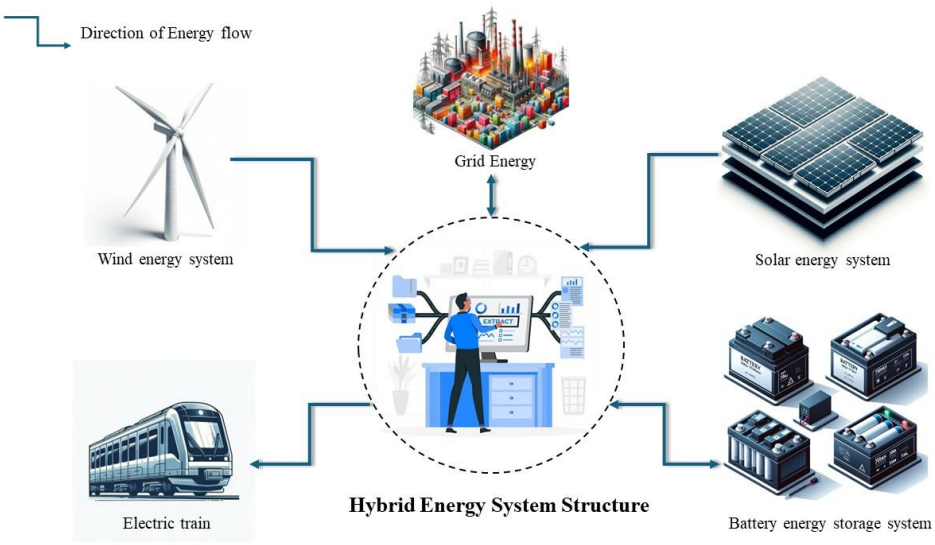

Figure 3. 1: The components of the hybrid energy system.

3.3. BESS strategic plan

The strategic plan for the Battery Energy Storage System (BESS) as outlined proposes an intelligent strategic plan, prioritizing the use of renewable energy generation over grid energy. Figure 3.2 represents the flow chart of the proposed strategic plan for the BESS integration. To ensure that storage is accessible during periods of shortfall, the BESS will charge when renewable energy generation exceeds the train's demand if the State of Charge (SOC) is less than 85%. Otherwise, the excess energy is fed back to the grid if the SOC is adequate, optimizing energy use

and potentially providing economic benefits through feed-in tariffs. On the other hand, when the train's demand surpasses RES generation, the BESS discharges if the SOC is above 20%, a threshold maintained to safeguard battery life and performance, while grid energy supplements any additional load requirements. This approach demonstrates a dedication to environmentally friendly energy management and illustrates the potential for advanced control systems to enhance renewable energy utilization.

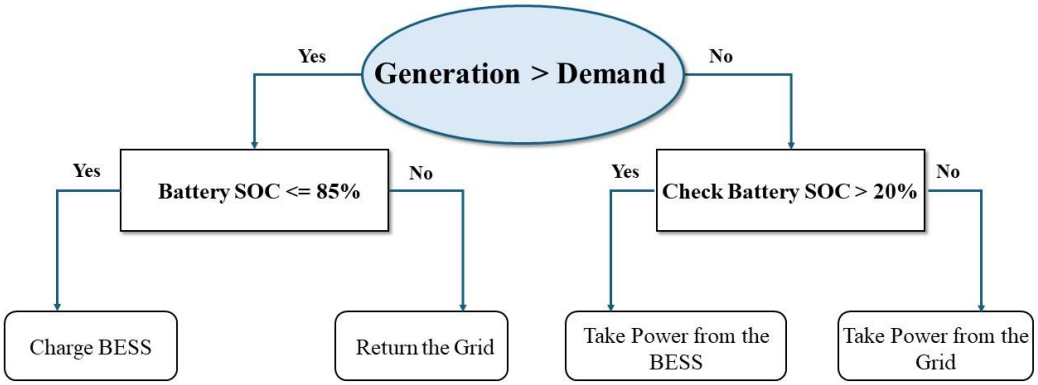

Figure 3. 2: The strategic plan for optimizing grid energy usage.

3.4. PSO optimization technique

Particle Swarm Optimization (PSO) is a bioinspired computer method for solving optimization problems by modeling the social behavior patterns of living things, such as fish schools and flocks of birds. According to [32], the PSO was developed in 1995 by Kennedy and Eberhart based on the idea that individual particles navigate the problem space by following the particles that are now optimal. Each particle in the PSO context is a possible solution to the optimization issue, and the objective function determines the fitness value associated with each particle [33]. Using their own experience as well as that of their neighbors or the entire swarm,

particles alter their location to explore the search space. All particles save information about their best position (p_{best}) and the best location any particle has reached in the swarm (g_{best}).

3.5. Case Studies

This master's thesis examines the integration of hybrid energy systems in Kazakhstan's railway network. The feasibility study is conducted for the "Talgo Tulpar" train moving from Astana to Almaty cities. As it is an electric train, the train moves fast, and it reaches its destination in less than one day. However, case studies 1, 2, and 3 are conducted for one full day (24 hours). This master's thesis considers three various case studies as follows:

- Case 1 (Solar PV Panel and Micro Wind Turbine): The solar panel and micro wind turbines are located on top of the moving train. This means that the railway energy network is supported only by solar panels and micro-wind turbines. This is a general base case, which is important in future comparisons.
- Case 2 (BESS and Renewable Energy Integration): The battery energy storage system (BESS) is included in the train's energy system in addition to the elements from the first case. A special strategic plan is applied to the system, which demonstrates proper usage of the storage system.
- Case 3 (Solar Sleeper Integration): The solar panels were put on the sleepers of the railway truck. This case includes all energy resources, which are solar PV panels and micro wind turbines, BESS, and solar sleepers.

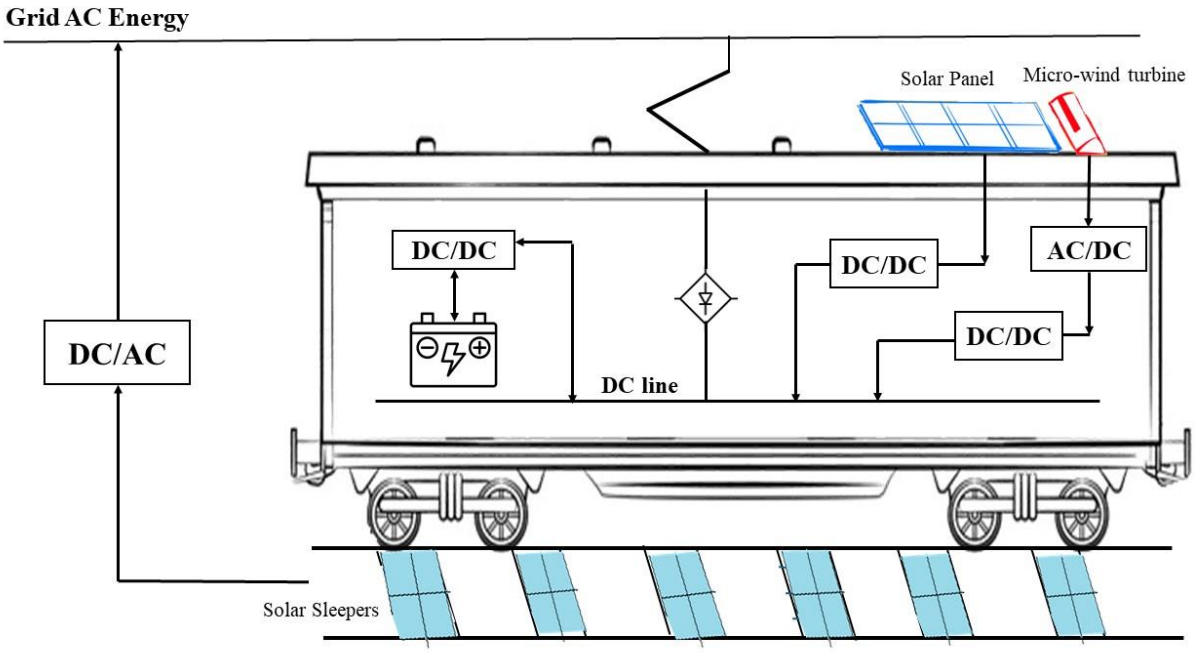

Figure 3. 3: The power flow illustration of case studies.

Chapter 4 - Mathematical Modeling

4.1. Solar energy systems

There are various factors that can influence the performance of solar energy systems. Mostly, solar irradiation and the temperature parameters are important considerations in designing the solar energy system. The power output related to solar irradiation can be evaluated through (4.1) shown below [34]:

$$p_{PV}(t) = P_{R,PV}\frac{R}{R_{ref}}\left[1 + N_T\left(T_C + T_{ref}\right)\right] \tag{4.1}$$

where, $p_{PV}(t)$ is the PV rated power. R_{ref} and R are the solar irradiation at the reference condition (1000 W/m^2) and the solar irradiation at the specific location, respectively. The latitude and longitude coordinates of the specific location can be seen in Appendix A. In addition, N_T is the temperature coefficient of the photovoltaic panel that can be found in the datasheet of the PV panel manufacture, and T_{ref} is the cell temperature at reference conditions (25 °C). The cell temperature T_C can be identified by applying (4.2) [34]:

$$T_C = T_{air} + \frac{(NOCT - 20)}{800}R \tag{4.2}$$

where, T_{air} is the air temperature, given in Celsius unit °C. *NOCT* is the nominal operating cell temperature, which can be found in the datasheet provided by the manufacturer. The varying parameter is the cell temperature, which is based on the solar irradiation and air temperature of the specific place. Information about the solar irradiation system will be received from the NASA database, where global radiation and air temperature for any place in the world at any time are freely available. Therefore, these two parameters were collected from NASA Prediction of

Worldwide Energy Resources [35], which is directed to allow solar and meteorological data sets from NASA research:

- Temperature at 2 meters (T2M): the average air temperature at 2 meters above the surface of the earth.
- The surface shortwave downward irradiance (Wh/m^2) under clear sky conditions.

4.2. Wind energy systems

It is important to note that the wind might not exist constantly in every location of the train route. It becomes complicated to produce efficient wind energy due to its variations in direction and speed. Therefore, this thesis considers the speed of the train as the speed of the wind. It is true that wind occurs due to the movement of the train at any location, which can be clearly seen in Figure 4.1. According to [23], the train generates air pressure in the opposite direction when it travels at an average speed of 50–60 km/h. Once a train is moving, a vacuum is created at its sides and back through the compression of the air, forcing it to its sides [23, 36, 37]. A massive amount of air pours into the train's sides and back to fill this vacuum [23]. The train's movement can create a wind, and in this thesis work, the wind speed is calculated accordingly. As mentioned before, the operation speed of the Talgo train in Kazakhstan is approximately 110 km/hour; thus, it can be stated that the movement of the train produces a wind. Das et al. [38] have demonstrated a practical mechanism where the wind is created by the speed of the train.

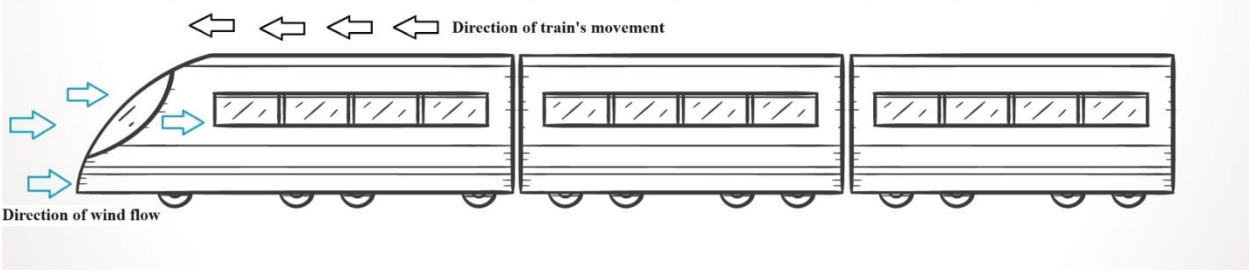

Figure 4. 1: Model of the wind flow

In [23, 24], the authors have demonstrated the feasibility of implementing the wind energy system on a moving train. According to [23], their proposed model of wind turbines on a moving train is expected to produce large amounts of power, which can be applied to feed the train's power needs. The power output of the wind turbine depends on its air density and wind speed, which are given in (4.3) [24, 25] below:

$$P_{Wind} = \frac{1}{2} \varrho_a A v^3 C_P \tag{4.3}$$

where, ρ_a is the mass density of the air (kg/m^2), A is the circular cross-sectional area (m^2), v is the wind velocity (m/s). The term C_P is turbine power coefficient, which is measured to be 0.4 based on the feasibility study [24, 25].

4.3. Battery energy storage system (BESS)

One of the important factors that can characterize the energy storage system is the “state of the charge” (SOC) parameter. This parameter can be identified based on (4.4) [39]:

$$SOC(t) = SOC(0) + \eta_c \sum_{m=1}^{N_{BESS}} P_{BESS}^{charg}(m,t) - \eta_d \sum_{n=1}^{N_{BESS}} P_{BESS}^{disch}(n,t) \tag{4.4}$$

where, η_c and η_d are charging and discharging efficiencies of the BESS. The working principle of the BESS can be characterized by the following constraint (4.5) [34]:

$$SOC_{min}(t) \leq SOC(t) \leq SOC_{max}(t) \tag{4.5}$$

where, $SOC_{min}(t)$ and $SOC_{max}(t)$ are the minimum and maximum limitations of the BESS at time *t*. The maximum charge $SOC_{max}(t)$ of the BESS can be identified by its nominal capacity. On the other hand, the minimum limitation $SOC_{min}(t)$ of the BESS can be defined by using the maximum depth of the discharge (DOD), which is given in (4.6) [34]:

$$SOC_{min}(t) = (1 - DOD)\, SOC_{max}(t) \tag{4.6}$$

The BESS power output is calculated based on its charging and discharging power values, which are illustrated in (4.7) [8 - 11]:

$$P_{out}(t) = P_{disch}(t) - P_{charg}(t) \tag{4.7}$$

where, $P_{disch}(t)$ and $P_{charg}(t)$ are discharging and charging power values of the battery at time t. This obtained output power of the BESS should follow the limitation given in (4.8) [8 - 11]:

$$-P_{charg}^{max} \leq P_{out}(t) \leq P_{disch}^{max} \tag{4.8}$$

Thus, it can be seen that the BESS is dependent on its charging and discharging limits, depth of the discharge, and the power coming from renewable energy resources, in this case, solar and wind energy systems.

4.4. Creation of the objective function

The purpose of the master's thesis is to investigate hybrid energy resources into the railway system, which helps minimize the energy coming from the grid. As mentioned in the previous sections, it considers the solar panels and wind turbines on top of the train, the battery energy storage system, and the solar panels on the sleepers of the railway track. Therefore, the objective function aiming to minimize grid energy usage and maximize renewable energy use while satisfying the load is subject to (4.9):

$$F_{minimize}(t) = P_{grid}(t) + P_{Solar}(t) + P_{Wind}(t) + P_{Sleeper}(t) + P_{BESS}^{disch}(t) - P_{BESS}^{charg}(t) - P_{load}(t) \tag{4.9}$$

where, $P_{grid}(t)$ is the power drawn from the grid at time *t*, $P_{Solar}(t)$ - the power generated by solar panels at time *t*, $P_{Wind}(t)$ - the power generated by wind turbines at time *t*, $P_{Sleeper}(t)$ - the power generated by sleeper solar panels at time *t*, $P_{BESS}^{charg}(t)$- the power directed to charging the BESS at

time t, $P_{BESS}^{disch}(t)$ - the power discharged from the BESS at time t, and $P_{load}(t)$ - the train load consumption at time t.

Chapter 5 - Simulation Study, Data Collection and Results

5.1. Train technical characteristics

Kazakhstan is one of the countries with the largest territory in the world. Most of the country's territory can be characterized by flat plains, known as Kazakh steppe. This has become one of the important factors in developing the railway network in Kazakhstan. In 2023, the Multilateral Investment Guarantee Agency of the World Bank invested in the project, which allows the modernization of railway infrastructure in Kazakhstan [40]. This master's thesis considers the Talgo Tulpar train in Kazakhstan, which is currently one of the most convenient high-speed trains manufactured by a Spanish company, "Patentes Talgo S.L.". In Spain, this Talgo 250 HSR train is named "RENFE S130". One of the popular routes of the Talgo Tulpar train in Kazakhstan is between Astana and Almaty, which are two of the main cities of our country. Through the application of the Talgo Tulpar train, the time taken for this route was significantly reduced, making it more comfortable. In addition, the technical specification of the train and its parameters are illustrated in Table 5.1. The route considered in this thesis is from Astana to Almaty, which has a length of 1200 km. The road trip from Astana to Almaty takes approximately 19 hours, and there are also stations where the train stops at a specific time. The map of the road trip can be seen in Figure 5.1. A detailed description of the timetable of the Talgo train from Astana to Almaty cities is illustrated in Table 5.2. As can be seen, the train leaves Astana station at approximately 12 pm and the trip duration is 19 hours. Therefore, the simulation studies were conducted by considering one full day, which means 24 hours (from 12:00 until 11:59 of the next day). In addition, to make the results clearer and more accurate, the location of the train at each hour has been identified. This can be seen in Appendix A, where the latitude and longitude, and the distance

from one location to the next are given. This information is useful in calculating the power output of renewable sources and in designing the speed profile of the train.

Table 5.1: Technical information of Tulpar Talgo 250 HSR train [24, 41, 42]

The parameters	**The value**
Length of wagon [m]	13.140
Width of wagon [m]	3.200
Height of wagon [m]	3.524
Weight of the train at full load [tons]	343
Maximum weight per motor axle (axle load), [tones]	18
Number of wagons	11 passenger wagons and 2 locomotive wagons
Weight of the wagon [tons]	61
The operating speed [km/hour]	110
Type of current	25 kV of AC, 50 Hz
Output power [kW]	2400
Traction system	Electric
Dimension of wagon in terms of GOST 9238	1-VM
Lifetime [years]	30
Manufacturer	Patentes Talgo S. L.

The detailed information of the considered trip is described in the following way:

- Train model: “Talgo Tulpar”
- Train route: Astana - Almaty
- Length of the route: 1200 km

- Trip duration: 18 hours and 49 minutes = 1129 minutes = 67740 seconds
- Number of the stopped stations: 11

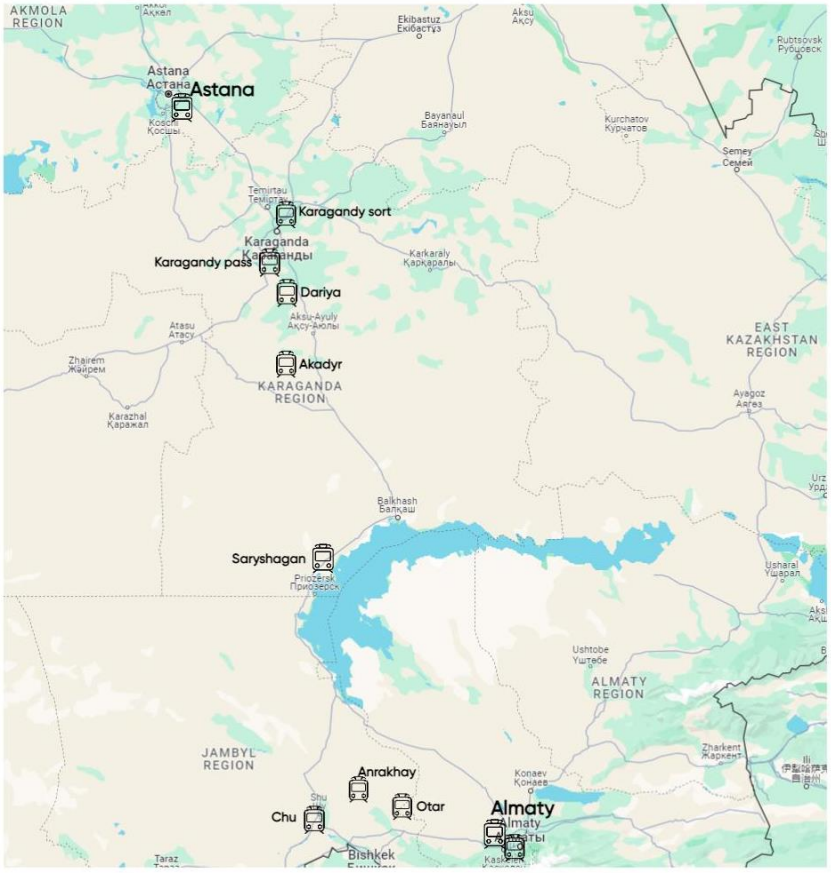

Figure 5. 1: Map of Talgo Tulpar train stations from Astana - Almaty

Table 5.2: The timetable of the route Astana - Almaty

№	Station	Arrival time (hours:minutes)	Length of parking time, minutes	Departure time (hours:minutes)	Time taken to reach the next station
1	Astana	-	-	11:45	2 hours 41 mins
2	Karagandy sort	14:26	2	14:28	24 mins
3	Karagandy pass	14:52	30	15:22	1 hour 9 mins
4	Dariya	16:310	3	16:34	1 hour 8 mins
5	Akadyr	17:42	15	17:57	3 hours 10 mins
6	Saryshagan	21:07	15	21:22	3 hours 47 mins
7	Chu	1:09	22	1:31	1 hour 40 mins
8	Anrakhay	3:11	22	3:33	31 mins
9	Otar	4:04	9	4:13	1 hour 55 mins
10	Almaty 1	6:08	5	6:13	21 mins
11	Almaty 2	6:34	-	-	-

5.2. Train energy and speed profile

To model the hybrid energy system, it is required to identify the train energy consumption. The energy consumption of the train is mainly based on its movement; therefore, it is significant to calculate the speed profile of the train. This thesis study considers the moving train “Talgo Tulpar” from Astana to Almaty in Kazakhstan. Therefore, it required real time data of the selected train’s speed or energy consumption. Since, there is no publicly available data about this train’s speed or energy profile. Thus, the speed profile of the selected train was created based on the model presented in [43]. Deng et al. [43] have demonstrated an optimization model of an urban rail transit train running curve under fast and slow train modes, which is based on the train's control parameters, such as speed and control force. In addition, Deng et al. [43] have created the speed

profile for fast and slow modes of the train by considering the train's speed variation from one station to the next. They illustrated specific stages of the train's speed, such as acceleration, cruising, coasting, and deceleration. Similarly, Ming et al. [44] investigated a model-based technique to simulate train motion, and they also analyzed the stages of the train's speed profile. Figure 5.2 illustrates the general speed profile from one station to the next. The position values for each speed variation are shown as s_1, s_2, s_3 for each stage in Figure 5.2. Points A and B indicate the starting station and the next one, respectively. Furthermore, Wang and Rakha [45] created a modeling framework for electric train energy consumption that takes instantaneous regenerative braking efficiency into account to facilitate in a rail simulation system. The author [45] first established the train speed model by considering its operational characteristics, train route and technical specifications. Based on the train's speed model demonstrated in [43, 44, 45], the speed profile for the "Talgo Tulpar" train moving from Astana to Almaty has been built.

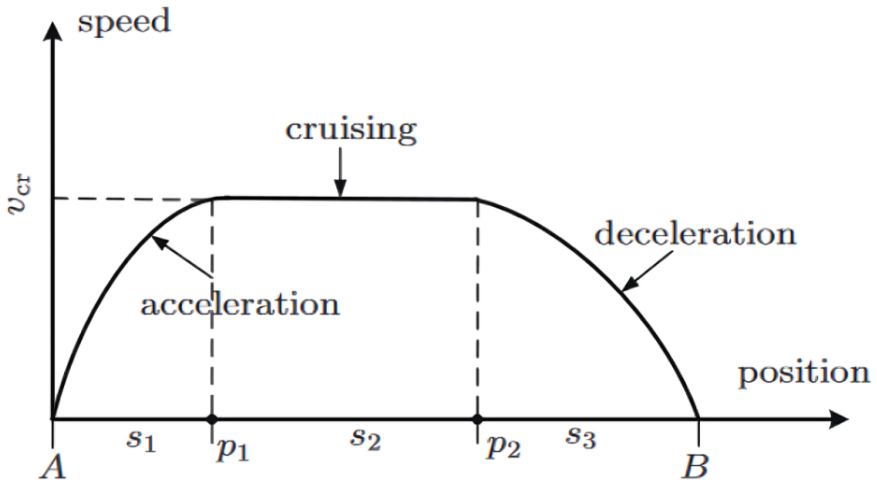

Figure 5. 2: The general train's speed profile from one station to another, taken directly from [44]

Based on the given information from the official website of the manufacturer [46] about the movement of the Talgo train, the train's speed profile was created:

- Maximum speed of the train: 250 km/h = 70 m/s

- The maximum speed of the train that can operate on Russian gauge (1520 mm) infrastructure: 220 km/h = 61 m/s
- The operation speed of the Talgo train in Kazakhstan: 110 km/h = 30.5 m/s

The train's speed profile has considered their acceleration and deceleration rates, the distance between each station and their cruising speeds, and the length of their parking time. According to Deng et al. [43], the acceleration and deceleration rates are the same, but the sign is different. Figure 5.3 demonstrates the graph of the Talgo train's speed profile, which is modeled based on research articles [43, 44]. It is important to note that the train's speed is given in m/s, while time variable, shown in seconds, means the duration of the trip from Astana to Almaty, which takes approximately 19 hours (that equals to 68400 seconds). Figure 5.3 provides 68400 data samples for illustrating the train's speed. In addition, it can be seen from Figure 5.3 that the train first reaches its maximum speed at approximately 61 m/s, as reported in its technical specification. Then the train starts to decelerate to reach its cruising speed, which means its operational and stable speed. The train's speed graph given in terms of seconds allows to clearly examine its characteristics.

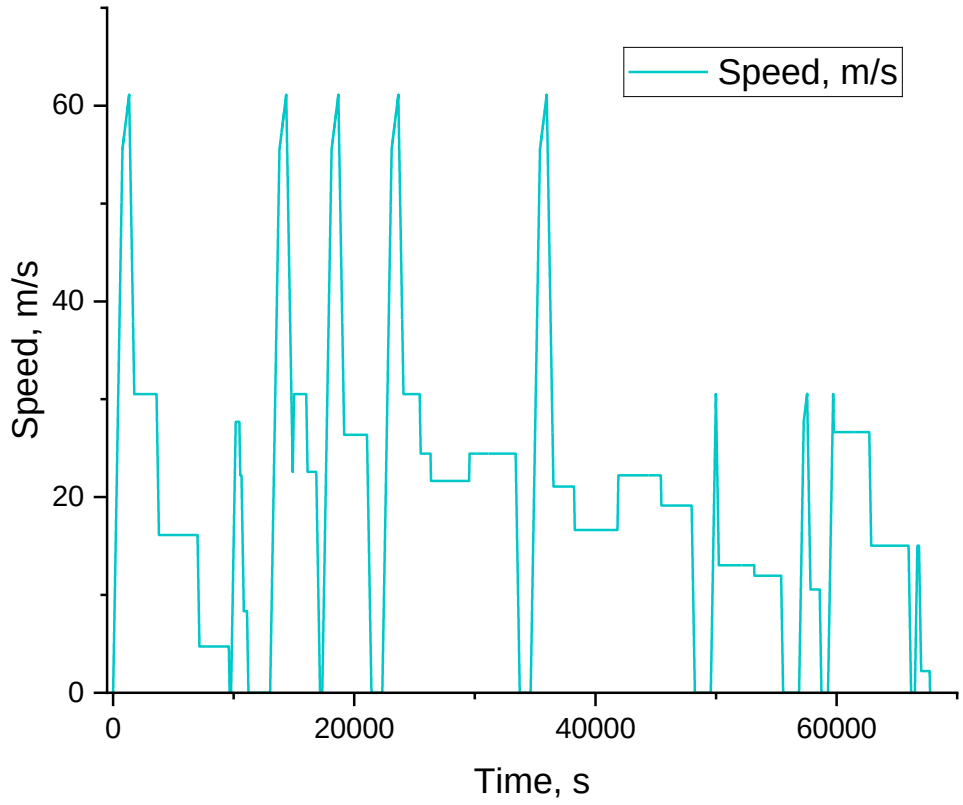

Figure 5. 3: The Talgo Tulpar train's speed profile

Furthermore, the train's energy consumption is estimated based on the obtained speed profile due to the unavailability of real-time data on the Internet. Therefore, the energy consumption data of the train is estimated based on the formulation given in article [47]. Lozano et al. [47] expressed the estimation process of the train's load, as an example, the formulation for the train Renfe in Spain has been considered in their studies. It is important to note that Spanish manufacturer of "Talgo Tulpar" train applies them with the name of Renfe in Spain. Therefore, the train load of "Talgo Tulpar" has been calculated based on the formulation, demonstrated in [47]. According to [47], the power is illustrated as the product of the traction force and the train's speed:

$$Power = F_t\, v \tag{5.1}$$

where, v is the train's speed and F_t is the tractive force (effort), which is identified based on (5.2) [47]:

$$F_t = \mu\, N \tag{5.2}$$

where, μ is the adhesion coefficient, which is affected by temperature, humidity, dirt, and speed when determining the rolling values for wheels and steel rails. In addition, N is the vertical response of the train, which is affected by the maximum axle load of the train. The adhesion coefficient for the electric train Renfe is calculated based on (5.3) [47]:

$$\mu = \mu_o\left(0.2115 + \frac{33}{42 + v}\right) \tag{5.3}$$

where, μ_o is the constant value, and it is equal to $\mu_o = 0.27$ for the Renfe train in Spain. Thus, the Talgo train's energy consumption has been calculated based on the method proposed for the Renfe train in Spain. It is important to note that the adhesion coefficient is also proportionally dependent on the train's speed. Therefore, the graph of the formulated energy consumption profile of the train can be similar to the speed's profile. Figure 5.4 illustrates the formulated train's energy consumption according to time in minutes. The train's speed profile is modelled based on the train's trip schedule (shown in Table 5.2) by following the proposed method in the studies. As can be seen in Table 5.2, the train's parking time is given in minutes and can be seen that the minimum stopping time is 2 minutes, while the maximum station time is 30 minutes. Therefore, to investigate properly and more accurately, the train's energy consumption load (kW) is reported in minutes. Furthermore, it is important to note that the electricity consumption of the train during its movement and parking time is also taken into account. This includes the train's wagon indoor

needs, such as lighting, air cooling, heating systems, and household appliances. However, train's electricity consumption in minute is significantly small in comparison to its high load indication.

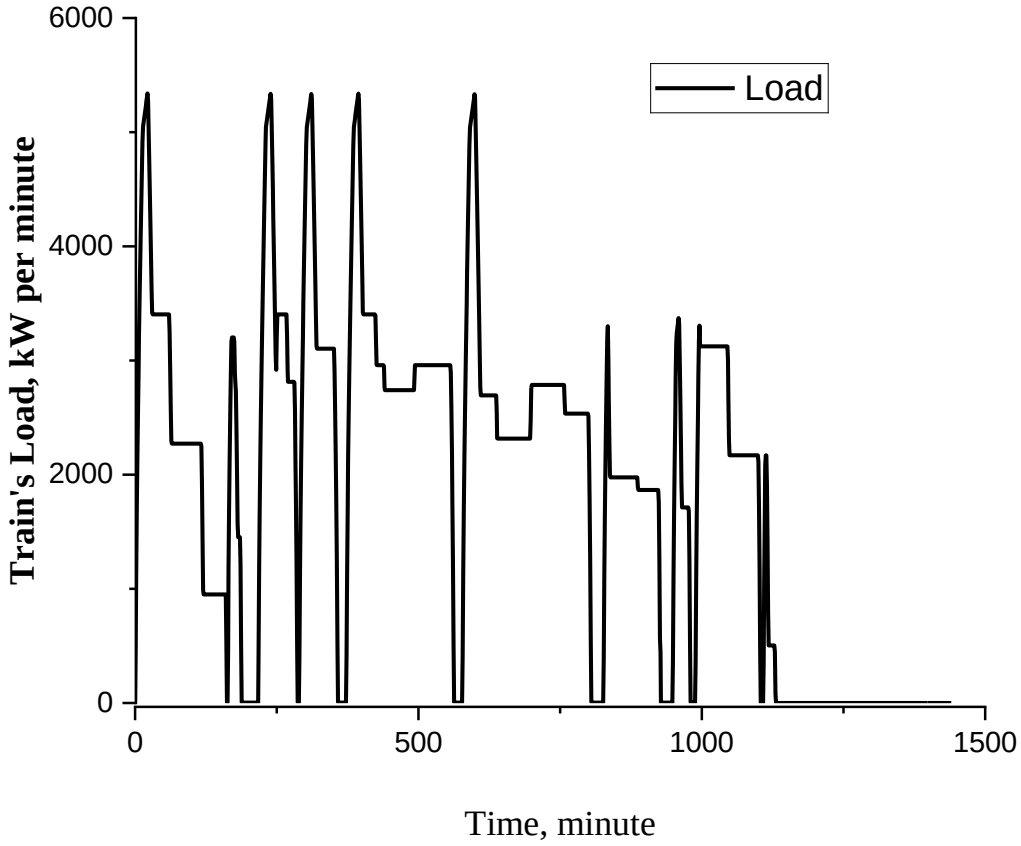

Figure 5. 4: The Talgo Tulpar train's real time energy consumption profile, given in kW per minutes.

5.3. Solar system selection

5.3.1. Type of solar cells

It is significant to choose the appropriate type of solar panel because it reflects on the performance, efficiency, and economic viability of the solar panel system. There are various factors that need to be considered before selecting a solar panel. One of the main steps in choosing the solar panel is to define the necessary type of solar cells for the system. Most applied types of

solar cells are silicon and thin film solar cells, which can be categorized as shown in Figure 5.5 [48].

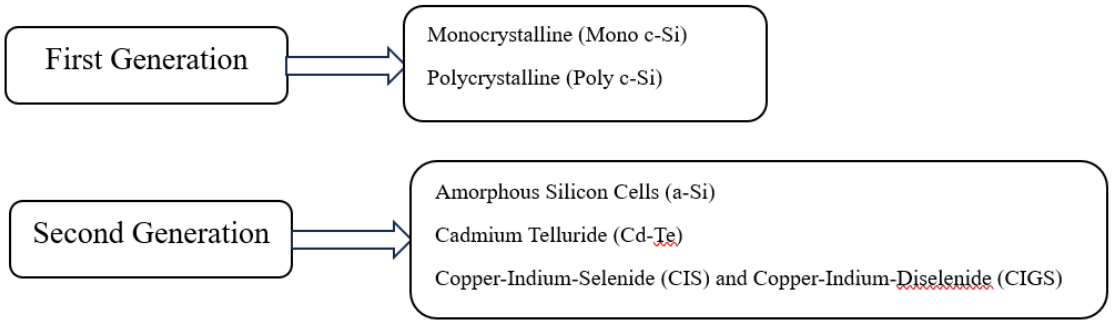

Figure 5. 5: The types of solar cells

As it can be seen, there are two main types of silicon solar cells: monocrystalline and polycrystalline solar cells. The difference between them is in the application of silicon in their production processes. Consequently, this makes polycrystalline silicon solar cells cheaper than monocrystalline. The reason for this is that polycrystalline silicon solar cells apply molten silicon by pouring rather than using it as a single crystal [48]. Even though crystalline silicon solar cells are the first generation of solar panel production, they are still the most efficient and most applied solar cells. According to [49], silicon solar cells have the highest efficiency of approximately 25%, also they are produced from one of the abundant materials. The silicon solar cells consist of two layers: a P-N type, which are positive and negative layers [48]. During the production process, silicon is often doped by boron, which helps to produce additional holes in the silicon lattice for the positive layer. On the other hand, to produce additional electrons in the silicon lattice for the negative layer, the silicon is doped with phosphorus [48].

According to Figure 5.5, the second generation of solar cells, which are defined as thin film, can be grouped into three: amorphous silicon, cadmium telluride (Cd-Te), and copper-indium-selenide (CIS). One of the advantages of thin film solar cells is their cost-effectiveness,

because they do not demand more materials for their production in comparison to the silicon solar cells [49]. Another difference is that they have very thin layers of $1 - 4\ \mu m$ thick [48]. However, thin film solar cells are not so efficient in comparison to the first-generation solar cells. Their energy efficiency per unit area is approximately 12% [49]. This value is sufficiently low in comparison to the first generation of solar cells.

As mentioned in previous sections, solar panels are going to be located on top of the roof of the train and on the sleeper of the railway track. The surface of the train's roof can be flat and curved; thus, the solar cells should be bendable and flexible. Also, another important aspect of choosing a solar panel type is its energy efficiency. Due to their limited implementation area, the selected solar panels have a small number of solar cells. Therefore, crystalline solar cells were selected because they are appropriate for the aspects.

5.3.2. Solar panels selection on the roof of the train

Nowadays, there are a wide range of manufacturers of solar panels. The 'Canadian Solar" CS6X-310M (310W) solar panel was selected after considering its cost-effectiveness and technical feasibility. This selected solar panel is aimed at being applied to the top of the train. In addition, the selected solar panel is a mono-crystalline type of solar cell. Table 5.3 demonstrates the technical characteristics of the selected solar panel [50].

Table 5.3: The technical parameters of the "Canadian Solar" CS6X-310M (310W)

Characteristic [unit]	**Specification**
Nominal operating maximum power, P_{max} [W]	310
Power tolerance [W]	± 5
Cell arrangement	72 (6×12)

Cell type	Mono-crystalline
Optimum operating voltage at P_{max}, V_{mp} [V]	36.7
Optimum operating current at P_{max}, I_{mp} [A]	8.44
Open circuit voltage, V_{oc} [V]	45.3
Short circuit current, I_{sc} [A]	8.95
Module efficiency, η [%]	16.16
Maximum series fuse rating, [A]	15
Nominal operating temperature, NOCT, [$^{\circ}$C]	45 ± 2
Linear power output warranty [years]	25
Weight [kg]	23
Dimensions (length $\times$ width $\times$ height) [m]	$1.954 \times 0.982 \times 0.04$
Surface area [m^2]	1.92

Based on the illustrated formula in the previous chapter, the power outputs for the selected solar panel are calculated for each season. It is true that the power generation of solar panels varies according to the seasons due to solar availability. The power outputs of the solar panels for the fall, winter, spring, and summer seasons are shown in Figure 5.6. It is important to highlight that the power output values are shown from 12 pm until 7 am based on the trip duration of the train. However, the simulation is considered one full day, which means from 12 pm until 11:59 am of another day. Based on the power outputs for each season, solar panels can produce the highest amount of power in the summer and spring seasons.

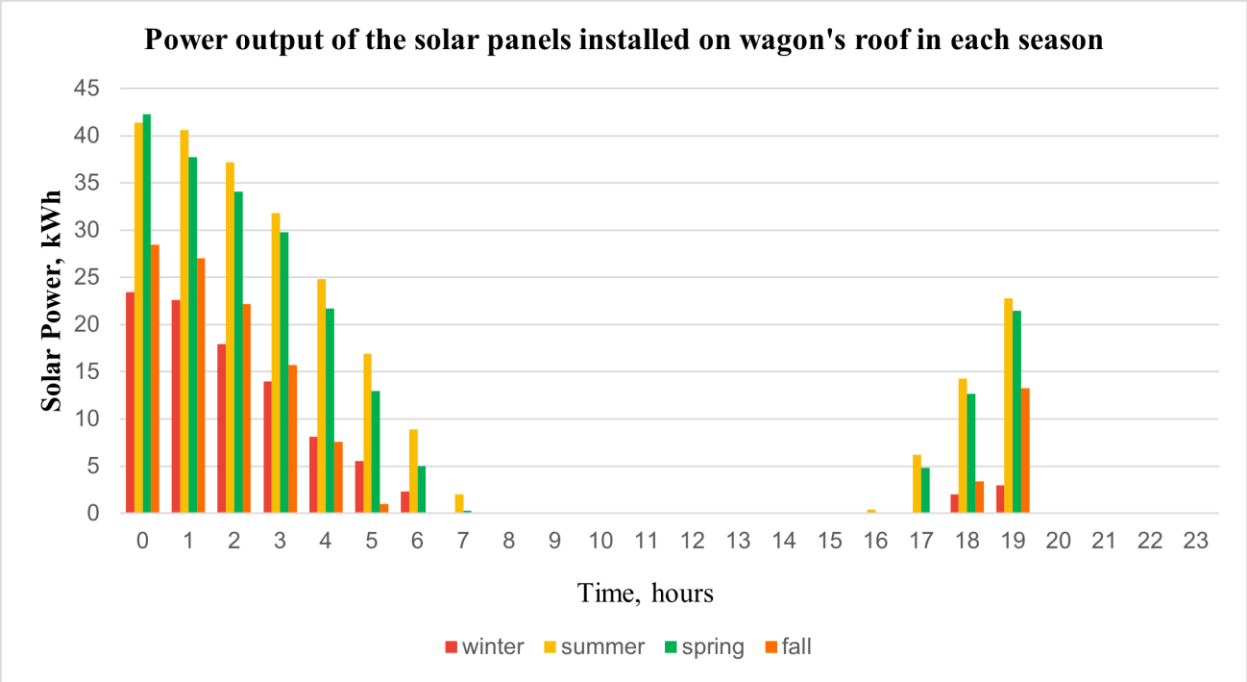

Figure 5. 6: The graph of the total power of solar panels on the train for each season: Winter, Summer, Spring, Fall.

5.3.3. Solar sleepers' selection.

The solar panels and micro wind turbines located on the roof of the moving electric trains would have insignificant energy generation that can satisfy the energy needs of the train. Therefore, we have also considered the application of solar panels on railway sleepers, as shown in Figure 5.7. Nowadays, British energy company Bankset is experimenting with the application of solar photovoltaic systems on the railway tracks in Germany. They demonstrated an ambitious project, which aims to establish gigawatts of solar PV on railway sleepers [51]. According to [16], there is a possibility to generate 0.1 MW of electricity per kilometer from the application of solar sleepers. This requires investigating the technical characteristics of the sleepers in Kazakhstan. The standard dimensions and technical specifications of the gauge tracks are different in Kazakhstan compared to European Union. According to [52], the European countries have a standard gauge of 1435 mm,

while Russian gauge tracks have a dimensions of 1524 mm. This Russian standard is also related to the countries of the Commonwealth of Independent States (CIS), where Kazakhstan is a part of this organization.

- Dimensions of the sleeper on the railway track [53]: 1524 mm × 250 mm.
- The distance or spacing between two sleepers [54]: 540 mm.

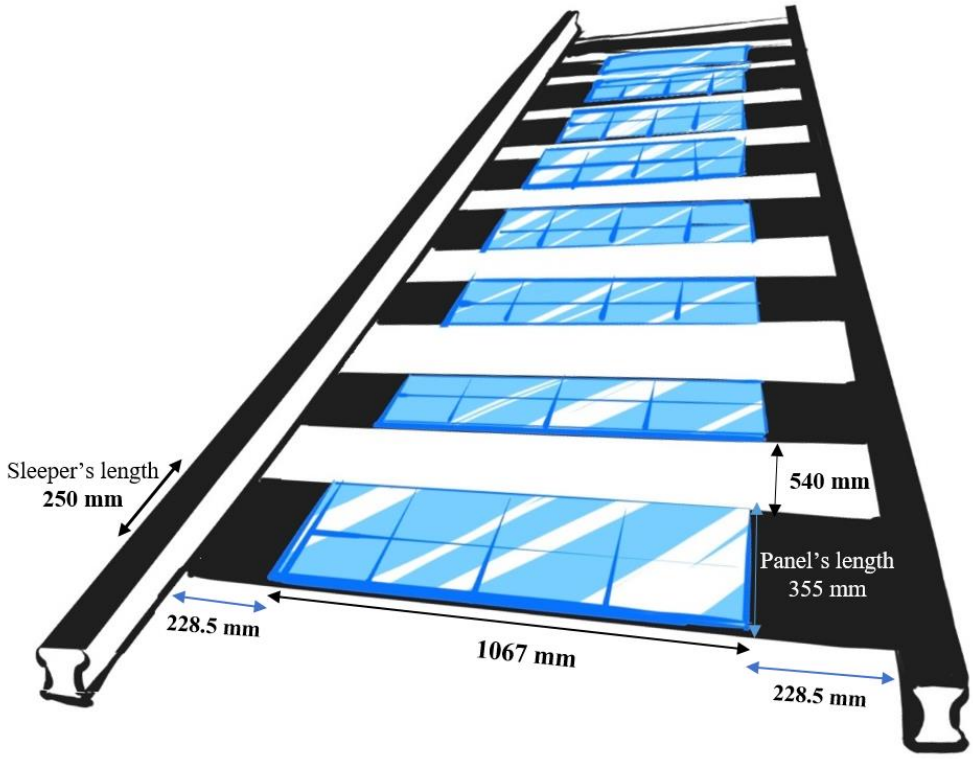

Figure 5. 7: The solar panels installed on the sleepers of the railway track.

It can be seen from the dimensions of the railway sleeper that small and slim solar panels can be installed. Based on its dimensions, it was chosen to install the LS-55FX2 monocrystalline solar panel from the "Lensunsolar" manufacturer [55]. This solar panel was found in the market for putting on the sleepers of the railway track on the route Astana - Almaty. Table 5.4 illustrates the technical specifications of the selected solar panel for sleepers [55].

Before calculating the energy output from the solar sleepers, it is important to identify the required number of sleepers on the track. From Table 5.4, the length of the selected solar panel fully suits the length of the sleeper. The length of the railway sleeper in Kazakhstan is 1524 mm, and it is decided to leave some space on both sides of the sleeper for maintenance purposes. Thus, the length of the sleeper for maintenance from both sides can be found:

$$Free\ space\ of\ \ the\ sleeper\ for\ maintenance = \frac{1524\ -\ 1067}{2} = 228.5\ mm$$

As can be seen, there is enough space for service work (as indicated in Figure 5.7). Furthermore, the width of the selected solar panel is equal to 350 mm, and the spacing between each sleeper is 540 mm in Kazakhstan. Based on this information, it is possible to calculate the total number of solar sleepers in 1 km.

$$Number\ of\ \ sleepers\ in\ 1\ km = \frac{1000\ m}{(0.35 + 0.44)\ \ m} = \frac{1000}{0.79} \approx 1265.8 \approx 1265$$

The distance between each location is given in Appendix A, and the total number of sleepers from one location to the other is calculated by multiplying the distance by the number of sleepers in 1 km. As an example, consider the total number of sleepers from Astana station to Oskarovka, which is the next location of the train after one hour:

$$Total\ number\ of\ \ sleepers\ \ (Astana\ -\ \ Oskarovka)\ \ =\ 109.83\ \times\ 1265\ =\ 138934$$

Table 5.4: The technical characteristics of the LS-55FX2 solar sleeper [55]

Characteristic [unit]	**Specification**
Nominal operating maximum power, P_{max} [W]	55
Power tolerance [W]	$\pm$ 5
Cell arrangement	20 (2×10)
Cell type	Mono-crystalline
Nominal operating temperature, NOCT, $^{\circ}$C	45 ± 2
Linear power output warranty [years]	25
Weight [kg]	2.2
Dimensions (length $\times$ width $\times$ height) [m]	$1.067 \times 0.355 \times 0.254$
Surface area [m^2]	0.379
Manufacturer	"Lensunsolar"

As discussed in chapter 4, the power output of the solar panel is calculated based on equations (4.1) and (4.2). Firstly, the power generation of solar sleepers for each location was calculated for the given time. Appendix A is applied to define the location in terms of its latitude and longitude. As mentioned before, the simulation study considers from 12 pm till 12 pm of another day. Secondly, the power output of solar sleepers for each location is summed based on their time to obtain the total generation power from Astana to Almaty cities. These can be represented in (5.4):

$$P_{total}(t) = \sum_{i=1}^{N} P_i(t) \tag{5.4}$$

where, $P_i(t)$ is the power output of solar sleepers in the *ith* section (kWh), N is the total number of sections between two cities, which is equal to 20. The total generation power of solar sleepers was calculated for each season, and there are estimated power outputs of each location in each season. This detailed information is available in Appendix B. Finally, the total power generation from solar panels, located from Astana to Almaty, for each season of the year is illustrated in

Figure 5.8. As can be seen from Figure 5.8, the energy generation of the solar sleepers is significantly high in comparison to the energy generation of the solar panels and wind turbines installed on the train's roof. As reported above, high energy generation from solar sleepers is influenced by the number of solar sleepers per each kilometer. The total length of the train's trip from Astana to Almaty is 1200 km, consequently, the high number of solar sleepers will be located over the railway track.

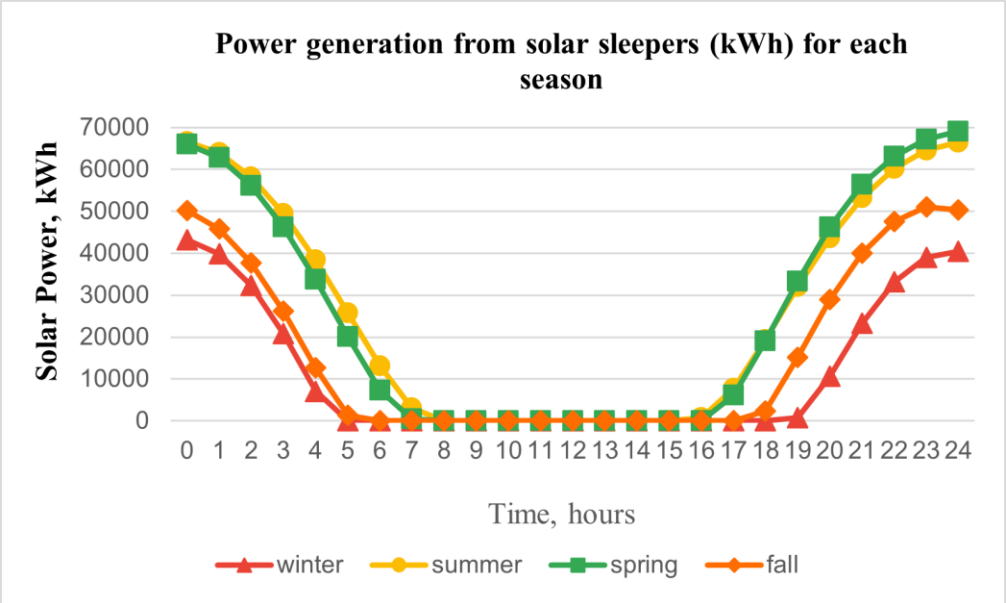

Figure 5. 8: The graph of the total power of solar sleepers Astana – Almaty for each season: Winter, Summer, Spring, Fall.

It is important to note that the obtained power output results differ based on the season due to daylight hours. In winter, it is true that night is longer than the sun, thus there is only 10 hours of sun availability in one day. On the other hand, in summer, the sun becomes available from 4 am till 8 pm. This means that the solar sleepers can generate a large amount of power in summer, which can also be seen in its output graph (Figure 5.8). For other seasons, fall and spring, the sun availability is approximately 12 hours in a day. Therefore, it can be concluded that the power generation of solar sleepers is highest in summer season, while the minimum energy generation is

counted in winter season. However, there are other factors which can also affect the performance of the solar sleepers of the railway track, which will be discussed in further chapters.

5.4. Wind turbine selection

The selected wind turbine (WT) is installed on the roof space of the train's wagon. Therefore, it means that the selected wind turbine should be small. As mentioned earlier, the wind turbine is chosen to be horizontally aligned micro VAWT, based on the feasibility study of [24]. Table 5.5 represents the technical characteristics of the selected wind turbine, produced by "Smartwind".

Table 5.5: The technical characteristics of the wind turbine [56]

Characteristic	**Specification**
Weight [kg]	10
Dimensions (length × width × height) [m]	0.7 × 0.7 × 1.2
Features	Vertical axis wind turbine (VAWT)
Maximum Voltage [V]	AC Three-phase 24
Peak Power [W]	300
Start-up Wind velocity [m/s]	0,9
Noise Level [dB]	< 40
Number of blades	6 blades
Warranty [years]	2
Configuration	Basic
Manufacturer	"Smartwind"

The power output of the wind turbine is calculated based on (4.3), where one of the varying parameters is speed. Therefore, the graph of the wind energy is similar to the speed profile of the train because it was assumed to neglect the environmental conditions that can affect the speed. Figure 5.9 demonstrates the graph of wind energy generation in terms of minutes. The maximum wind energy is reached at 1000 kW, which is equal to the acceleration stage of the train. When a train accelerates, it tries to reach its maximum velocity based on its technical specifications. Therefore, the graphs of the train's load and power of the wind turbines reach their maximum level at the acceleration stage. During the acceleration stage, the train reaches its maximum speed that is equal to 61 m/s (220 km/h). It is true that there is a high-speed limitation for generating energy from wind turbines. However, this proposed micro wind turbine should be designed in a way that can meet the highest speed of the wind. On the other hand, the minimum required speed for generating energy from small scale wind turbines is given in Table 5.5. There can be seen that the cut-in speed is 0.9 m/s, which means that wind turbines start to generate energy at the minimum speed of 0.9 m/s. This power output of the wind turbine is assumed to be the same for each season.

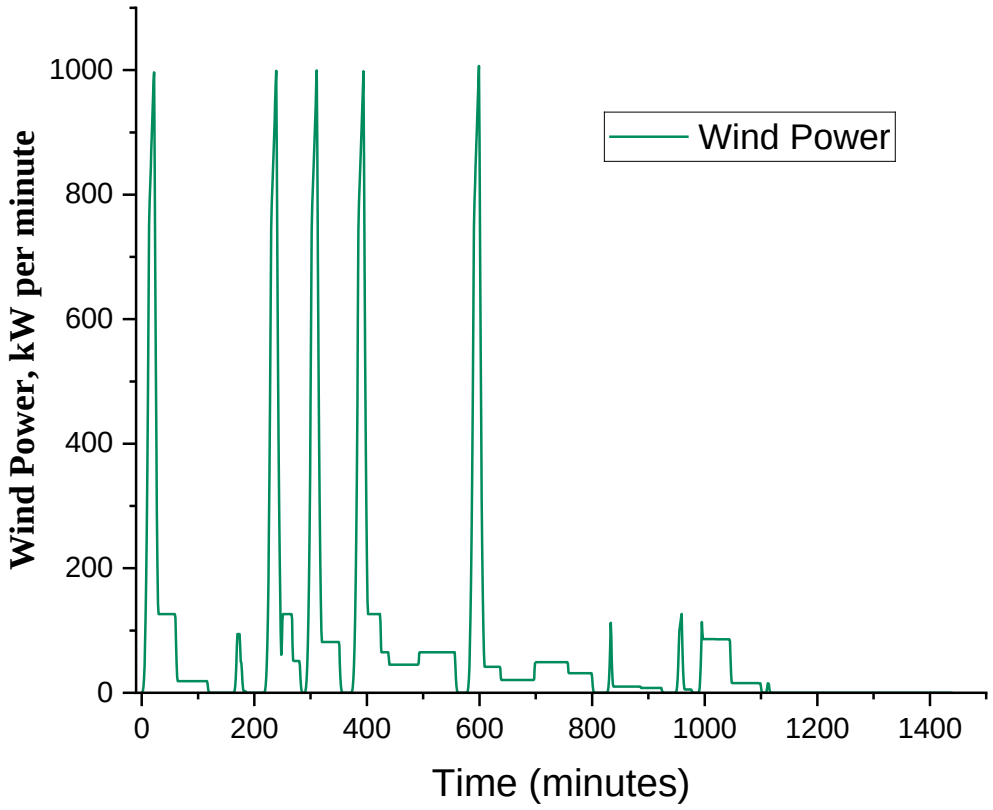

Figure 5. 9: The graph of the total power of wind turbines moving from Astana - Almaty

5.5. Solar panels and wind turbines arrangement

According to Table 5.1, the length and the width of the wagon are 13.140 m and 3.200 m, respectively, and the dimensions of the wagons are given in terms of 1-VM standard. Figure 5.10 represents the top view of the standard wagon 1-VM [46, 57].

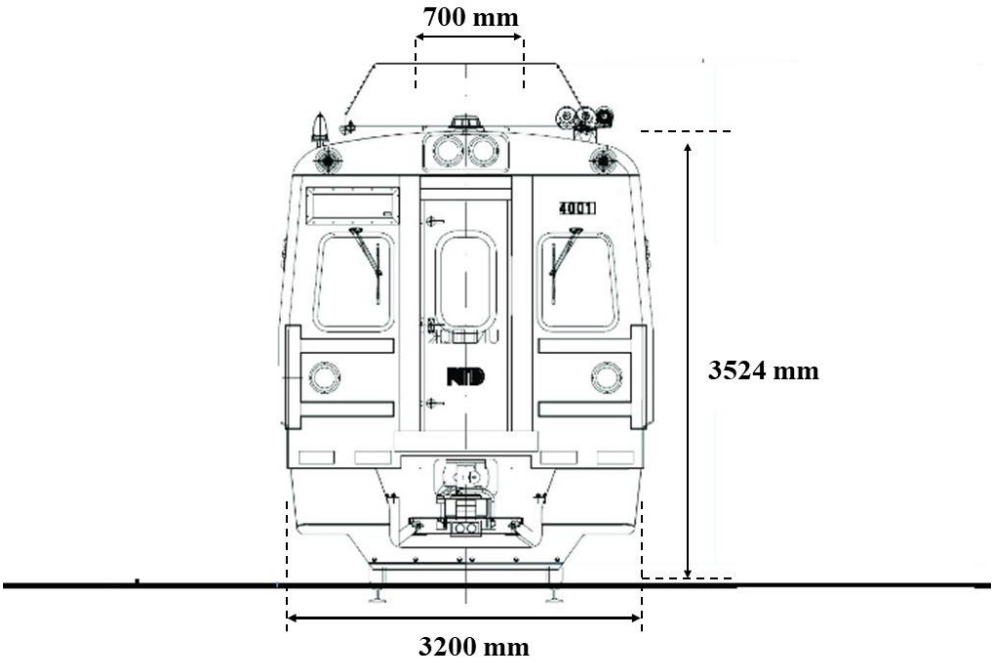

Figure 5. 10: The face view of the Talgo Tulpar train's wagon (dimensions in mm), taken and modified from [57]

It can be seen that the middle of the wagon's roof is taken for maintenance purposes. Thus, the available width is calculated:

$$Available\ width = 3200 - 700\ mm = 2500\ mm = 2 \times 1250\ mm$$

Furthermore, it is required to identify the available length for installations. Figure 5.11 represents the side view of the train's wagon. Similarly, it is assumed to leave 500 mm from both sides for the service and maintenance purposes. Thus, the available length for the installations is calculated to be:

$$Available\ length = 13140 - 500 \times 2 = 12140\ mm$$

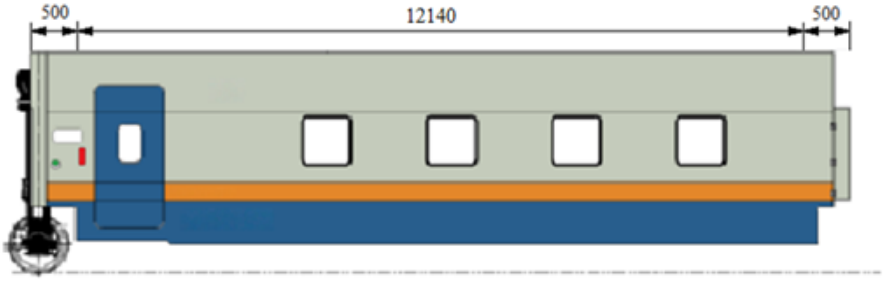

Figure 5. 11: The side view of the Talgo Tulpar train's wagon (dimensions in mm), taken and modified from [46, 57]

The next step is to calculate the required number of solar panels and wind turbines on the roof of the wagon. From Table 5.3, the selected solar panel "Canadian Solar" CS6X-310M has a surface area of $1.954 \times 0.982\ m^2$, and the width of the solar panel suits fully the required width of the wagon (0.982 < 1.250 m). From Table 5.5, the selected wind turbine has dimensions $0.7 \times 0.7\ m$, similarly, the width of the turbine fits fully the available wagon's width (0.7 < 1.250 m). Therefore, the total number of solar panels and wind turbines that can be installed on the roof is defined to be:

$$Total\ number\ of\ PV\ and\ WT = 2 \times \frac{12.140}{1.954 + 0.7} \approx 2 \times 4.57 \approx 2 \times 4 = 8$$

This means that there can be installed in total 8 units of each source. Figure 5.12 shows the visual illustration of solar panels and wind turbines installation on top of the train's wagon. There can be seen 4 rows of wind turbines, which model is based on [24], similarly, 4 rows of solar panels.

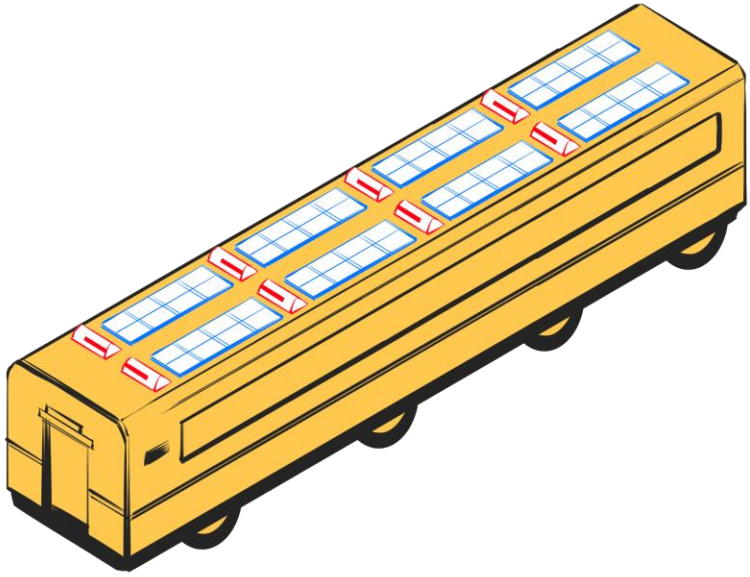

Figure 5. 12: The conceptual design of the solar panels and wind turbines installation on a moving train

5.6. Battery energy storage system (BESS) selection

The battery energy storage system stores energy coming from the solar panels and wind turbines that are located on top of the train. Generally, the capacity of the BESS is defined by over fulfillment of up to 120 % [58]. This means that the upper limit of the BESS capacity is calculated as follows (5.5):

$$P_{max} = 1.2\, P_{nominal} \tag{5.5}$$

According to the technical specifications given in Table 5.3 and 5.4, the rated power of solar panel and wind turbine is equal to 310 W and 300 W, respectively. Thus, by considering the total number of renewable energy systems, the BESS capacity for each wagon is estimated as follows:

$$BESS\ capacity\ for\ each\ train's\ wagon\ =\ 1.2(\,310\times 8\ +300\times 8)\ =5.856\ kW$$

As mentioned before, the Talgo Tulpar train has 11 wagons, thus the total BESS capacity for full train is estimated to be:

$$BESS\ capacity\ for\ the\ train\ fully\ = 5.865 \times 11\ = 64.515\ kW$$

Chapter 6 - Results and Discussion

6.1. Case study 1

Case study 1 considers the performance of solar panels and micro wind turbines on a moving train, which can be seen as general or base case. This base case is important to compare with other cases, where the integration of storage systems and solar sleepers are considered. As mentioned earlier, the simulation results are obtained in terms of one randomly chosen day in each season. Therefore, all case studies are examined for each season. Figure 6.1 shows the graph representation of the grid energy usage, the train's load, and renewable energy usage during the train's movement in summer season. As can be seen, the train's load is mostly dependent on the main energy network (grid energy). Similar scenarios can be noticed in other season's graphs (Figures 6.3, 6.5, 6.7). The renewable energy usage indication demonstrates the summation of energy generation from the small-scale solar panels and wind turbines for each season, which graphs are shown separately in Figures 6.2, 6.4, 6.6, and 6.8. It is important to note that the simulation results are shown for one full day (12 pm till 11:59 am of the next day). However, the applied data are illustrated in terms of time taken for the train to move from Astana – Almaty. To be more exact, this case considers only renewable energy resources installed on the train. Therefore, their data are shown for 1140 minutes, which is the time taken for the train to reach its destination. The considered solar panels and wind turbines are small scale applications, therefore the generated energy from them is insufficient to meet the energy consumption of the train. In addition, the total generated energy from renewable energy resources and the energy savings are obtained from simulation, which is shown in Table 6.1. There can be seen that mostly summer and spring seasons demonstrate better results in comparison to other seasons. This is understandable

because the generation of solar energy is directly dependent on irradiation. Even though the renewable energy resources are installed in small-scale applications, there is an energy savings of around 4% in each season. This means that through the integration of micro wind turbines and solar panels on top of the train, it is able to minimize a particular amount of demand energy. The code implemented in case 1 is given in Appendix C.

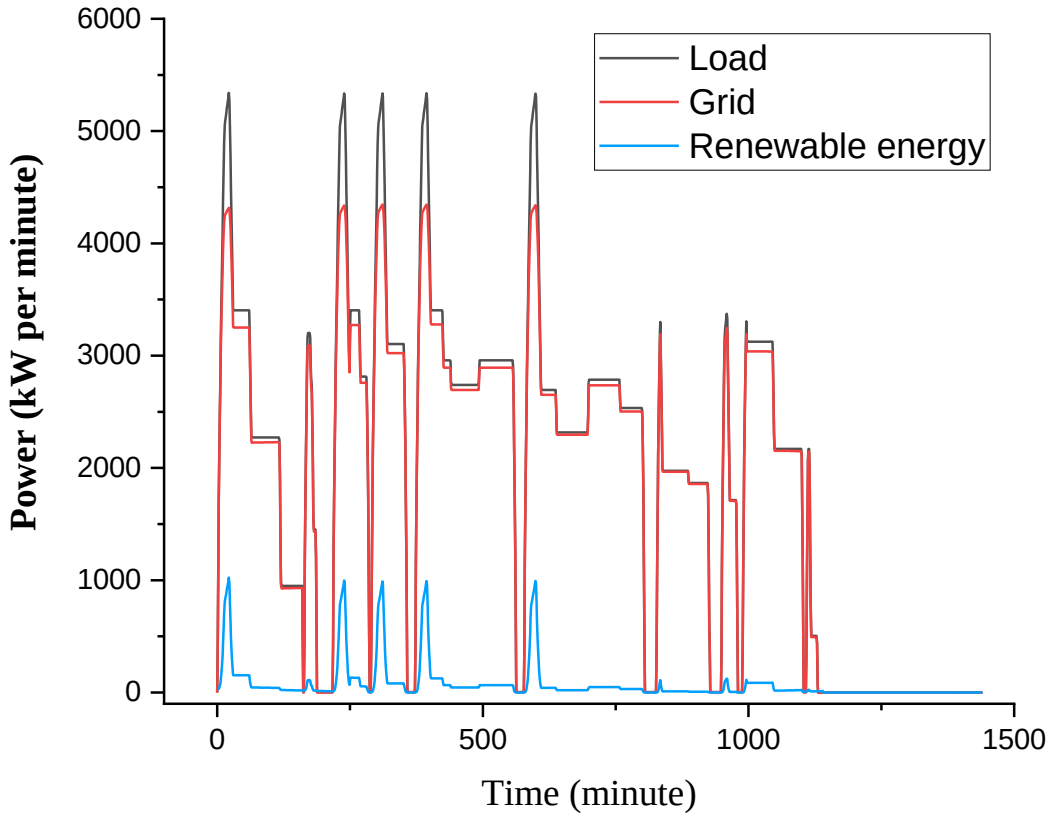

Figure 6. 1: Case 1 - The graph of the grid energy usage, the train's load, and renewable energy usage during the trip Astana-Almaty in Fall season.

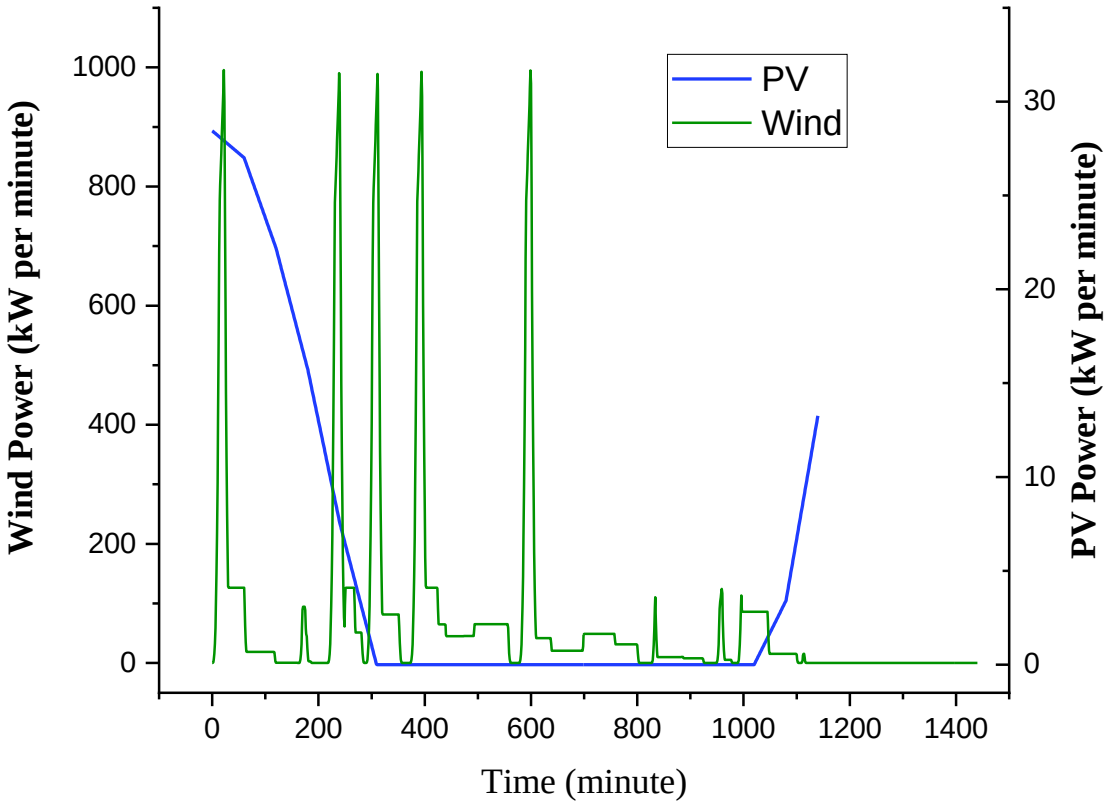

Figure 6. 2: Case 1 – The graph of the elements of renewable energy usage parameter: PV panels and Wind turbines installed on train's roof in Fall season.

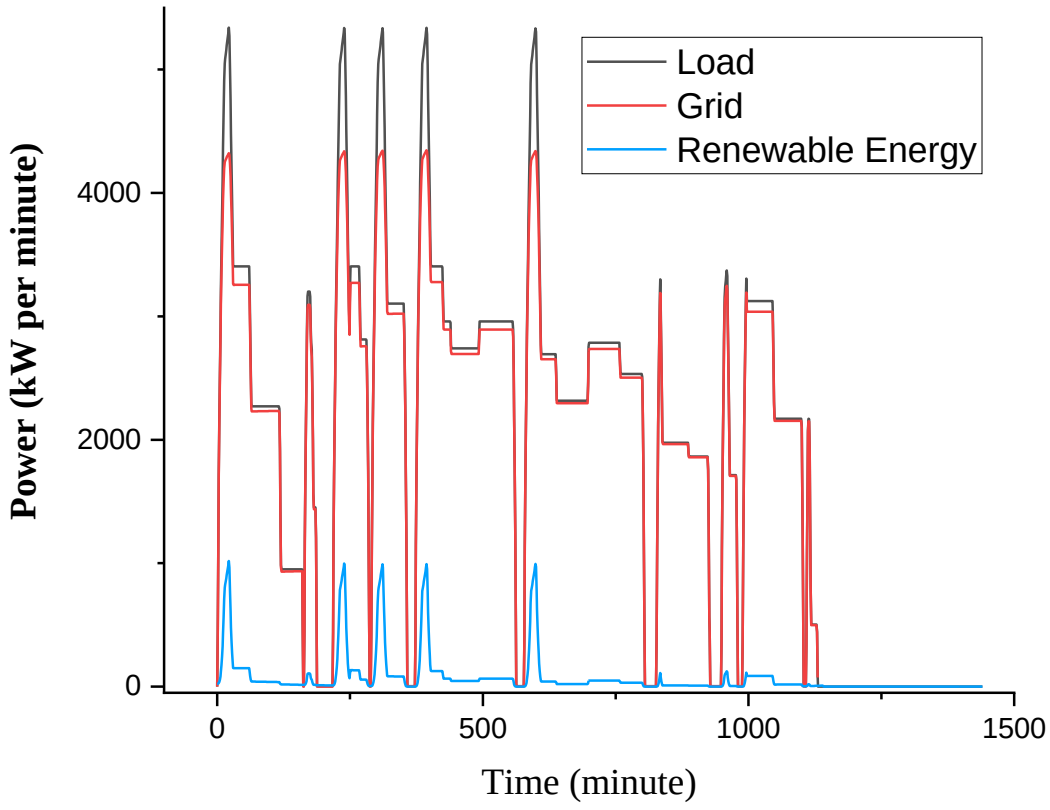

Figure 6. 3: Case 1 - The graph of the grid energy usage, the train's load, and renewable energy usage during the trip Astana-Almaty in Winter season.

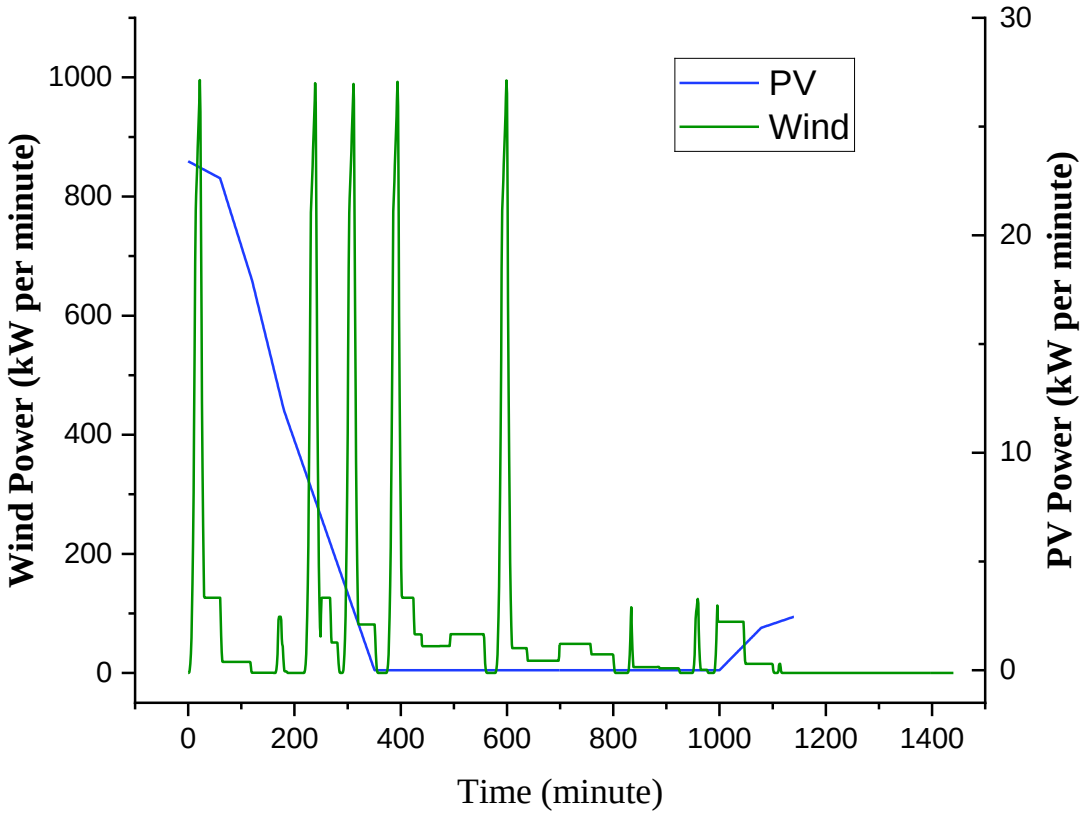

Figure 6. 4: Case 1 - The graph of the elements of renewable energy usage parameter: PV panels and Wind turbines installed on train's roof in Winter season.

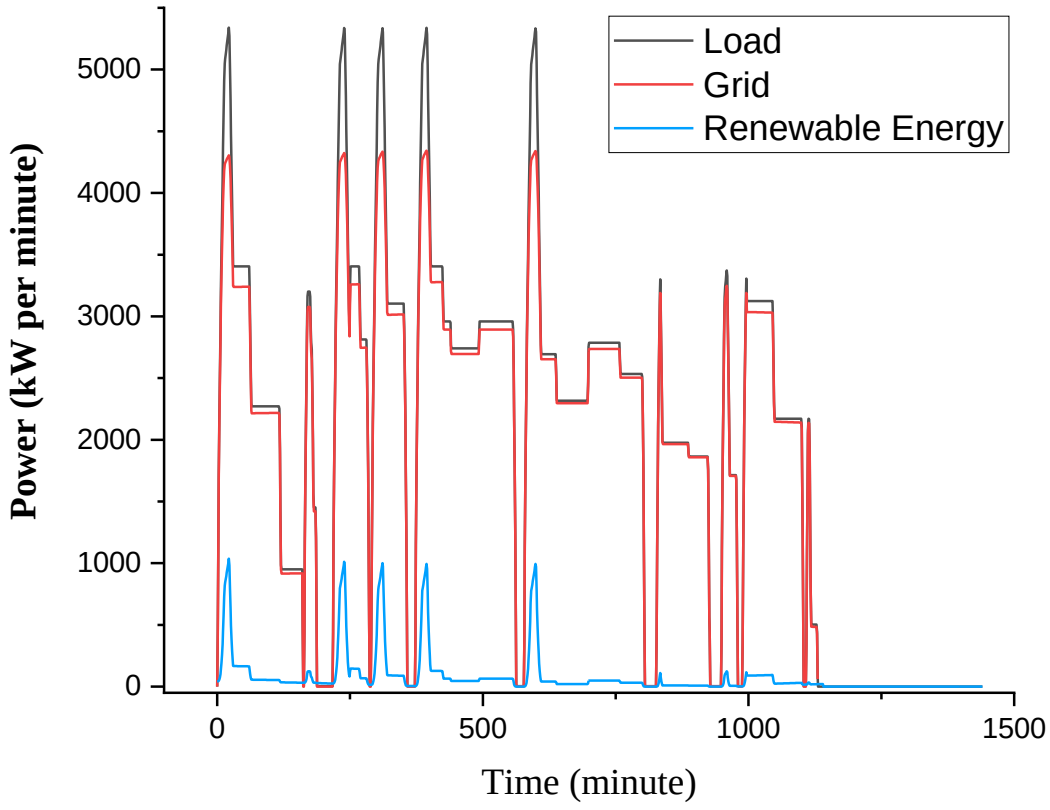

Figure 6. 5: Case 1 - The graph of the grid energy usage, the train's load, and renewable energy usage during the trip Astana-Almaty in Spring season.

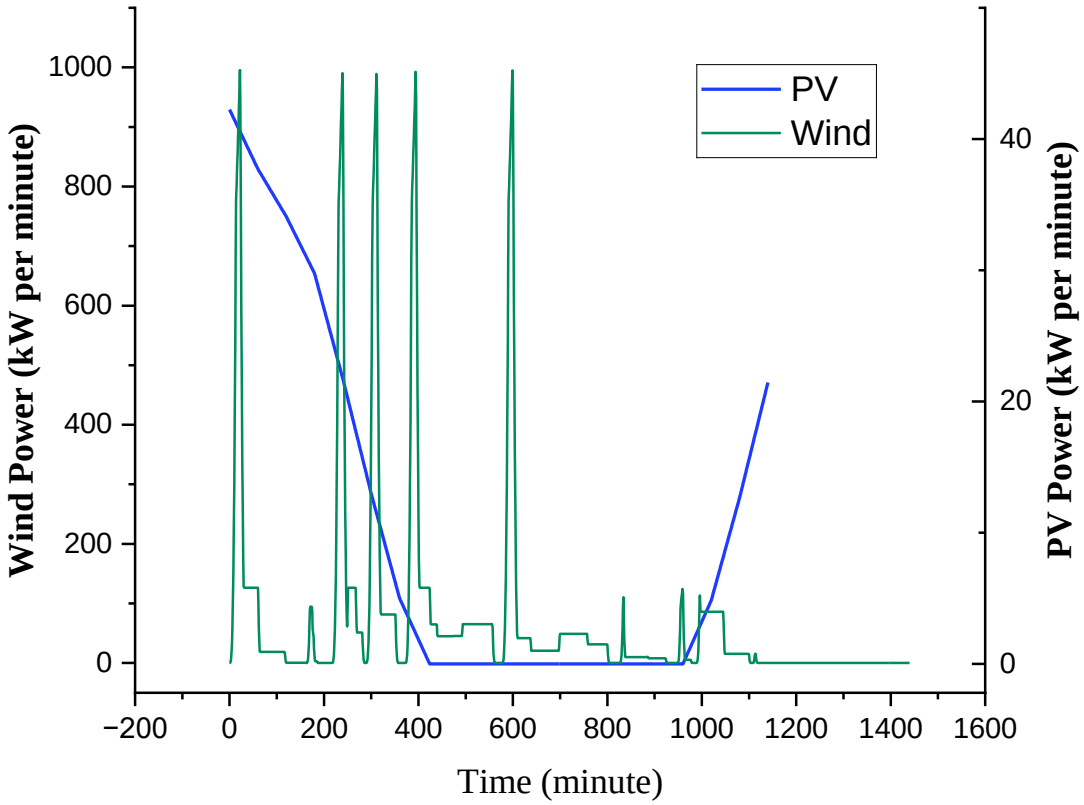

Figure 6. 6: Case 1 - The graph of the elements of renewable energy usage parameter: PV panels and Wind turbines installed on train's roof in Spring season.

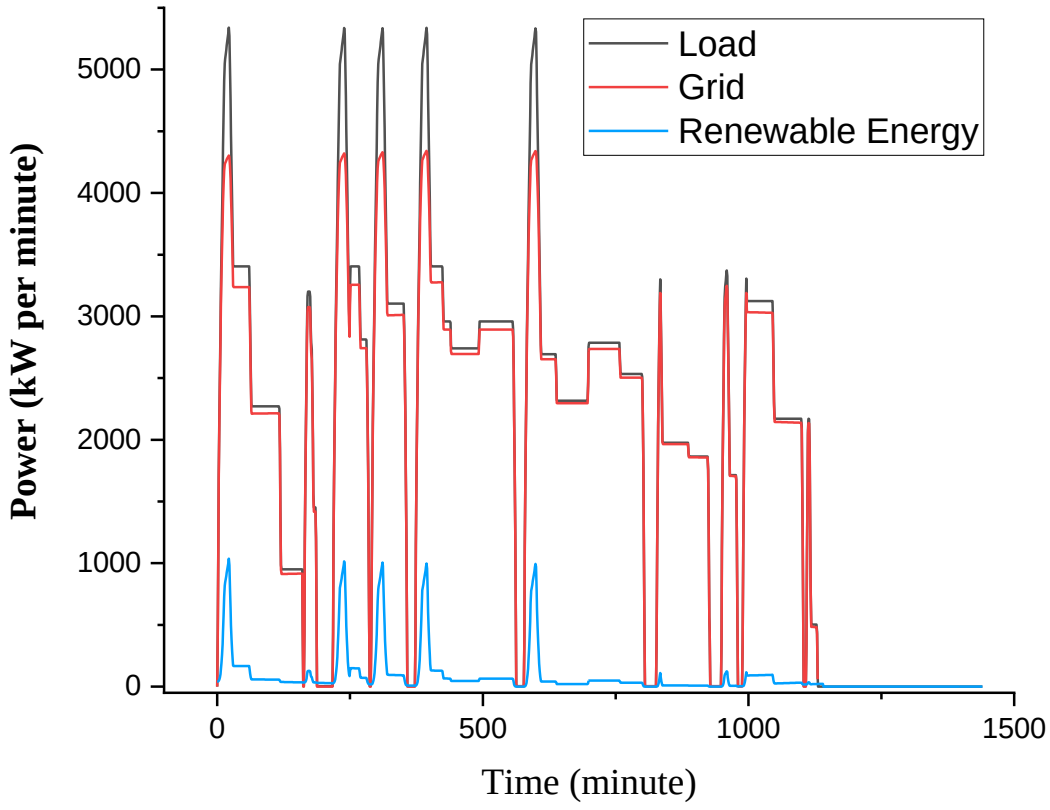

Figure 6. 7: Case 1 - The graph of the grid energy usage, the train's load, and renewable energy usage during the trip Astana-Almaty in Summer season.

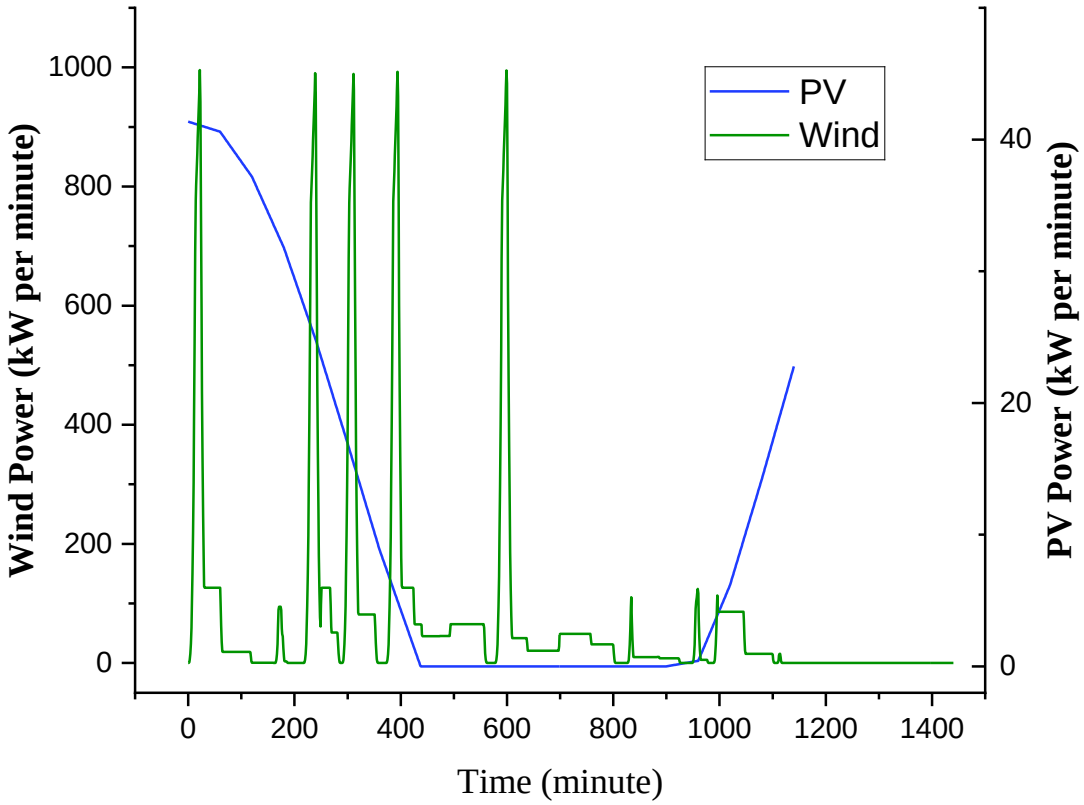

Figure 6. 8: Case 1 – The graph of the elements of renewable energy usage parameter: PV and Wind turbines installed on train's roof in Summer season.

Table 6.1: The obtained results for each season from case 1 study

	Summer	**Winter**	**Fall**	**Spring**
Total Energy Generated by Renewable energy sources [kWh]	2007.39	1873.34	1890.12	1983.75
Total Solar Generation [kWh]	214.95	80.91	97.69	191.32
Total Wind Generation [kWh]	1792.43	1792.43	1792.43	1792.43
Energy savings [%]	4.42	4.15	4.18	4.37

6.2. Case study 2

Case study 2 considers the application of solar panels and wind turbines in small-scale applications, also the battery energy storage system is applied to the train's energy system. The aim of this case is to investigate the effect of the BESS on the train's energy system. This case considers the strategy plan of the BESS in hybrid energy system proposed in Chapter 3. There are operating limitations on the State of Charge (SOC) of the BESS. More specifically, to guarantee battery longevity and operational dependability, the SOC should stay between 20% and 85%. If the SOC after any time step is outside these boundaries, the objective function applies a severe penalty (a huge arbitrary value, like 10,000). In order to avoid these fines, the PSO will look for ways to maintain the SOC within the authorized range. Figures 6.9, 6.12, 6.15, and 6.18 illustrate the graph of grid energy usage, train's load, and renewable energy resources during the trip for fall, winter, spring, and summer seasons, respectively. It is important to note that the simulation is conducted for one full day, 24 hours. Furthermore, by following the strategy plan, the PSO tries to optimize the charging and discharging conditions of the BESS. Figures 6.10, 6.13, 6.16, and 6.19 demonstrate the optimal BESS SOC levels for each season: fall, winter, spring, and summer, respectively. From obtained results, it can be seen that the BESS SOC level is mostly satisfying its constraint (between 20% - 85%). Consequently, Figures 6.11, 6.14, 6.17, and 6.20 illustrate the power of the BESS based on the SOC level for each season. There can be seen the charging and discharging condition of the BESS. The positive values of the BESS power demonstrate the charging condition of the BESS, while the negative indications of the BESS power demonstrate the discharging condition of the BESS. Positive power indicates that energy is flowing into the battery, increasing its stored energy. On the other hand, negative values on the graph indicate that the energy is flowing out of the battery to meet the system's energy demand.

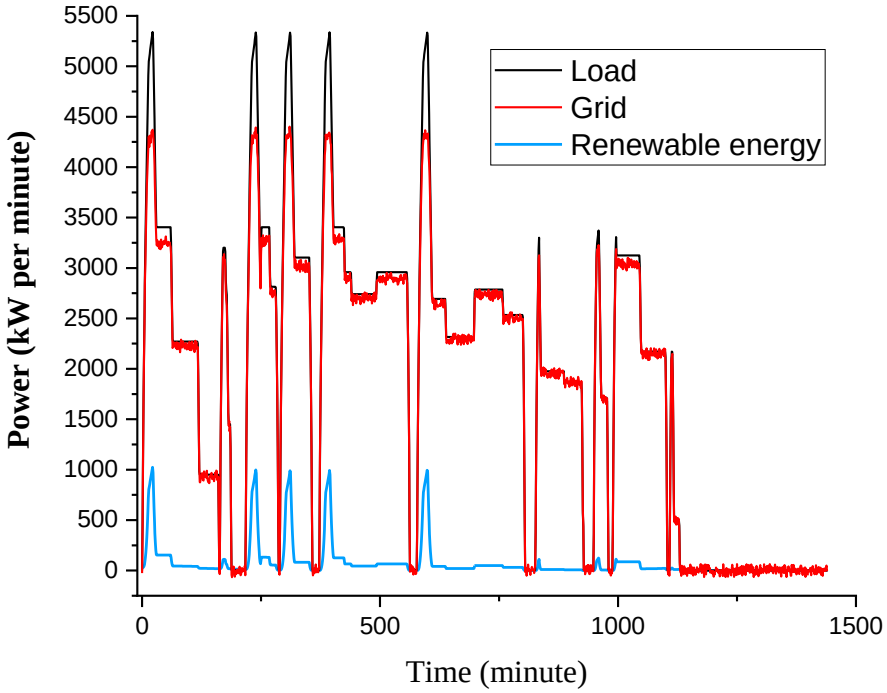

Figure 6. 9: Case 2 - The graph of the grid energy usage, the train's load, and renewable energy usage during the trip Astana-Almaty in Fall season.

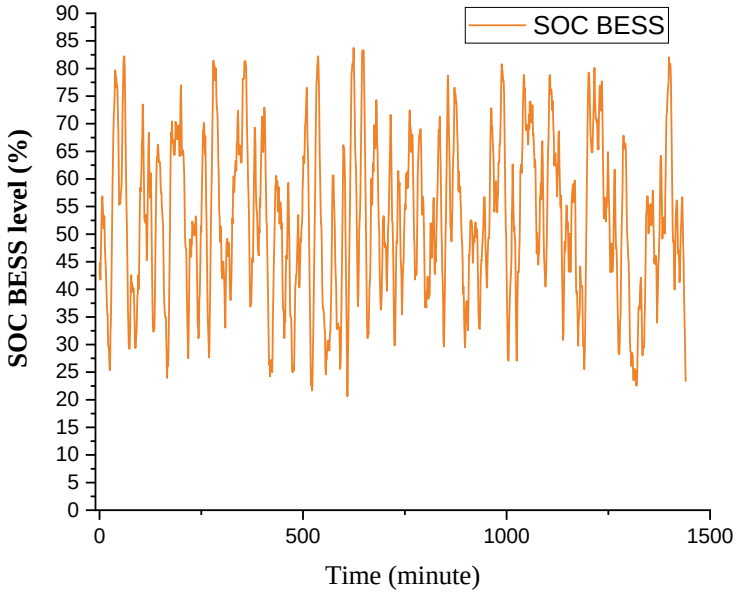

Figure 6. 10: Case 2 - The optimized BESS SOC level over the given time, Fall season.

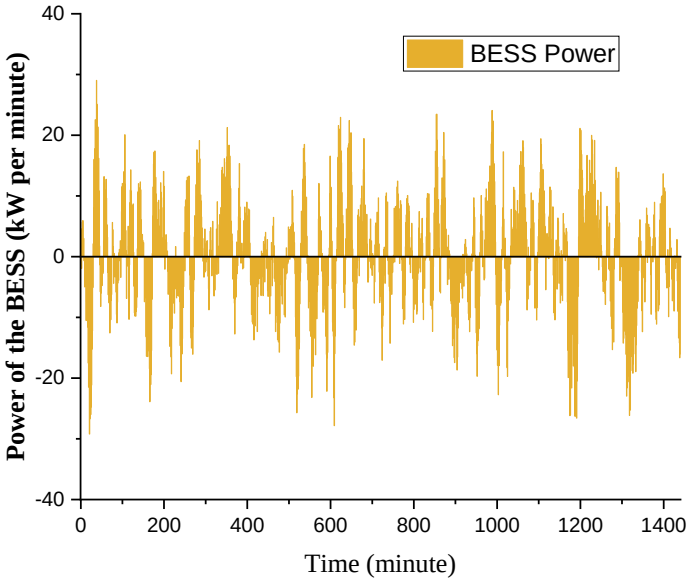

Figure 6. 11: Case 2 – The optimized BESS Power changes over the given time, Fall season.

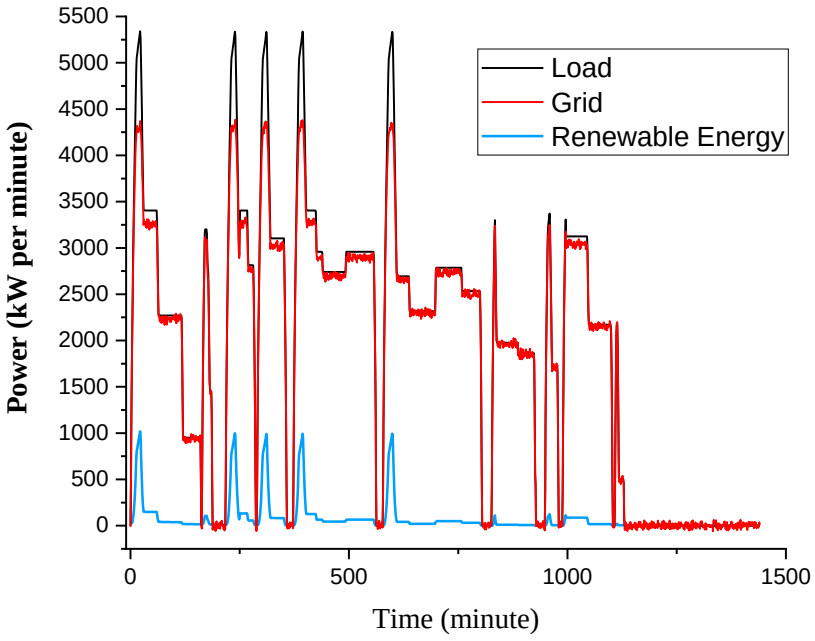

Figure 6. 12: Case 2 - The graph of the grid energy usage, the train's load, and renewable energy usage during the trip Astana-Almaty in Winter season.

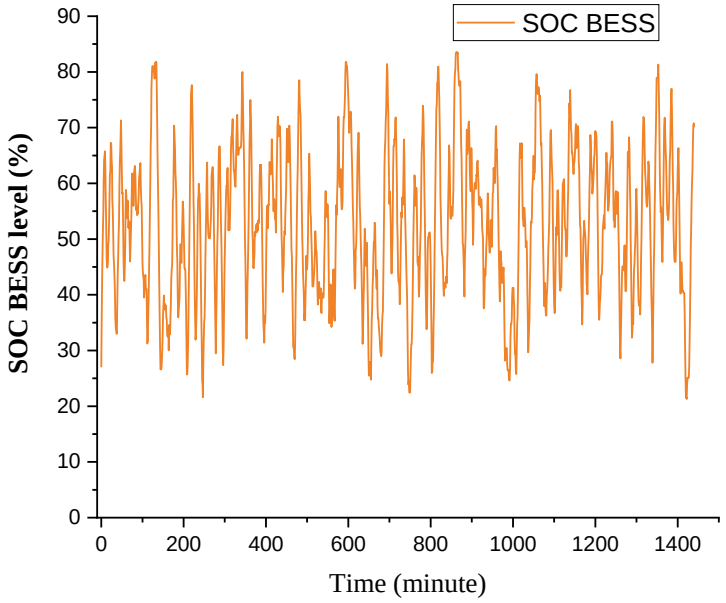

Figure 6. 13: Case 2 – The optimized BESS SOC level over the given time, Wimter season.

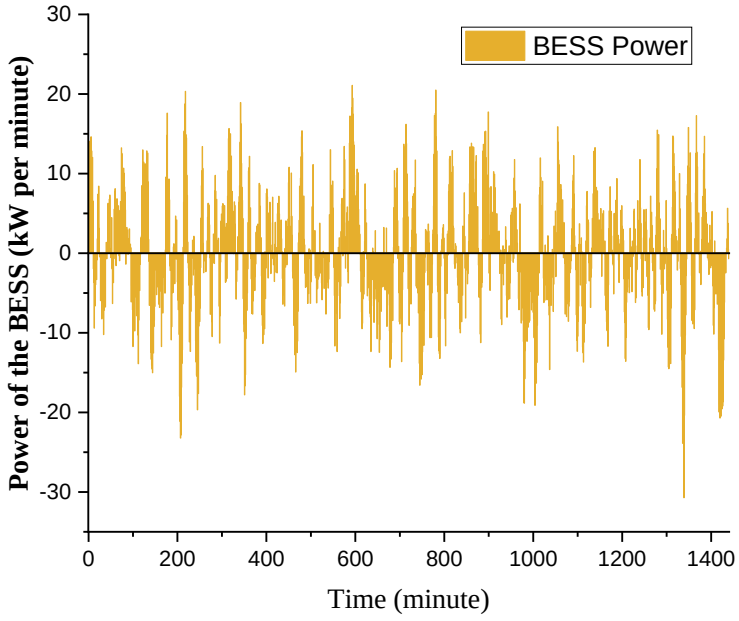

Figure 6. 14: Case 2 - The optimized BESS Power changes over the given time, Winter season.

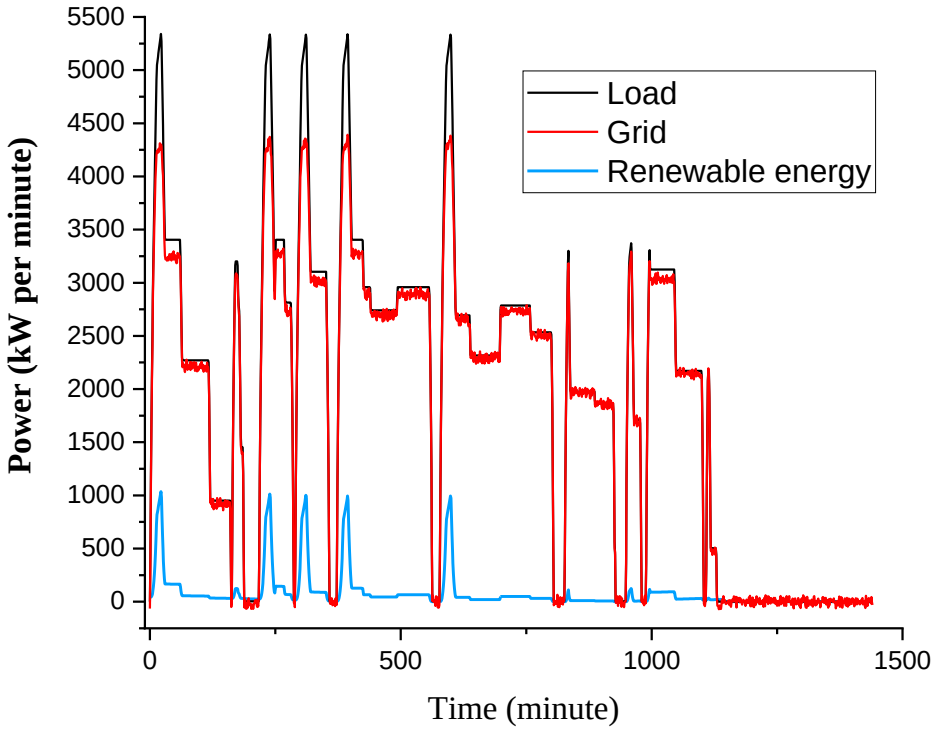

Figure 6. 15: Case 2 - The graph of the grid energy usage, the train's load, and renewable energy usage during the trip Astana-Almaty in Spring season.

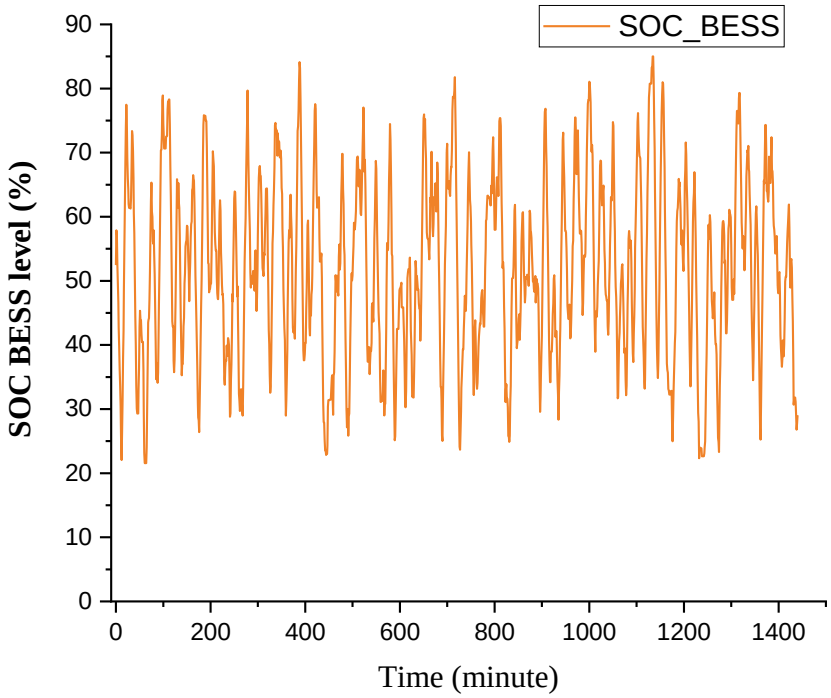

Figure 6. 16: Case 2 – The optimized BES SOC level over the given time, Spring season.

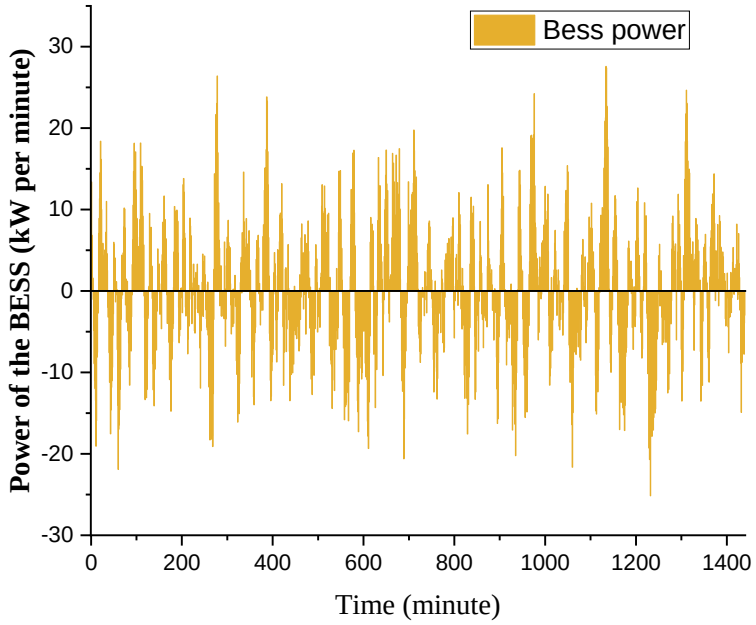

Figure 6. 17: Case 2 - The optimized BESS Power changes over the given time, Spring season.

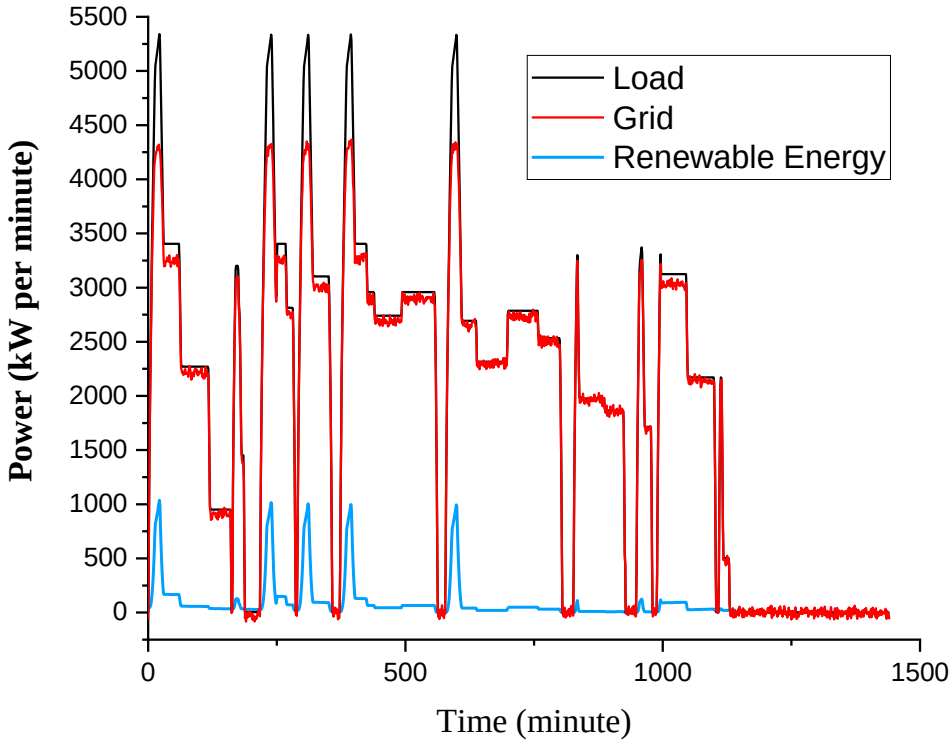

Figure 6. 18: Case 2 - The graph of the grid energy usage, the train's load, and renewable energy usage during the trip Astana-Almaty in Summer season.

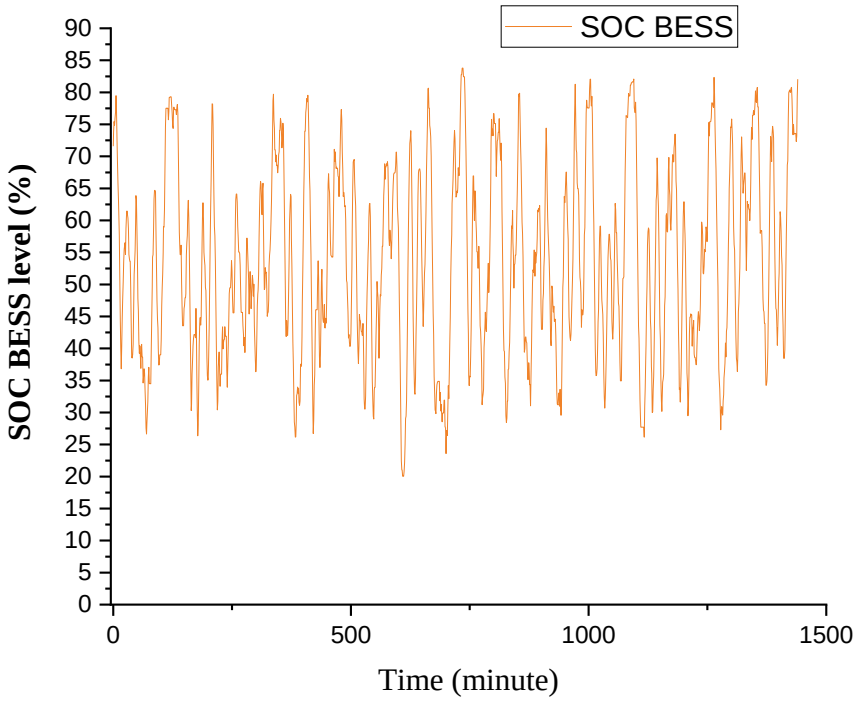

Figure 6. 19: Case 2 - The optimized BESS SOC level over the given time, Summer season.

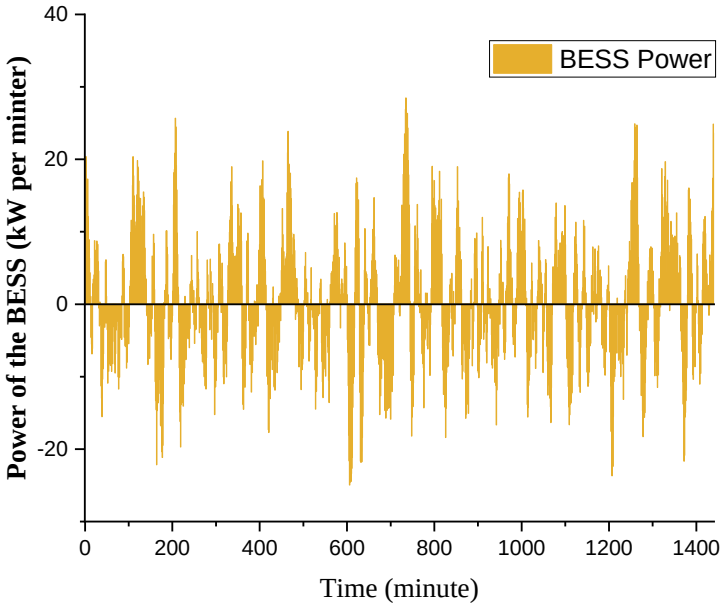

Figure 6. 20: Case 2 - BESS Power changes over the given time, Summer season.

Based on the obtained graphs of the BESS SOC and its power, it can be concluded as follows:

- This graph displays the BESS's SOC changes over the course of the day, with values ranging from roughly 50 % to 90 %. These fluctuations demonstrate that the BESS is actively being charged and discharged.
- The SOC rarely stays at a constant level, suggesting a dynamic system that responds to varying conditions such as changes in load or renewable energy generation. Due to the high train's load, the BESS condition is significantly changing to meet the energy demand of the system, which means its active working principle based on the proposed strategy plan.
- It can be seen that the SOC levels do not go to minimum or maximum (100 %) levels. They often remain within a healthy range, which is beneficial for battery lifetime.
- The existence of both positive and negative values suggests that the BESS is being used to supply energy to the load (when demand exceeds generation) as well as store energy when renewable generation is probably surpassing demand.
- The fluctuating nature of renewable energy sources and the related modifications in BESS activity to balance the system are also reflected in the variability of the BESS power flow.

However, the generation of renewable energy resources are not at the level to meet fully the train's energy demand. This can be seen in Table 6.2, where the total grid energy usage, total renewable energy generation, and total BESS energy storage values are demonstrated for each season. The grid energy usage is significantly high compared to renewable energy generation. However, it is understandable because the integrated solar panels and wind turbines are small scale, and they are located on top of the train. Even though the renewable energy generation is small, the BESS is actively charging or discharging. This means that the designed operational system gives preference to system characteristics, such as maintaining a high SOC to manage abrupt demand spikes or to

have a reserve for times when renewables aren't producing. The implemented code for this case can be found in Appendix D.

Table 6.2: The obtained results for each season from case 2 study

	Summer	**Winter**	**Fall**	**Spring**
Total Grid Energy Usage [kWh]	43077.72	43201.32	43180.37	43101.53
Total Energy Generated by Renewable energy sources [kWh]	2007.39	1873.34	1890.12	1983.75
Total Solar Generation [kWh]	214.95	80.91	97.69	191.32
Total Wind Generation [kWh]	1792.43	1792.43	1792.43	1792.43
Total BESS energy storage [kWh]	-0.441	3.154	5.550	1.823

6.3. Case study 3

Case study 3 examines the application of solar panels over the railway track, BESS, solar panels, and wind turbines located on top of the train’s wagon. The aim of this case is to investigate the effect of solar sleepers on the railway energy network. It is significant to report that this energy generation method over the railway track is currently a new one. This method of generating electricity is not widely demonstrated in the literature, however, they have a high potential for generating huge amounts of energy. Figures 6.21, 6.24, 6.27, and 6.30 illustrate the graph of grid energy usage, train’s load, and renewable energy resources during the trip for summer season. As can be seen, the generated energy from total renewable energy resources is very high, which makes the excess energy return to the grid. The blue line in the graph shows the total generation of hybrid

energy resources. It is important to note that the generated energy from solar sleepers is significantly high, which can be noticed in Chapter 5. The negative illustration of the grid energy means that most of the energy is returning to the grid. This means that the solar sleepers can meet the train's energy demand. However, the performance of the solar sleepers is directly dependent on the climate that characterizes their instability in generating energy. Furthermore, this case 3 also considers BESS, thus the proposed strategic plan has followed to optimize the BESS charging and discharging decision choices. Figures 6.22, 6.25, 6.28, and 6.31 show the optimized BESS SOC levels for fall, winter, spring, and summer seasons, respectively. In addition, Figures 6.23, 6.26, 6.29, and 6.32 illustrate the BESS power indications based on the optimized charging and discharging decisions for each season. Significant variations in the SOC show that the BESS is actively being charged and discharged during the duration of the observation. The SOC appears to be kept above 30%, indicating that the BESS is not being over-discharged. Similarly, it can be seen that the BESS power also has a lot of variability, with the power frequently switching between charging (positive values) and discharging (negative values). This might suggest that the system could be optimized further for stability to reduce the wear and tear on the BESS. The BESS power flow demonstrates that positive and negative numbers are distributed reasonably evenly, suggesting a balance between charging during surplus and discharging during high demand or low generation periods.

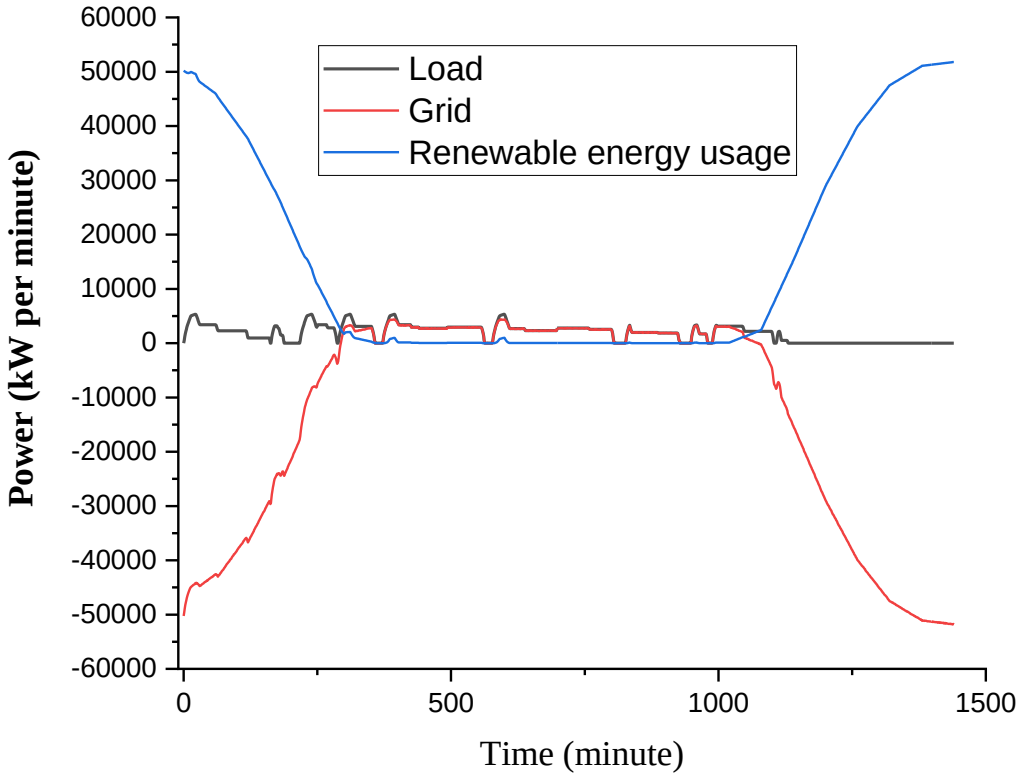

Figure 6. 21: Case 3 - The graph of the grid energy usage, the train's load, and renewable energy usage during the trip Astana-Almaty in Fall season.

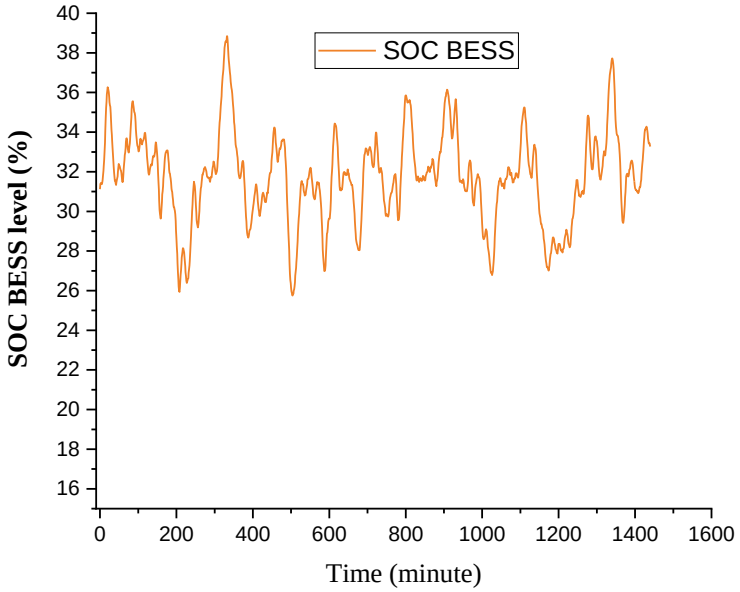

Figure 6. 22: Case 3 – The optimized BESS SOC level over the given time, Fall season.

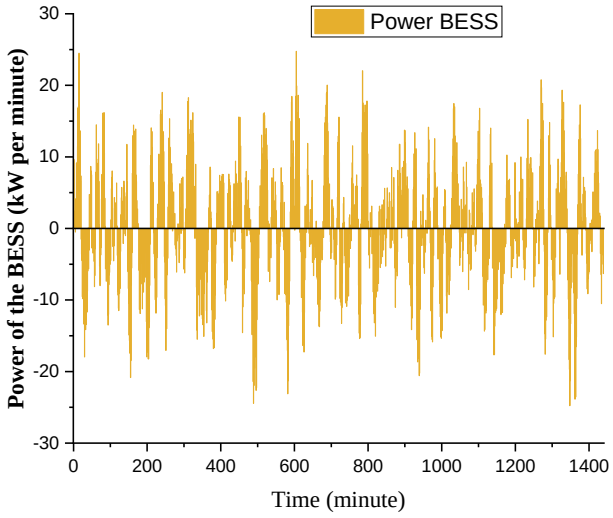

Figure 6. 23: Case 3 - The optimized BESS Power changes over the given time, Fall season.

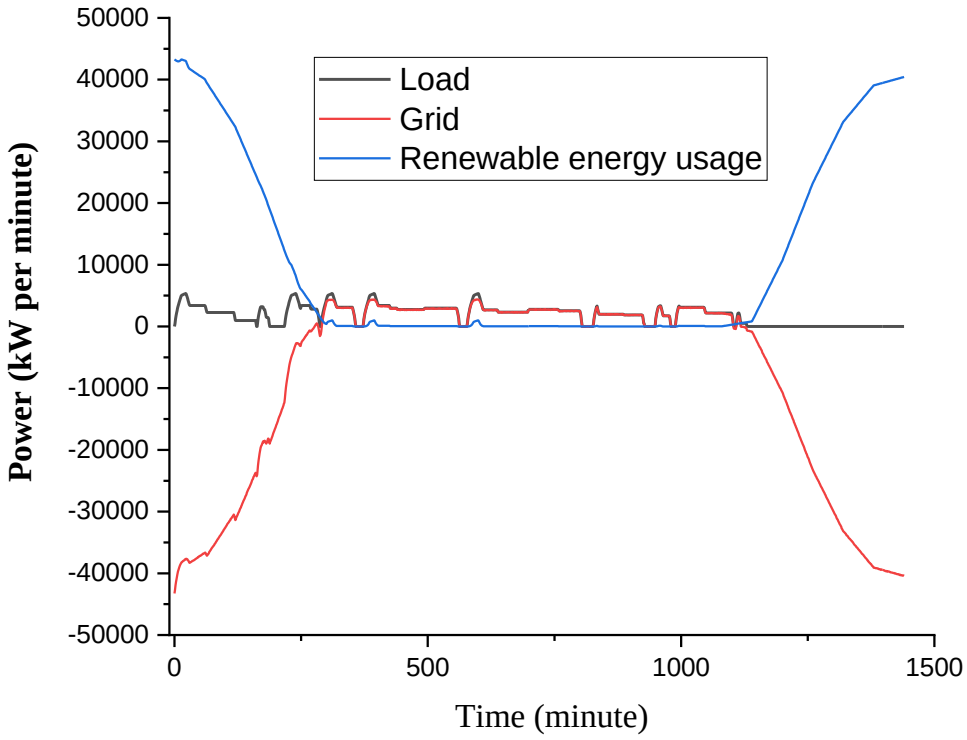

Figure 6. 24: Case 3 - The graph of the grid energy usage, the train's load, and renewable energy usage during the trip Astana-Almaty in Winter season.

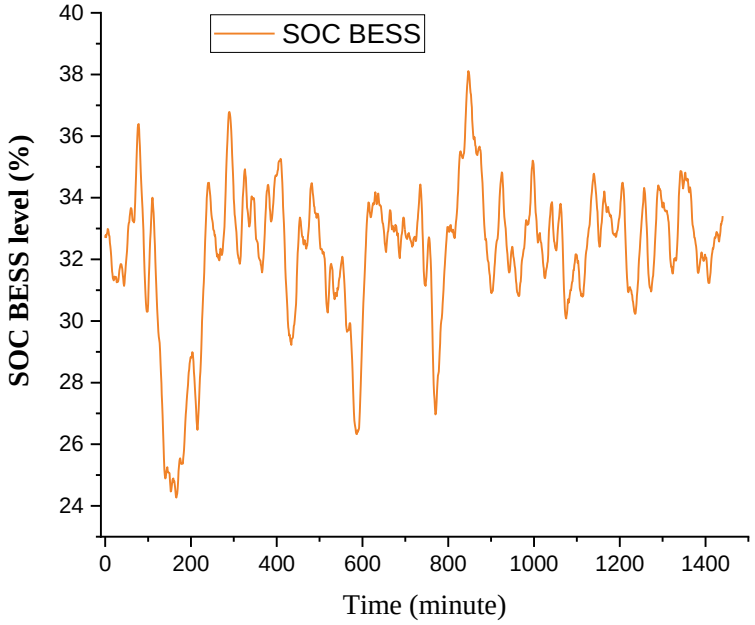

Figure 6. 25: Case 3 – The optimized BESS SOC level over the given time, Winter season.

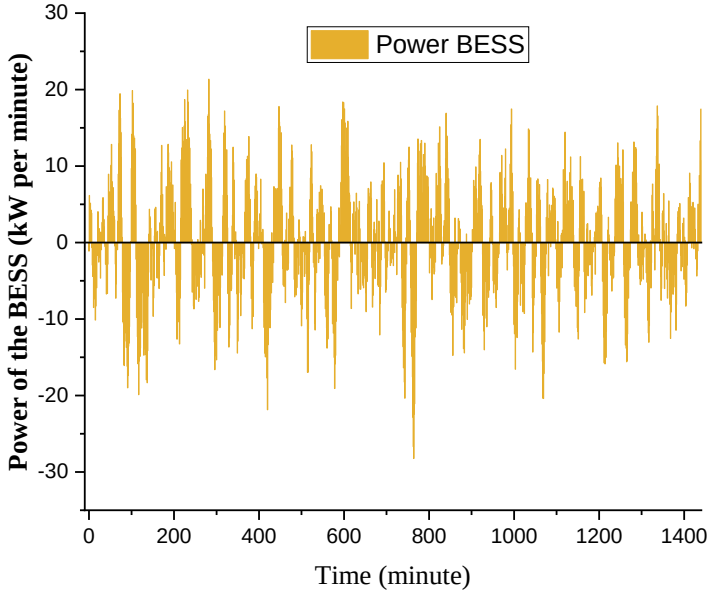

Figure 6. 26: Case 3 - The optimized BESS Power changes over the given time, Winter season.

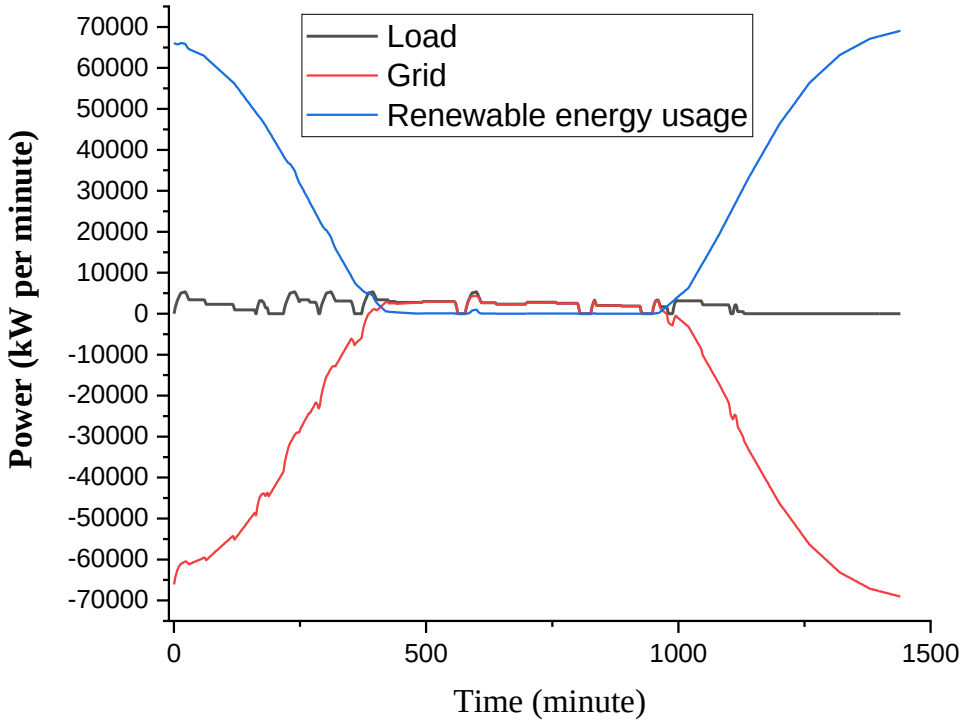

Figure 6. 27: Case 3 - The graph of the grid energy usage, the train's load, and renewable energy usage during the trip Astana-Almaty in Spring season.

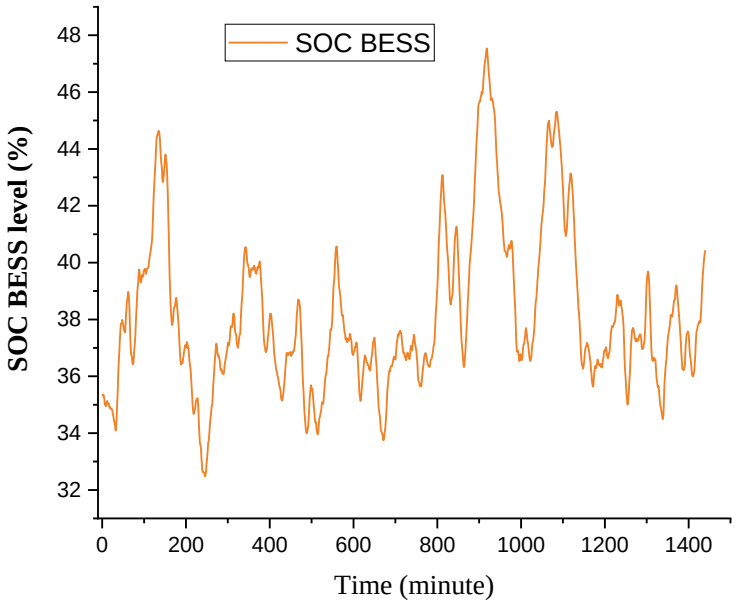

Figure 6. 28: Case 3 – The optimized BESS SOC level over the given time, Spring season.

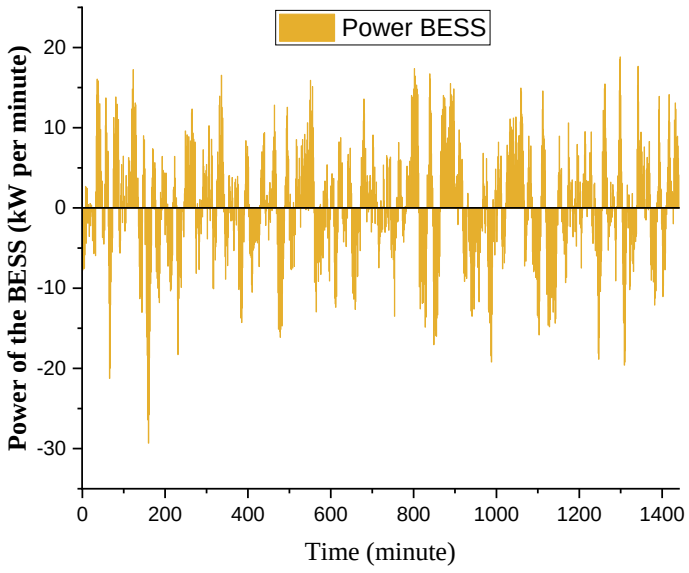

Figure 6. 29: Case 3 - The optimized BESS Power changes over the given time, Spring season.

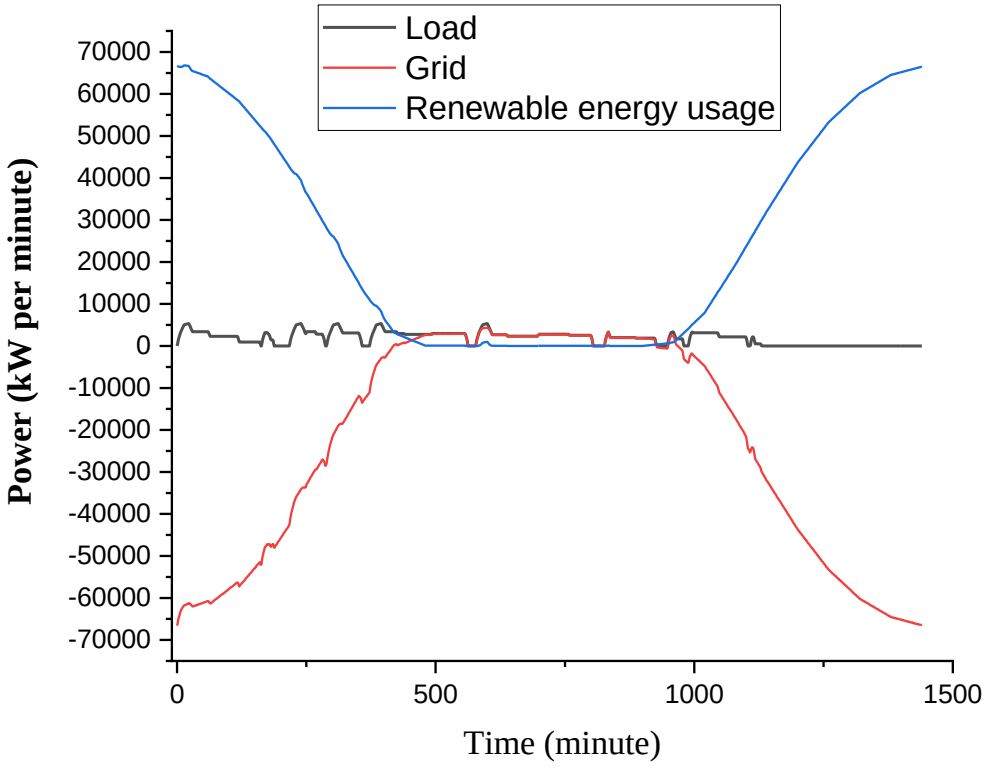

Figure 6. 30: Case 3 - The graph of the grid energy usage, the train's load, and renewable energy usage during the trip Astana-Almaty in Summer season.

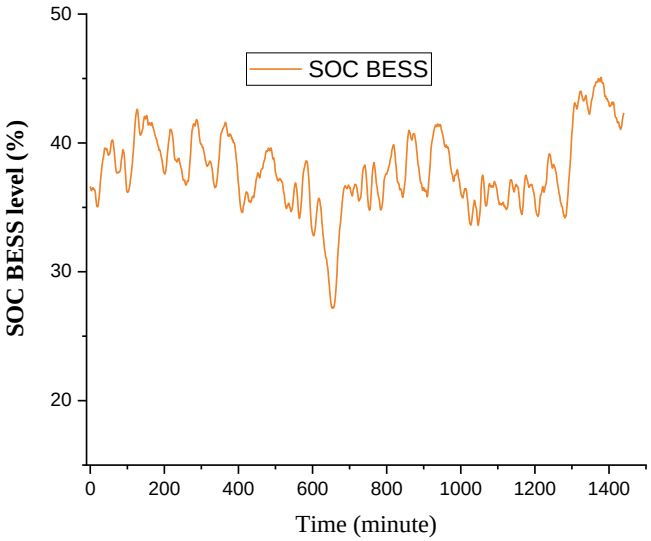

Figure 6. 31: Case 3 – The optimized BESS SOC level over the given time, Summer season.

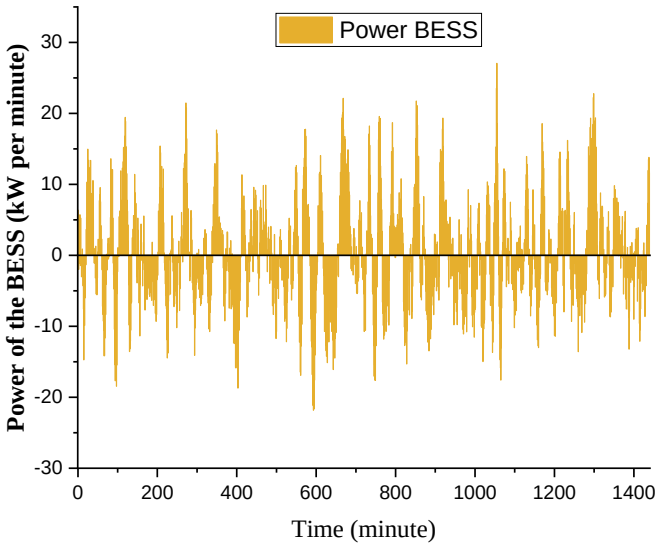

Figure 6. 32: Case 3 - The optimized BESS Power changes over the given time, Summer season.

Table 6.3 illustrates the characteristics of the energy network that includes solar sleepers and designed according to the proposed strategic plan. The solar sleepers provide huge amounts of energy, which allows us to minimize the energy coming from the main grid. However, solar sleepers are not available during the full day. In the absence of solar sleepers, the train's load is mostly dependent on the grid energy. This can be seen from Figures 6.21, 6.24, 6.27, and 6.30, where red line (grid energy) covers black line (train's load). This is related to the period approximately from 6 pm till 7 am. In comparison to other cases, the indication of the energy savings in this study case is significantly higher. For example, in the summer season, the proposed design can save approximately 58.4 % of the grid energy. In general, the summer season is one of the most efficient periods of time, which allows the solar energy systems to reach the highest value. In addition, this case also allows to save grid energy significantly in other seasons. However, it is not fully possible to rely on hybrid energy systems. Each considered energy resources demonstrate a different amount of energy generation due to their application scale. The considered train's load index is also different in comparison to the generated energy from hybrid energy systems. The solar panels and wind turbines are small scale applications, consequently, the capacity of the BESS is also relatively at this size. As can be seen from the obtained results after optimizing the BESS charging and discharging decisions, the BESS is actively working to meet the high energy demand from train's load. In addition, solar sleepers are applied on the railway track from Astana to Almaty, which has a length of 1200 km. Therefore, the energy generation index of each considered element is various. To minimize grid energy usage appropriately, the energy generation index from each resource should be stabilized. The code implemented in case study 3 is given in Appendix E.

Table 6.3: The obtained results for each season from case 3 study

	Summer	**Winter**	**Fall**	**Spring**
Total Grid Energy Usage [kWh]	18728.61	32116.01	29150.11	21163.13
Total Energy Generated by Renewable energy sources [kWh]	603229.12	251460.59	362265.23	588896.42
Total Solar Generation [kWh]	214.95	80.91	97.69	191.32
Total Wind Generation [kWh]	1792.43	1792.43	1792.43	1792.43
Excess Energy [kWh]	576951.80	238562.57	346407.45	565057.20
Energy Savings [%]	58.40	28.66	35.24	52.98
Total BESS energy storage [kWh]	9.364	-0.00048544	4.267	1.396

Chapter 7 - Conclusion

This master's thesis proposed a feasibility study of the integration of hybrid energy harvesting solutions in the rail transportation system. The aim of the study was to explore the integration of hybrid energy systems, especially solar and wind energy resources, to meet the energy requirements of the rail transportation system in Kazakhstan. To be more exact, it considered a small-scale application of solar and wind energy with a battery energy storage system (BESS) on a moving electric train, named the Talgo Tulpar. One of the most well-known routes of this train is between Astana and Almaty cities in Kazakhstan. However, due to small scale generation, these energy resources were insufficient to meet the train's energy demand. Therefore, to support the energy network of the railway, the application of solar panels over the sleepers of the railway track were considered.

The core of this study was the development of a comprehensive mathematical model, combined with detailed MATLAB simulations, to assess the performance and energy generation capabilities of a proposed hybrid energy system. Based on the proposed objective function and the mathematical model of each energy resource, the data collection process and analytical calculations were conducted. To operate properly, the study demonstrated the energy management system, which aims to minimize the energy coming from the grid and maximize the renewable energy usage.

In order to obtain clearer and more accurate results, this study considered three study cases. The first case was taken into consideration solar panels and wind turbines located on top of the train. This case allowed us to analyze the difference of the system when other additional energy resources are applied. In the second case, the BESS was enhanced to meet the train's demand. The strategic plan has been preceded in this case and tried to optimize the charging/discharging

conditions of the BESS. Finally, the third case investigated the application of solar sleepers. The solar sleepers are independent from the movement of the train. They are located along the train's route by connecting two cities. Furthermore, this study was conducted a seasonal analysis of the integration of hybrid energy harvesting solutions by considering these three cases.

The results of this study indicate that there is potential to greatly lessen dependency on the main energy grid through the combination of solar and wind energy sources with a successful energy management system. To be more precise, the modeling findings show that even modest installations of solar panels and wind turbines aboard the train can result in energy savings. An additional layer of efficiency is added with the addition of a BESS. This allows for more efficient energy storage and usage, acting as a buffer against the intermittent nature of renewable energy sources. Furthermore, nowadays the application of solar sleepers is an innovative approach, and this master's thesis investigated the high potential of the solar sleepers.

Chapter 8 - Future works and Recommendation

Based on the obtained results, it can be seen that the solar and wind energy systems cannot fully meet the electric train's energy demand. The generated energy from solar panels and micro-wind turbines can be useful for train's indoor energy demands, such as lightning and air conditioning systems. The considered train is an electric train with 11 passenger wagons, which means the required energy for its movement is very high. Therefore, this thesis considered the application of solar sleepers. Even though the solar sleepers applied along the train's route can generate a huge amount of energy, there are some challenges that need to be considered. Firstly, solar energy is not available for the whole day, and this also relates to the solar panels located on the train's roof. In summer, the solar availability is the longest that allows us to generate the highest amount of electricity. However, it becomes complicated for solar sleepers in winter. This is due to the short days and long nights in winter. Also, solar sleepers require active cleaning processes due to the dust, snow, and dirtiness in winter. There is a possibility that solar sleepers might be unavailable during the harsh weather conditions. Therefore, it is important to investigate an effective solution for these challenges.

Furthermore, future studies should investigate more about optimizing the hybrid energy resources in the rail transportation network, which allows to maximize energy generation. This master's thesis has considered only energy generation and technical aspects. It is important to analyze other sectors of this study, such as environmental and economic aspects. Future works should analyze the scalability of the proposed hybrid energy system by examining different routes and trains. By implementing these suggestions and participating in the planned future projects, the rail transportation industry may make great progress toward achieving sustainability objectives.

References

[1] S. H. I. Jaffery, M. Khan, H. A. Khan, S. Ali, "A study on the feasibility of solar powered railway system for lightweight urban transport", in Proceedings of World Renewable Energy Conference, Denver, 2012, pp. 1-5.

[2] L. Jia, J. Ma, "A Perspective on Solar Energy-powered Road and Rail Transportation in China", *CSEE journal of power and energy systems,* vol. 6, 4, pp. 760-771, 2020.

[3] O. US EPA, "Sources of Greenhouse Gas Emissions," *www.epa.gov,* Dec. 29, 2015. [Online]. Available: https://www.epa.gov/ghgemissions/sources-greenhouse-gas-emissions#:~:text=In%202021%2C%20greenhouse%20gas%20emissions

[4] M. Nazari-Heris, B. Mohammadi-Ivatloo, "Application of Robust Optimization Method to Power System Problems", in *Classical and Recent Aspects of Power System Optimization*, 1st edition, A. F. Zobaa, S. H. E. Abdel Aleem, A. Y. Abdelaziz, Ed. London: Academic Press, 2018, pp. 19-32.

[5] R. Hemmati and H. Saboori, "Emergence of hybrid energy storage systems in renewable energy and transport applications - A review", Renewable and Sustainable Energy Reviews, vol. 65, pp. 11 - 23, 2016.

[6] T.Jamal, S.Salehin, "Hybrid renewable energy sources power systems", in Hybrid Renewable Energy Systems and Microgrids, 1st edition, E. Kabalci, Ed. London: Academic Press, 2021, pp. 179-214.

[7] J. Teng, L. Li, Y. Jiang, R. Shi, "A Review of Clean Energy Exploitation for Railway Transportation Systems and Its Enlightenment to China", *Sustainability*, vol. 14, 17, pp. 1-9, 2022.

[8] E. Fouladi, H. R. Baghaee, M. Bagheri, and G. B. Gharehpetian, "Power management of microgrids including PHEVs based on maximum employment of Renewable Energy Resources," *IEEE Transactions on Industry Applications*, vol. 56, no. 5, pp. 5299–5307, 2020.

[9] E. Fouladi, H. R. Baghaee, M. Bagheri, M. Lu, G. B. Gharehpetian, "BESS Sizing in an Isolated Microgrid Including PHEVs and RERs", in *IEEE international conference on environment and electrical engineering,* Spain, pp. 1 - 5, 2020.

[10] E. Fouladi, H. R. Baghaee, M. Bagheri and G. B. Gharehpetian, "Smart V2G/G2V Charging Strategy for PHEVs in AC Microgrids Based on Maximizing Battery Lifetime and RER/DER Employment," in *IEEE Systems Journal*, vol. 15, no. 4, pp. 4907-4917, Dec. 2021, doi: 10.1109/JSYST.2020.3034045.

[11] E. Fouladi, H. R. Baghaee, M. Bagheri and G. B. Gharehpetian, "A Charging Strategy for PHEVs Based on Maximum Employment of Renewable Energy Resources in Microgrid," *2019 IEEE International Conference on Environment and Electrical Engineering and 2019 IEEE Industrial and Commercial Power Systems Europe (EEEIC / I&CPS Europe)*, Genova, Italy, 2019, pp. 1-5, doi: 10.1109/EEEIC.2019.8783742.

[12] A. García-Olivares, J. Sole, O. Osychenko, “Transportation in a 100% renewable energy system”, *Energy Conversion and Management,* vol. 158, pp. 266-285, 2015.

[13] Automostory. (2021). *First Solar Car* [Online]. Available: https://www.automostory.com/first-solar-car.htm

[14] A. Fayad, H. Ibrahim, A. Ilinca, S. S. Karganroudi, and M. Issa, “Energy Efficiency Improvement of Diesel–Electric Trains Using Solar Energy: A Feasibility Study”, *Applied Sciences,* vol. 12, no. 5869, pp. 1-15, 2022.

[15] C. P. Nazir, “Solar Energy for Traction of High-Speed Rail Transportation: A Techno-economic Analysis”, *Civil Engineering Journal,* vol. 5, pp. 1566-1576, 2019.

[16] V. Kuznetsov, P. Hubskyi, A. Rojek, M. Udzik, and K. Lowczowski, “Progress and Challenges connected with the integration of renewable energy sources with railway distribution networks”, Energies, vol. 17, 489, pp. 1-19, 2024.

[17] J. W. McCurry. (2012, March). R&D crossroads [Online]. Available: https://siteselection.com/issues/2012/mar/belgium.cfm

[18] H. Hayashiya, H. Itagaki, Y. Morita, Y. Mitoma, T. Furukawa, T. Kuraoka, Y. Fukasawa, T. Oikawa, “Potentials, Peculiarities and Prospects of Solar Power Generation on the Railway Premises”, in *International Conference on Renewable Energy Research and Applications (ICRERA)*, Japan, 2012, pp. 1-6.

[19] X. Li, D. Hui, and X. Lai, “Battery Energy Storage Station (BESS)-Based Smoothing Control of Photovoltaic (PV) and Wind Power Generation Fluctuations”, *IEEE Transactions on Sustainable Energy,* vol. 4, no. 2, pp. 464 - 473, 2013.

[20] M. Bakhtvar, A. Al-Hinai, “Robust Operation of Hybrid Solar-Wind Power Plant with Battery Energy Storage System”, *Energies,* vol. 14, no. 3781, pp. 1-18, 2021.

[21] A. K. Bulbul, A. R. Laskar, W. T. Sayeed Chy, M. Sahariat, “Energy Harvesting for Electric Train: Application of Multi-Renewable Energy Sources with Sophisticated Technology”, *European Journal of Advances in Engineering and Technology,* vol. 4, no. 11, pp. 858-865, 2017.

[22] M. K. Johari, M. A. A Jalil, M. F. Mohd Shariff, “Comparison of horizontal axis wind turbine (HAWT) and vertical axis wind turbine (VAWT)”, *International Journal of Engineering and Technology,* vol. 7, pp. 74 - 80, 2018.

[23] B. Sindhuja, “A Proposal for Implementation of Wind Energy Harvesting System in Trains”, in *International Conference on Control, Instrumentation, Energy & Communication*, India, 2014, pp. 696-702.

[24] V. Nurmanova, M. Bagheri, T. Phung, S. K. Panda, “Feasibility study on Wind Energy Harvesting System Implementation in moving trains”, *Electrical Engineering,* vol. 100, pp. 1837-1845, 2018.

[25] V. Nurmanova, M. Bagheri, A. Sultanbek, A. Hekmati and H. Bevrani, "Feasibility study on wind energy harvesting system implementation in moving trains," *2017 International Siberian Conference on Control and Communications (SIBCON)*, Astana, Kazakhstan, 2017, pp. 1-6, doi: 10.1109/SIBCON.2017.7998495.

[26] A. H. Fathima, K. Palanisamy, "Optimization in microgrids with hybrid energy systems – A review", *Renewable and Sustainable Energy Reviews,* vol. 45, pp. 431-446, 2015.

[27] K. C. Divya, J.Ostergaard, "Battery energy storage technology for power systems—An overview", *Electric Power Systems Research,* vol. 79, no. 4, pp. 511- 520, 2009.

[28] X. Li, D. Hui, and X. Lai, "Battery Energy Storage Station (BESS)-Based Smoothing Control of Photovoltaic (PV) and Wind Power Generation Fluctuations", *IEEE Transactions on Sustainable Energy,* vol. 4, no. 2, pp. 464 - 473, 2013.

[29] M. Bakhtvar, A. Al-Hinai, "Robust Operation of Hybrid Solar-Wind Power Plant with Battery Energy Storage System", *Energies,* vol. 14, no. 3781, pp. 1-18, 2021.

[30] T. Molla, B. Khan, P. Singh, " A comprehensive analysis of smart home energy management system optimization techniques", Journal of Autonomous Intelligence, vol. 1, no. 1, pp. 15-21, 2018.

[31] A. R. Tabrizi, "Energy Management System Optimization for Grid Connected Microgrids in Presence of Energy Storage", presented at the HORA, Ankara, Turkey, June 09-11, 2022, pp.1-7.

[32] M. N. Alam, "Particle Swarm Optimization: Algorithm and its Codes in MATLAB". 2016. doi: 10.13140/RG.2.1.4985.3206.

[33] X. Hu, R. Eberhart, "Solving Constrained Nonlinear Optimization Problems with Particle Swarm Optimization".

[34] A. Maleki, F. Pourfayaz, "Optimal sizing of an autonomous hybrid photovoltaic/wind/battery power system with LPSP technology by using evolutionary algorithms", *Solar Energy,* vol. 115, pp. 471 - 483, 2015.

[35] Data access viewer, NASA prediction of worldwide energy resources, 2023. doi: https://power.larc.nasa.gov/#resources

[36] G. Prasanth and T. Sudheshnan, "A Renewable Energy Approach By Fast Moving Vehicles", *Proceedings of the National Seminar & Exhibition on Non-Destructive Evaluation,* vol. 6, pp. 232 - 236, 2011.

[37] S. Bharathi, G. Balaji, V.A.Saravanan, S. Suresh, "A Method for Generating Electricity by Fast Moving Vehicles: A Renewable Energy Approach", *Applied Mechanics and Materials,* vols 110-116, pp. 2177-2182, 2012.

[38] S. Das, D. Mazumder, N. Mia, S. Rahman, "A Review on Power Generation from Wind Power Created By Fast Moving Train Perspective Bangladesh", in *IEEE International Conference on Technology, Engineering, Management for Societal impact using Marketing, Entrepreneurship and Talent (TEMSMET),* Bengaluru, India, pp. 1-5, 2020.

[39] T. Adefarati, R. C. Bansal, "Reliability, economic and environmental analysis of a microgrid system in the presence of renewable energy resources", *Applied Energy,* vol. 236, pp. 1089 - 1114, 2019.

[40] "MIGA backs modernization of Kazakhstan's railway network". Multilateral Investment Guarantee Agency of the World Bank (MIGA). https://www.miga.org (accessed 19 November, 2023).

[41] JSC "NC Kazakhstan Temir Zholy". “Technical Specifications. Reports”. https://railways.kz/ (accessed 19 November, 2023).

[42] Renfe. “S-130”. https://www.renfe.com/es/en/renfe-group/renfe-group/fleet-of-trains/s-130 (accessed 19 November, 2023).

[43] L. Deng, L. Cai, G. Zhang, S. Tang, “Energy consumption analysis of urban rail fast and slow train modes based on train running curve optimization”, Energy Reports, vol. 11, pp. 412-422, 2024.

[44] X. X. Ming, L. Ke-Ping, and Y. Li-Xing, “Discrete event model-based simulation for train movement on a single-line railway”, *Chinese Physics B,* vol. 23, No. 8, pp. 1 - 7, 2014.

[45] J. Wang, H. A. Rakha, “Electric train energy consumption modeling”, *Applied Energy,* vol. 193, pp. 346 - 355, 2017.

[46] Talgo. “Kazakhstan”. https://www.talgo.com/kz-passenger-cars (accessed 19 November, 2023).

[47] J. A. Lozano, J. Félez, J. de D. Sanz, and J. M. Mera, “Railway Traction in Reliability and Safety in Railway, *InTech*, 2012, ch1, pp. 3-28.

[48] K. Ranabhat, L. Patrikeev, A. Antal’evna, K. Andrianov, V. Lapshinsky, E. Sofronova, “An introduction to solar cell technology,” *Journal of Applied Engineering Science*, vol. 14, no. 4, pp. 481-491, 2016.

[49] A. M. Bagher, M. M. Abadi Vahid, M. Mohsen, “Types of Solar Cells and Application”, *American Journal of Optics and Photonics*, vol. 3, no. 5, pp. 94 -113, 2015.

[50] Canadian Solar, “Maxpower CS6U-315 | 320| 325| 330P”, V5.52P2_NA, Nov. 2016. [Revised Nov. 2023].

[51] L. Ji, F. Ning, J. Ma, L. Jia, “SWOT Analysis for orchestrated development of a solar railway system in China”, *IET Renewable Power Generation,* vol. 14, no. 18, pp. 3628-3635, 2020.

[52] F. de Kemmeter, “Europe and its Russian gauge tracks”, *Mediarail.be – Rail Europe News.* 2022. https://mediarail.wordpress.com/europe-and-its-russian-gauge-tracks/ (accessed 19 November, 2023).

[53] 1520. “Our Track Gauge 1520”. https://1520.ru/about/track/?language=en#:~:text=The%20standard%20Russian%20railway%20gauge,Vladivostok%2C%20Murmansk%2C%20and%20Baku (accessed 19 November, 2023).

[54] R. S. Ortega, J. Pombo, S. Ricci, M. Miranda, “The importance of sleepers spacing in railways”, *Construction and Building Materials*, vol. 300, pp. 1 - 15, 2021.

[55] Amazon. “55W 12V ETFE Black Flexible Solar Panel, PERC Mono Solar Cells, Ultrathin Ultra Lightweight for Campers”. https://www.amazon.com/ (accessed 19 November, 2023).

[56] Makemu Green Energy. “Generatore Eolico SMARTWIND 300W/400W/500W”. https://www.makemu.it/prodotto/generatore-eolico-smartwind/ (accessed 19 November, 2023).

[57] N. Ghaviha, “Energy Optimal Operation of Electric Trains: Development of a Driver Advisory System.” 2016. Accessed: Nov. 19, 2024. [Online]. Available: https://www.diva-portal.org/smash/get/diva2:925586/FULLTEXT02.pdf

[58] U. Schlachter, A. Worschech, T. Diekmann, B. Hanke, K. von Maydell, “Optimal Capacity and Operating Strategy for Providing Frequency Containment Reserve with Batteries and Power-to-Heat”, *Journal of Energy Storage*, vol. 32, 101964, pp. 1 - 12, 2020.

Appendices

Appendix A

The thesis considers the application of renewable energy resources on a moving electric train from Astana to Almaty, which takes approximately 19 hours to reach the destination. In order to obtain the power outputs of the renewable energy resources, it is required to identify the location of the train. Table A.1 provides the latitude and longitude coordinates of the train at each hour.

Table A.1. The data of the train's location according to hours

Time, hours	Actual time	Location of the train	Latitude of the location in degree	Longitude of the location in degree
0	12:00 PM	Astana	51.11271	71.53210
1	1:00 PM	Oskarovka	50.5333858161779	72.65025502509447
2	2:00 PM	Temirtau	50.07918283465947	72.92090285199694
3	3:00 PM	Karagandy pass	49.79334	73.09503
4	4:00 PM	Uzhnyi	49.36118742496513	72.90986511166221
5	5:00 PM	Uspenski	48.665566376316896	72.71103384245644
6	6:00 PM	Akadyr	48.26332777932332	72.85918129912986
7	7:00 PM	Akbulak	47.58870628948525	73.28561137436674
8	8:00 PM	Karazhyngyl	46.91493647011182	73.46172522820338
9	9:00 PM	Saryshagan	46.11945	73.60895
10	10:00 PM	Mynaral	45.45561236252802	73.64851267597983
11	11:00 PM	Buraybaltay	44.970626653766075	74.10213926486894
12	12:00 AM	Hantau	44.2678858111061	73.76592190754447
13	1:00 AM	Chu	43.6011701791115	73.75109095544974
14	2:00 AM	Moyunkum	43.59579497361071	74.36171090249954
15	3:00 AM	Anrakhay	43.69527034703366	74.83118084017495
16	4:00 AM	Otar	43.543326827665275	75.19459651965887
17	5:00 AM	Uzynagash	43.22696354739212	76.29627104404047
18	6:00 AM	Almaty-1	43.34109322840262	76.94981332646272
19	7:00 AM	Almaty-2	43.27373941351145	76.93949946052555

Table A.2. The distance between locations of the train

From	To	Distance, km
Astana	Oskarovka	109.83
Oskarovka	Temirtau	58.16
Temirtau	Karagandy pass	30
Karagandy pass	Uzhniy	50
Uzhniy	Uspenski	78.7
Uspenski	Akadyr	47.18
Akadyr	Akbulak	83.14
Akbulak	Karazhyngyl	73.31
Karazhyngyl	Saryshagan	78.36
Saryshagan	Mynaral	78
Mynaral	Buraybaltay	61.48
Buraybaltay	Hantau	80.95
Hantau	Chu	70
Chu	Moyunkum	44.86
Moyunkum	Anrakhay	41
Anrakhay	Otar	33.71
Otar	Uzynagash	96.28
Uzynagash	Almaty-1	54
Almaty-1	Almaty-2	7.4

Appendix B

This Appendix represents the obtained power outputs of the solar sleepers for each location of the trip route during one full day (12 pm till 11:59 am of another day), which is important in estimating the total generation of power from solar sleepers. It contains the power outputs of one randomly chosen day in a season. The period shown in graphs relates to 12:00 pm – 11:59 am (another day).

B.1. Fall season, October

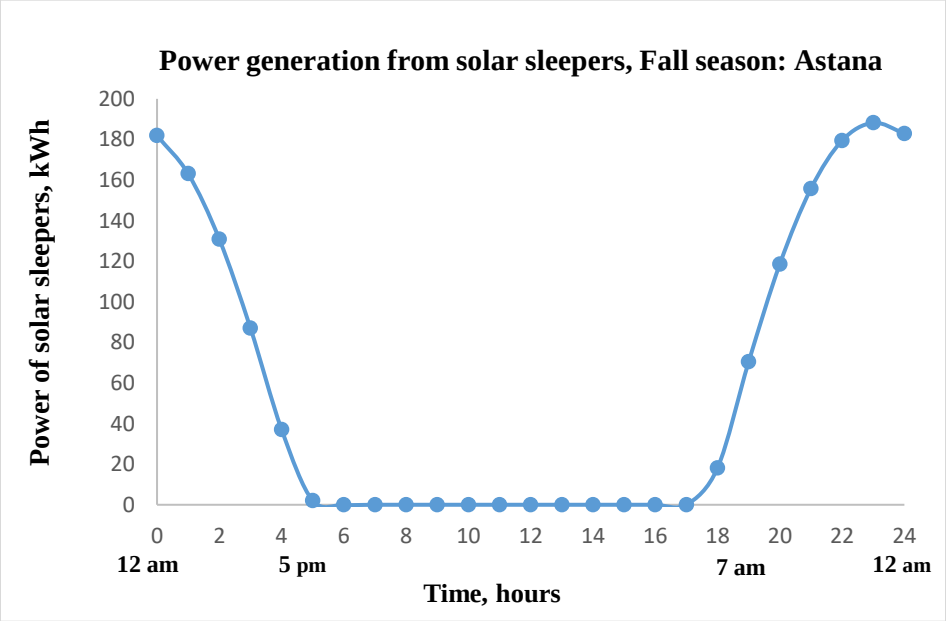

Figure B.1. The power of solar sleepers (kWh), fall season: Astana

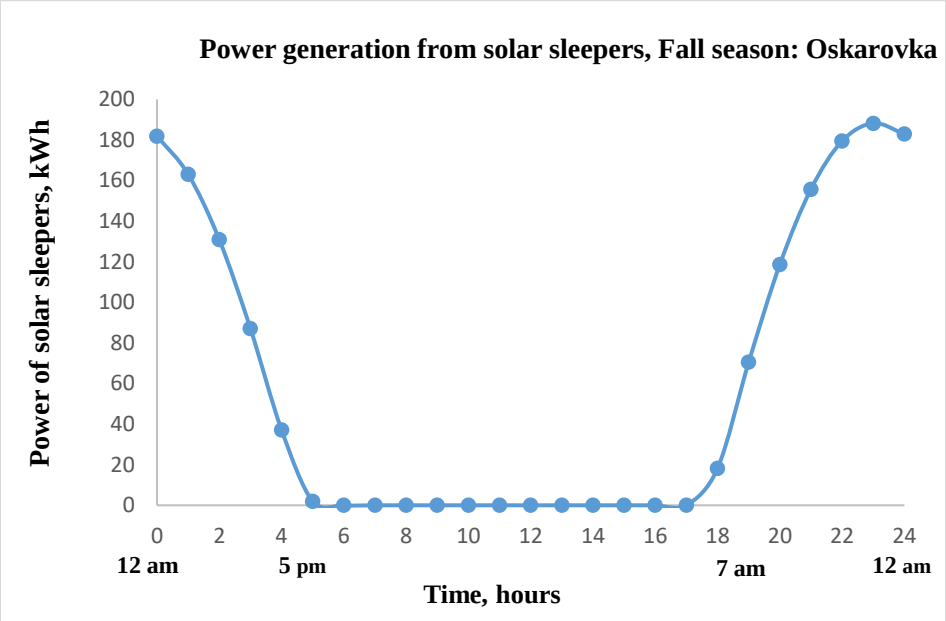

Figure B.2. The power of solar sleepers (kWh), fall season: Oskarovka

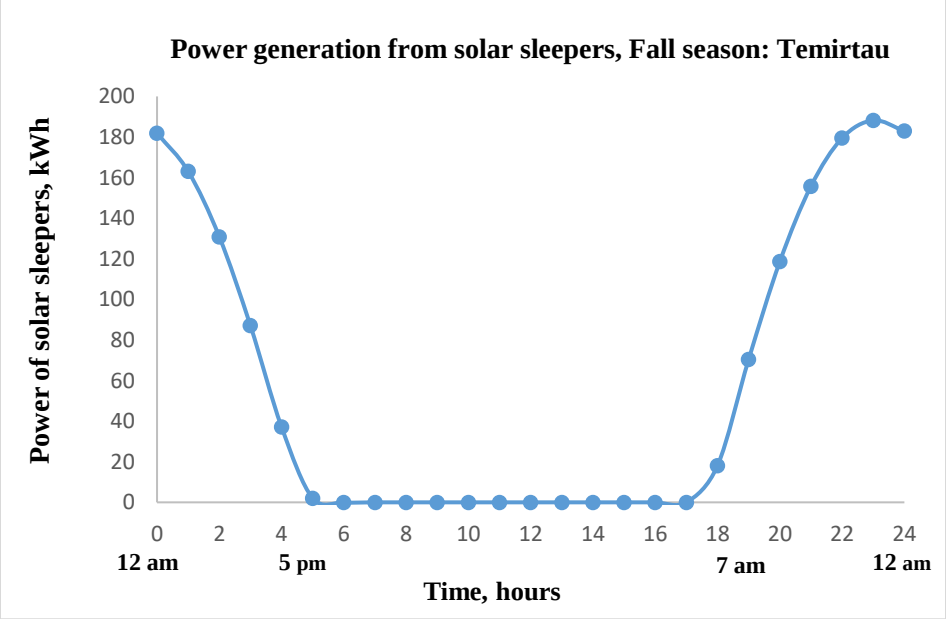

Figure B.3. The power of solar sleepers (kWh), fall season: Temirtau

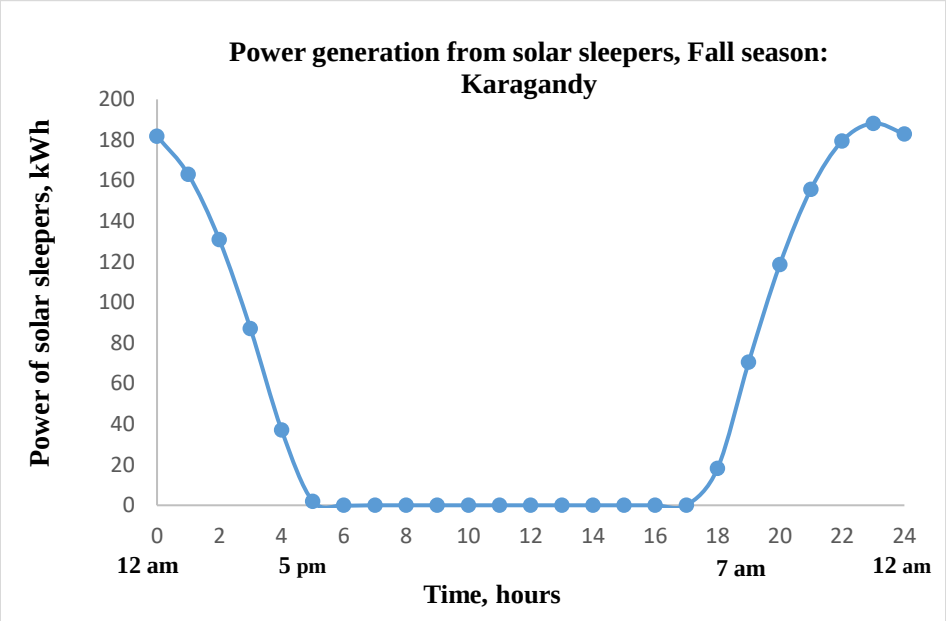

Figure B.4. The power of solar sleepers (kWh), fall season: Karagandy

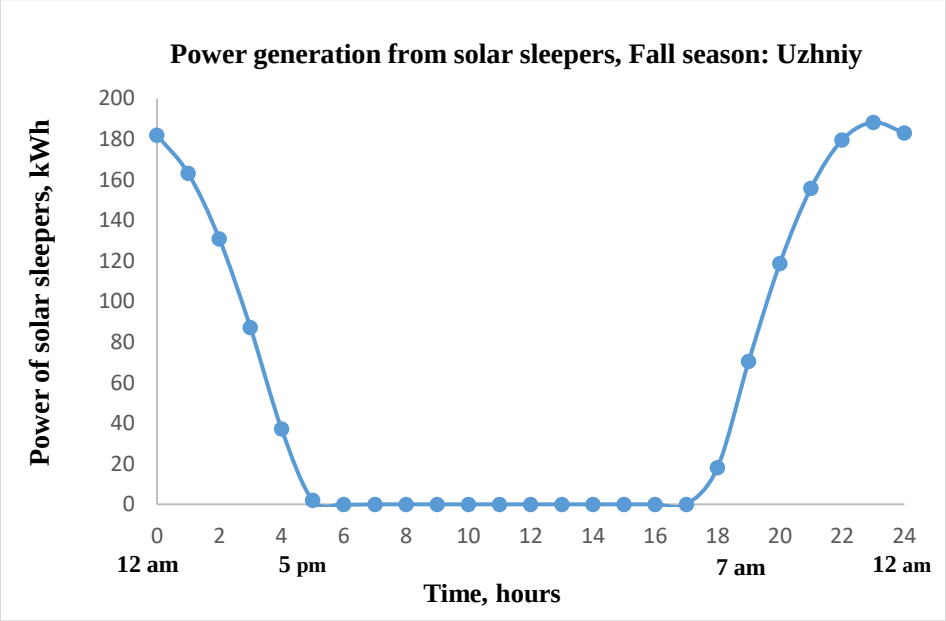

Figure B.5. The power of solar sleepers (kWh), fall season: Uzhniy

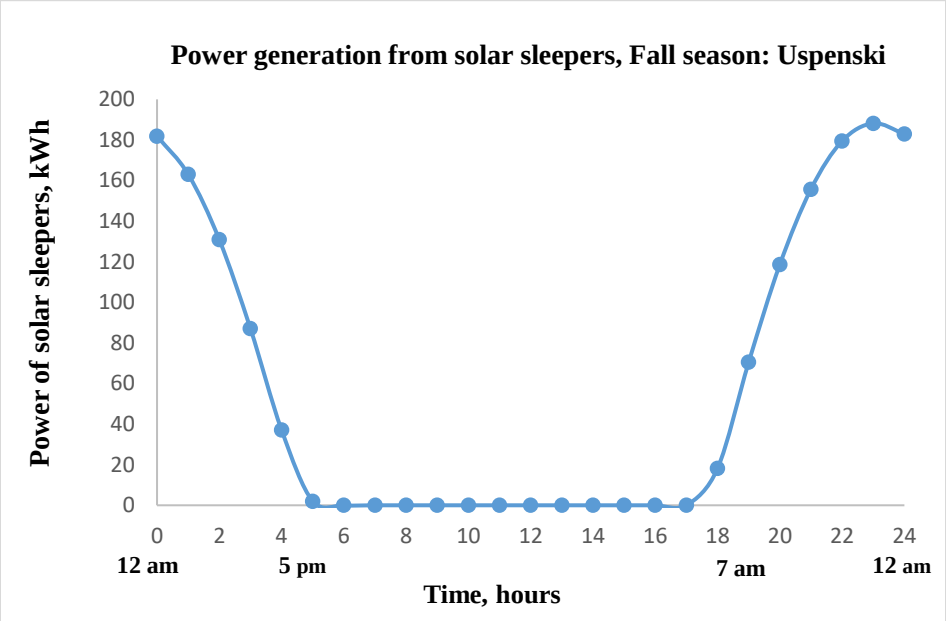

Figure B.6. The power of solar sleepers (kWh), fall season: Uspenski

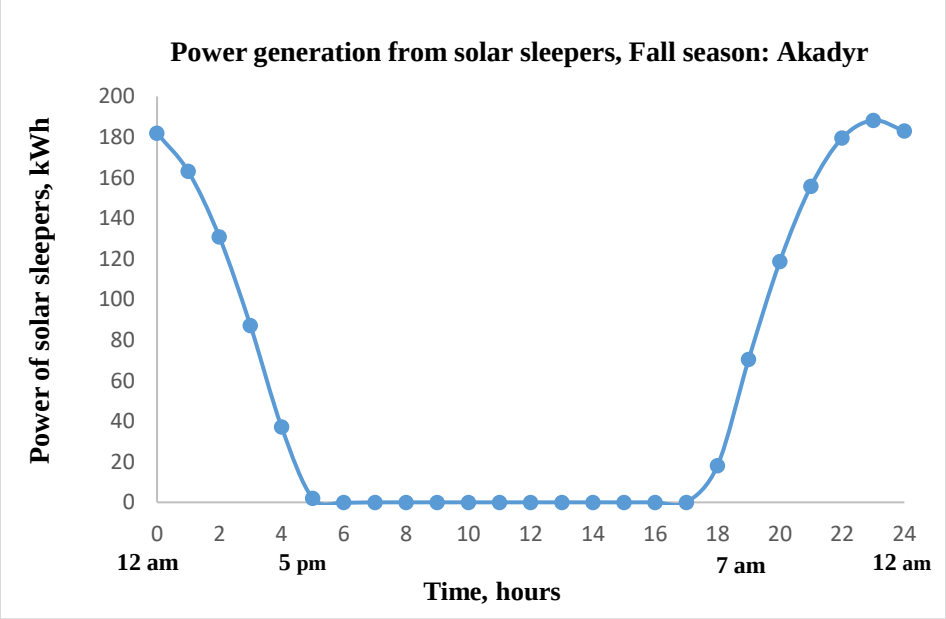

Figure B.7. The power of solar sleepers (kWh), fall season: Akadyr

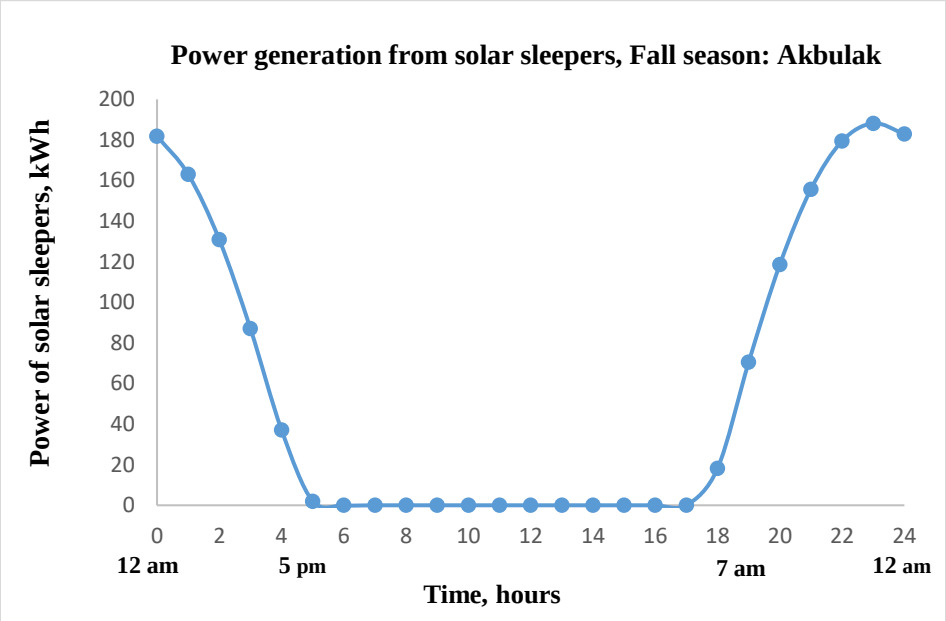

Figure B.8. The power of solar sleepers (kWh), fall season: Akbulak

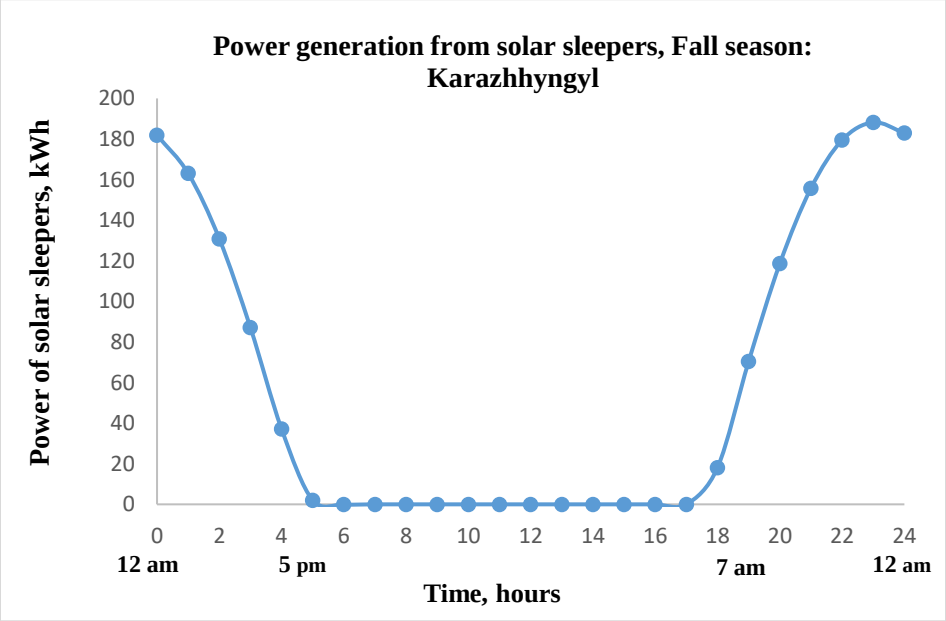

Figure B.9. The power of solar sleepers (kWh), fall season: Karazhyngyl

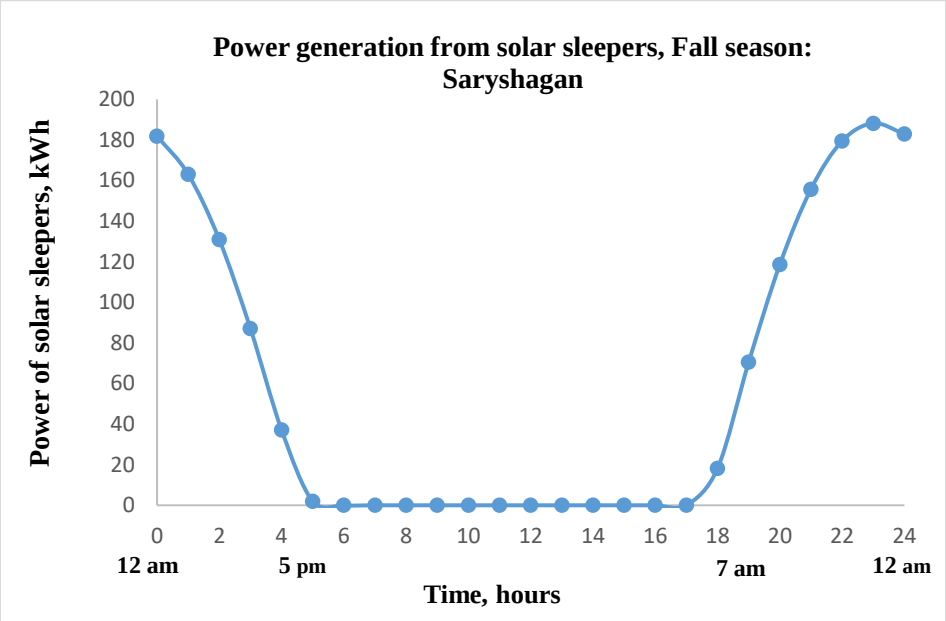

Figure B.10. The power of solar sleepers (kWh), fall season: Saryshagan

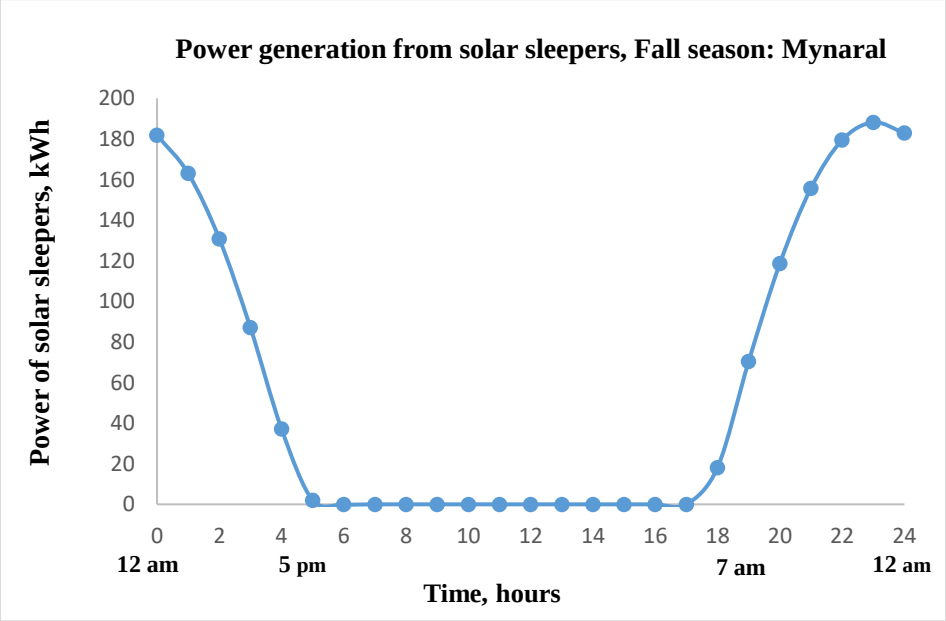

Figure B.11. The power of solar sleepers (kWh), fall season: Mynaral

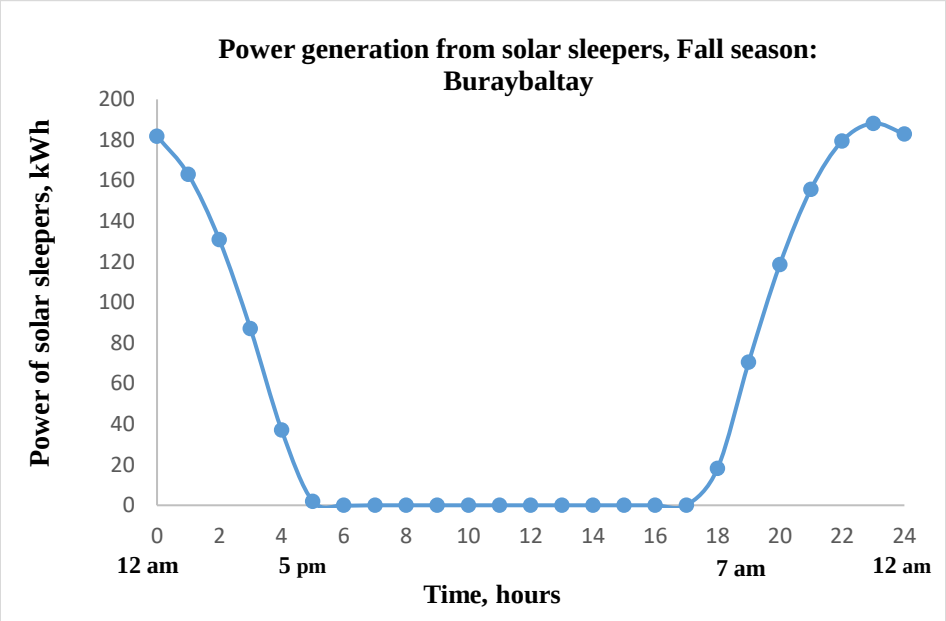

Figure B.12. The power of solar sleepers (kWh), fall season: Buraybaltay

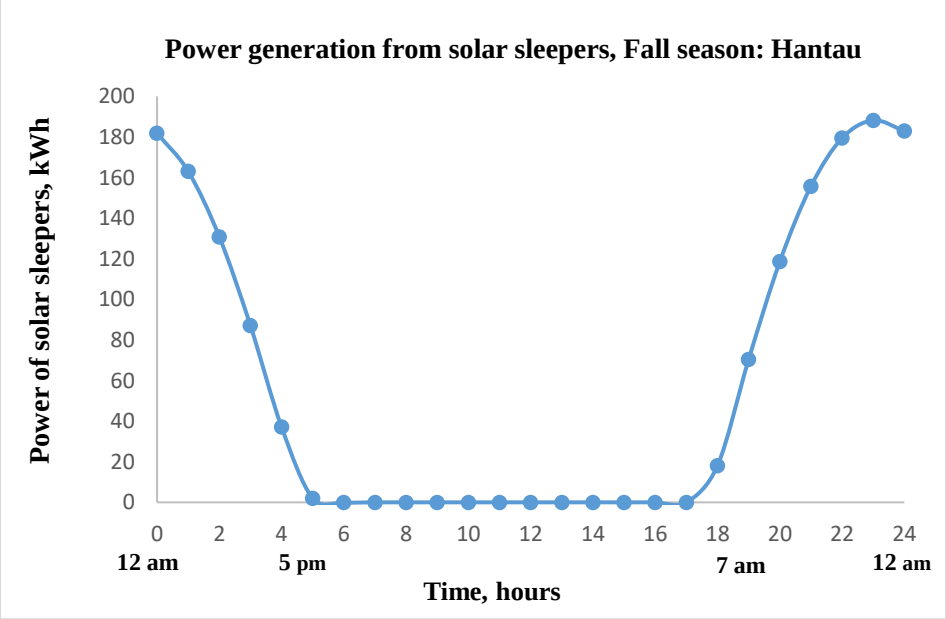

Figure B.13. The power of solar sleepers (kWh), fall season: Hantau

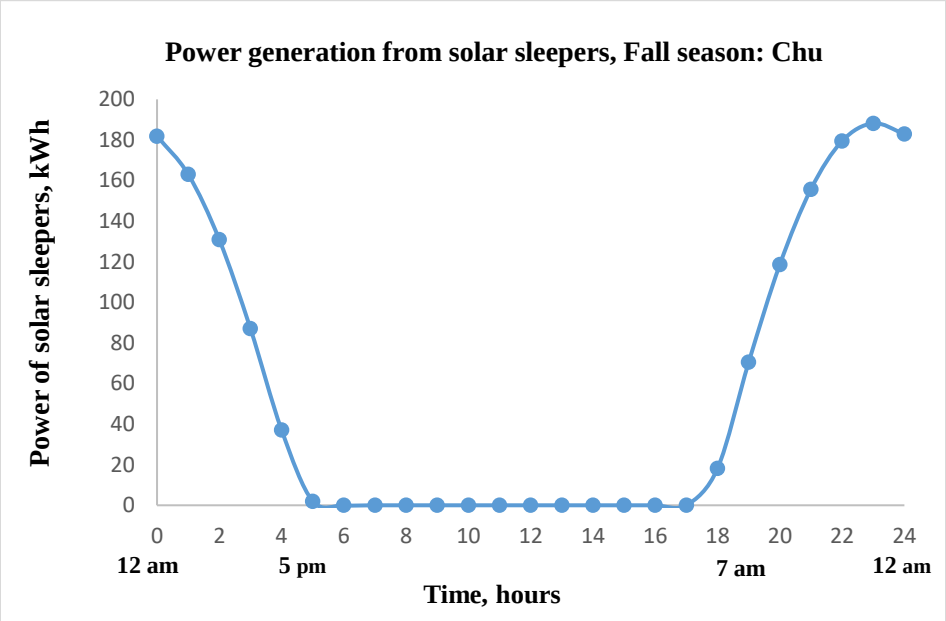

Figure B.14. The power of solar sleepers (kWh), fall season: Chu

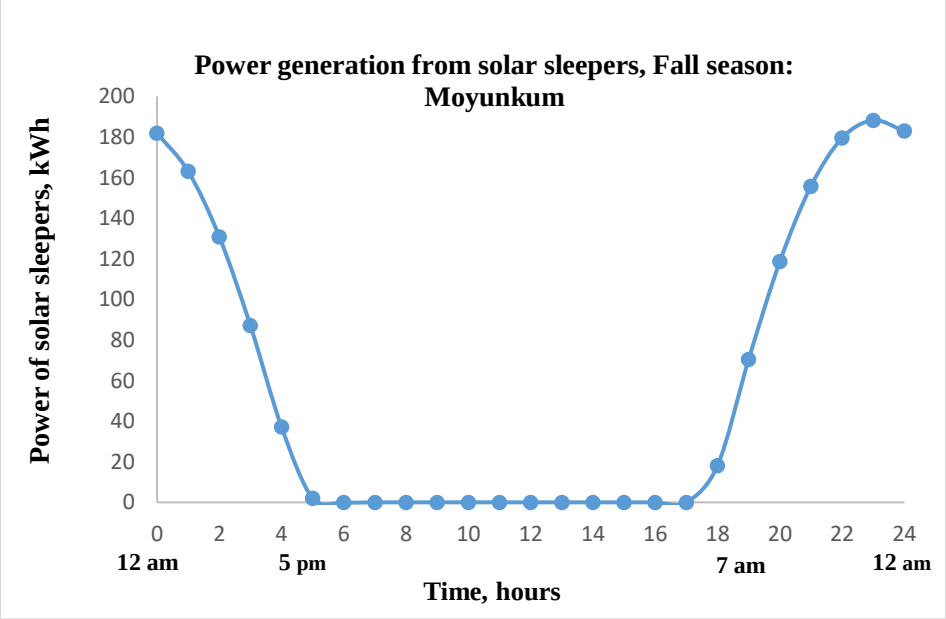

Figure B.15. The power of solar sleepers (kWh), fall season: Moyunkum

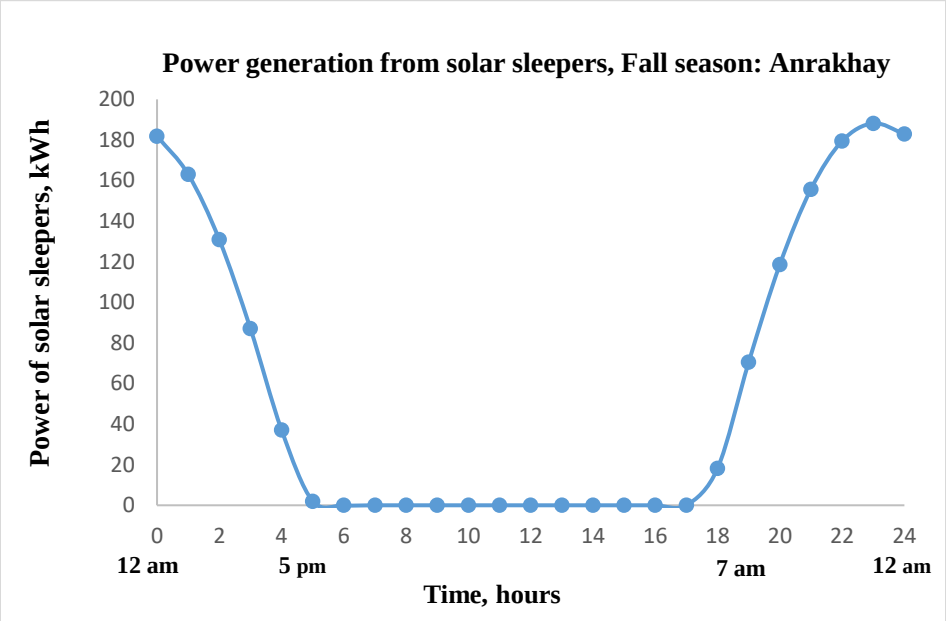

Figure B.16. The power of solar sleepers (kWh), fall season: Anrakhay

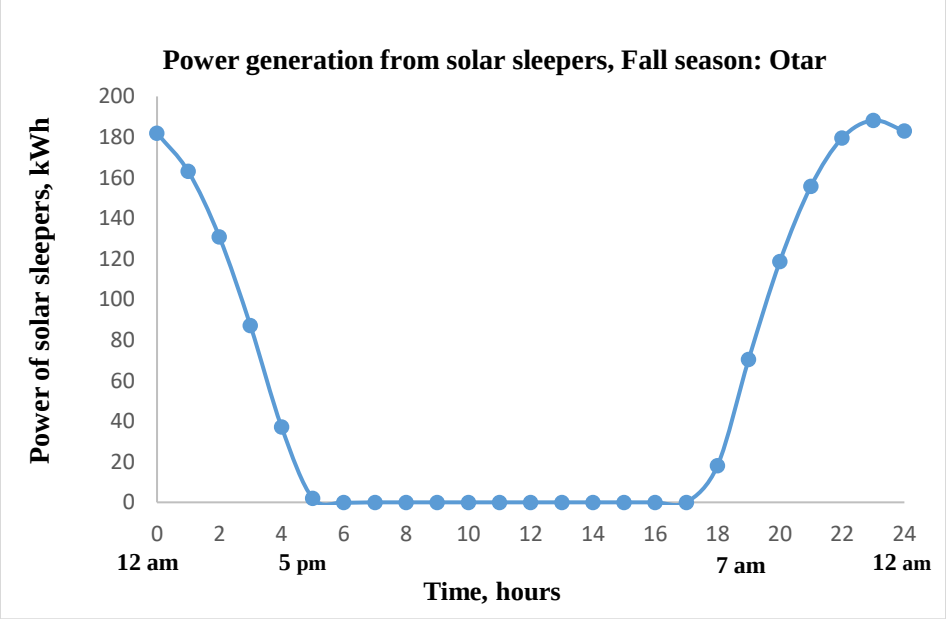

Figure B.17. The power of solar sleepers (kWh), fall season: Otar

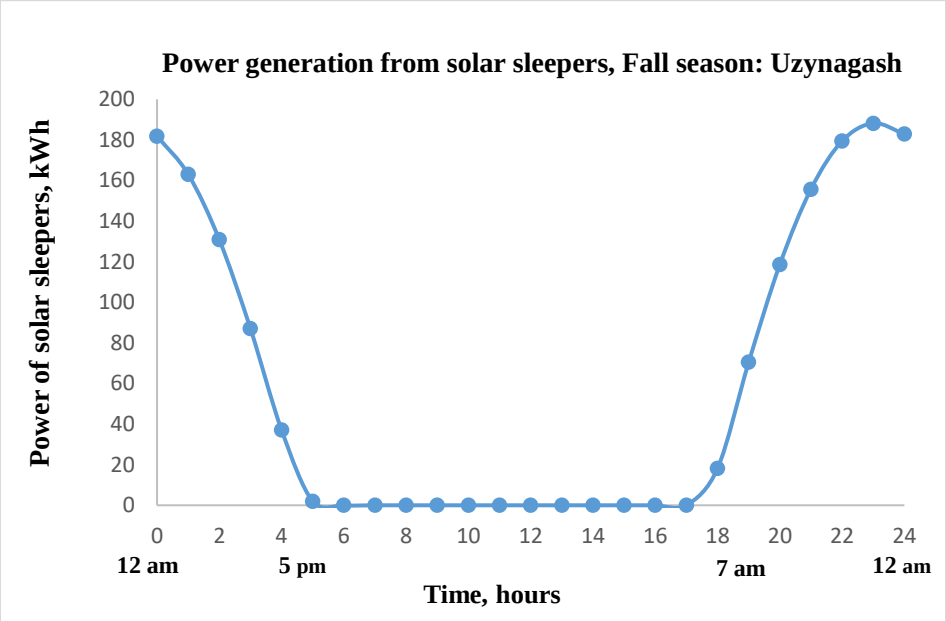

Figure B.18. The power of solar sleepers (kWh), fall season: Uzynagash

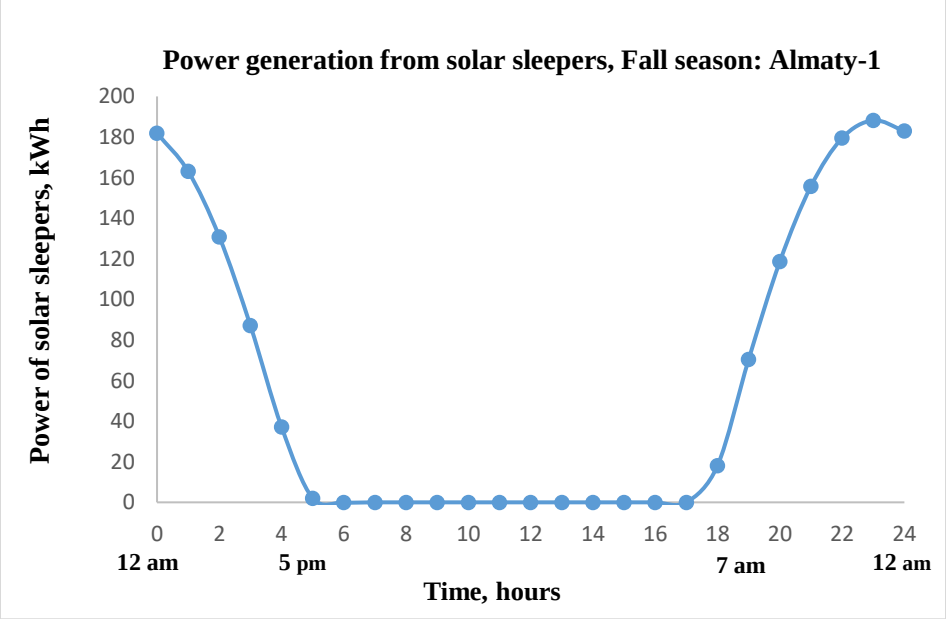

Figure B.19. The power of solar sleepers (kWh), fall season: Almaty-1

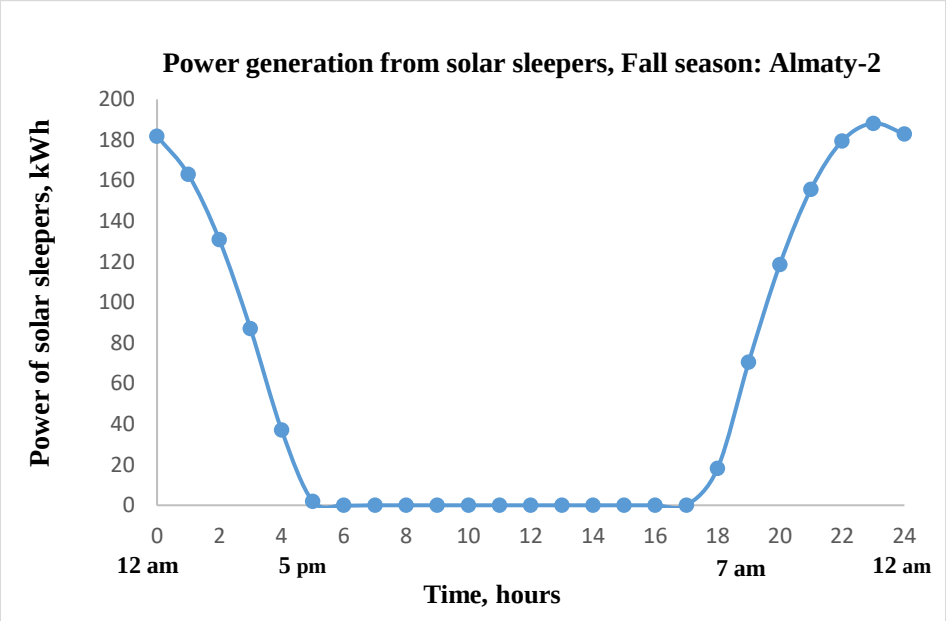

Figure B.20. The power of solar sleepers (kWh), fall season: Almaty-2

B.2. Winter season, February

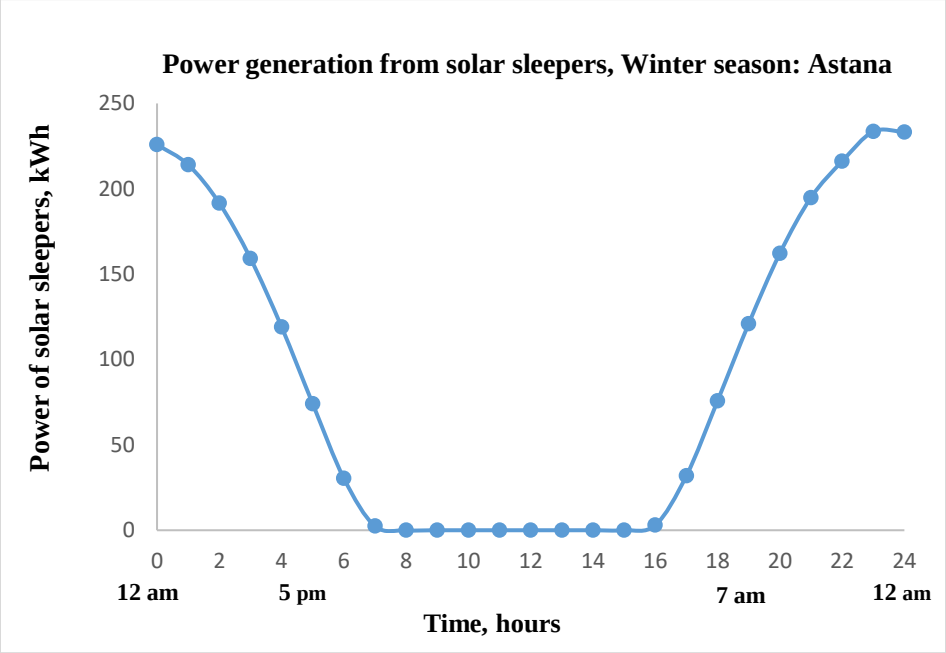

Figure B.21. The power of solar sleepers (kWh), winter season: Astana

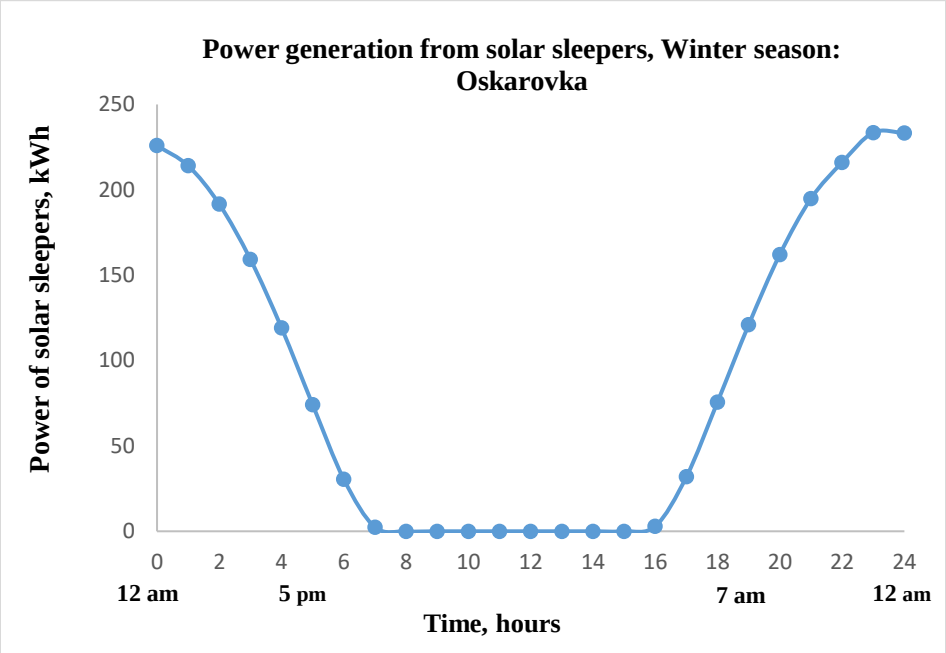

Figure B.22. The power of solar sleepers (kWh), winter season: Oskarovka

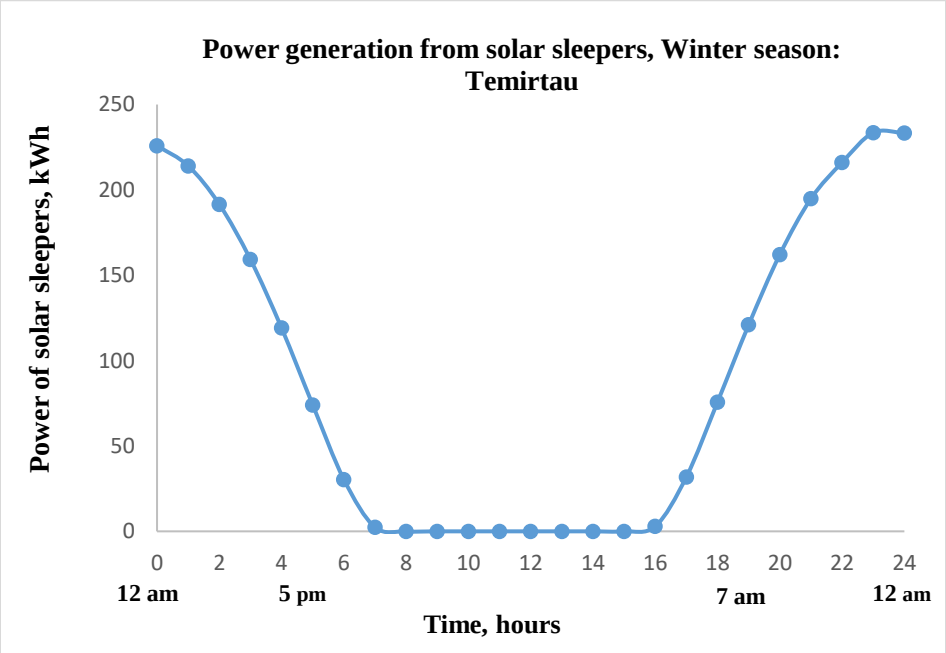

Figure B.23. The power of solar sleepers (kWh), winter season: Temirtau

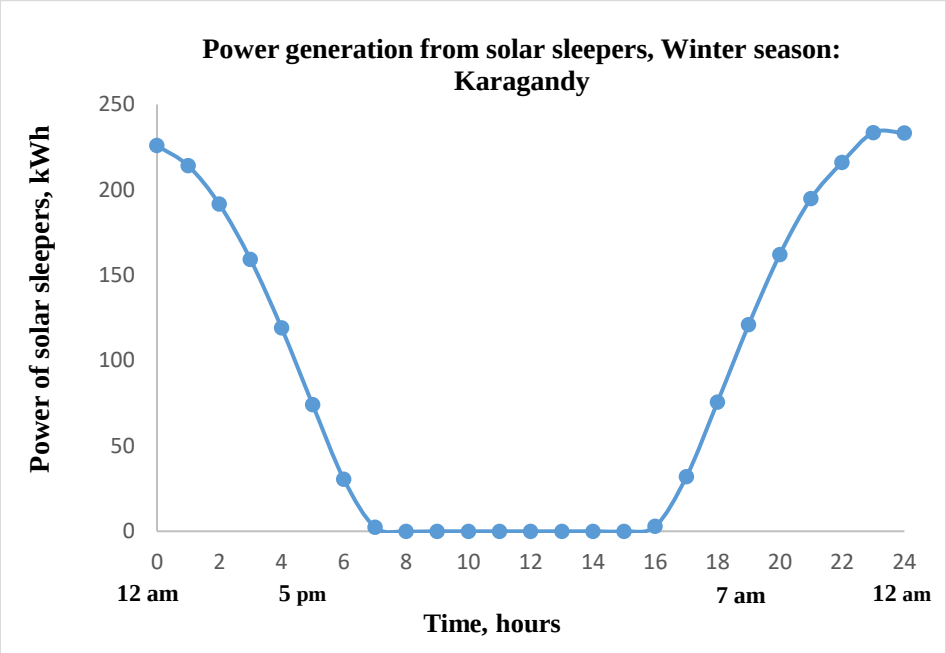

Figure B.24. The power of solar sleepers (kWh), winter season: Karagandy

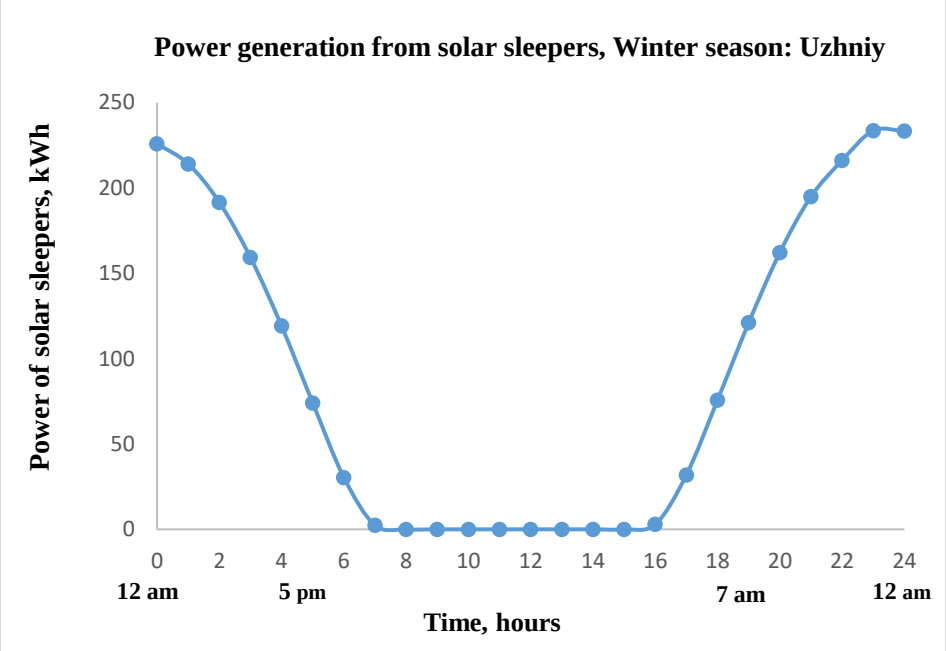

Figure B.25. The power of solar sleepers (kWh), winter season: Uzhniy

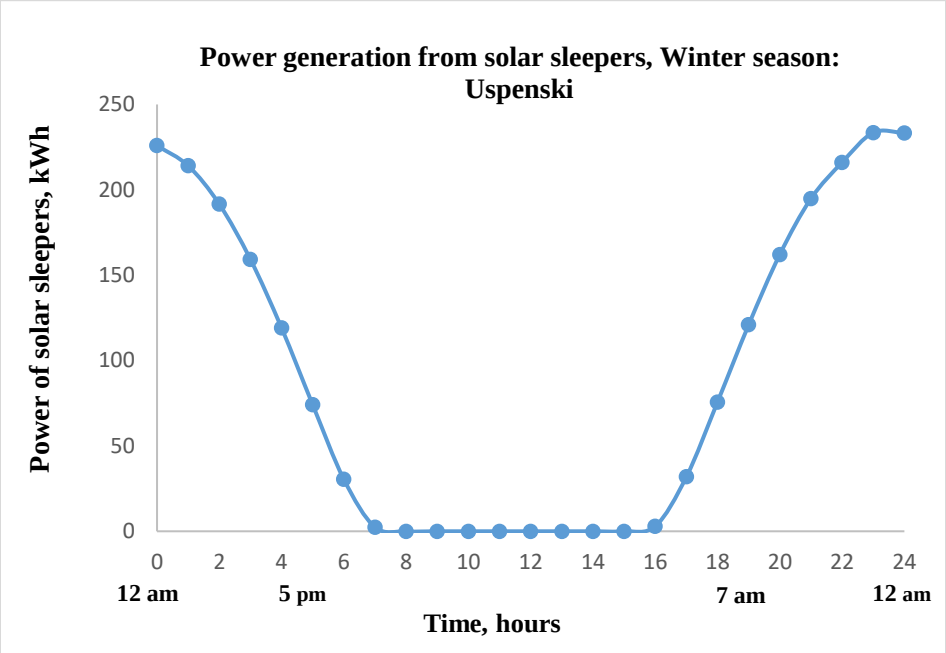

Figure B.26. The power of solar sleepers (kWh), winter season: Uspenski

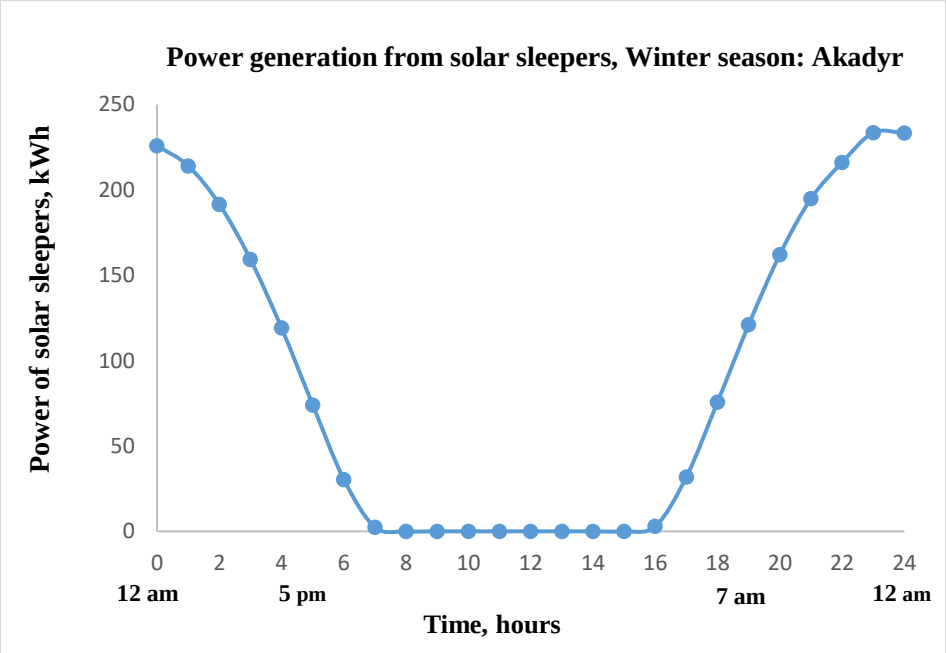

Figure B.27. The power of solar sleepers (kWh), winter season: Akadyr

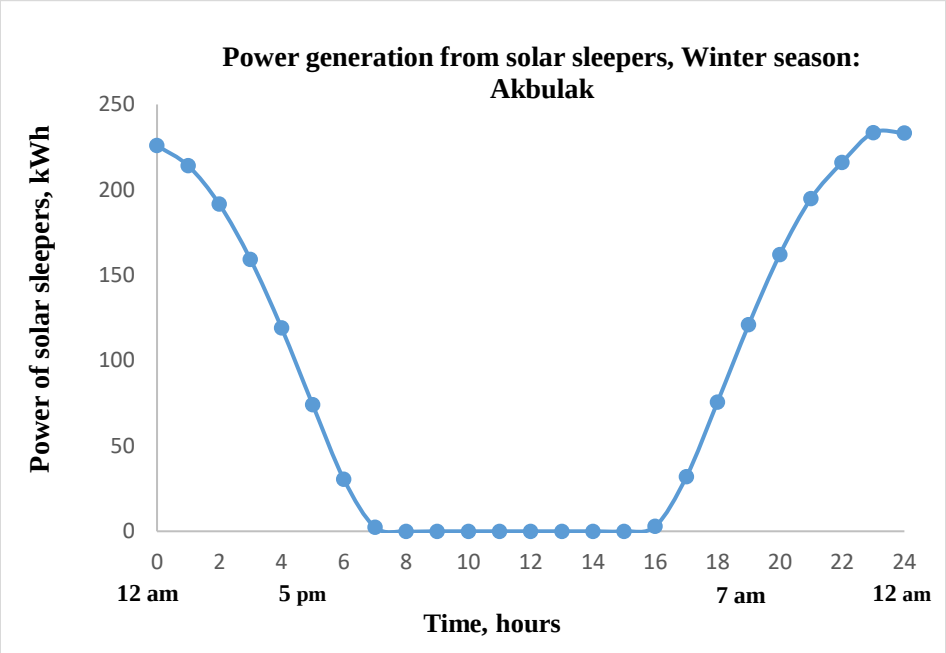

Figure B.28. The power of solar sleepers (kWh), winter season: Akbulak

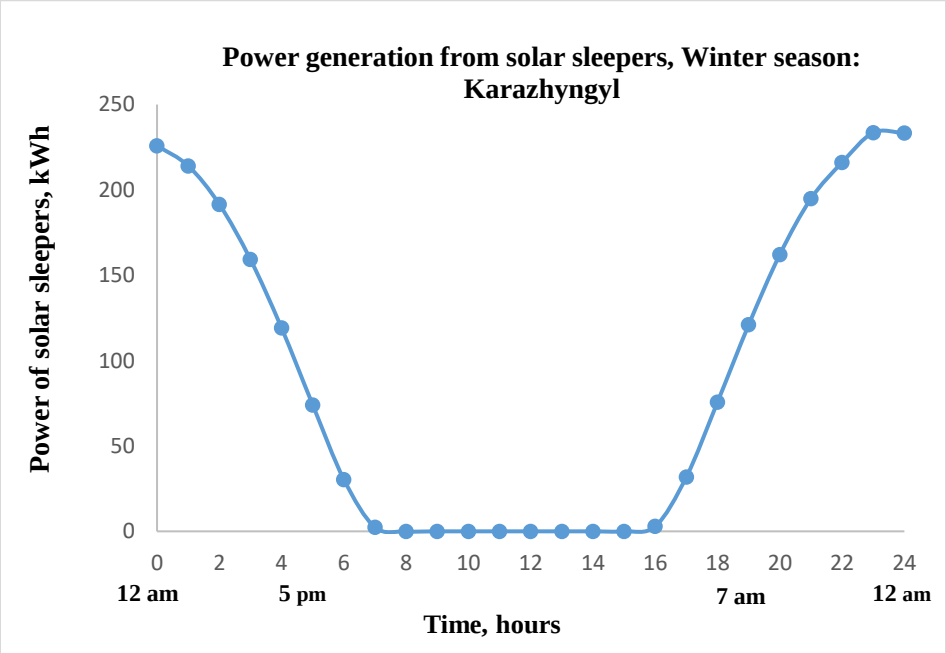

Figure B.29. The power of solar sleepers (kWh), winter season: Karazhyngyl

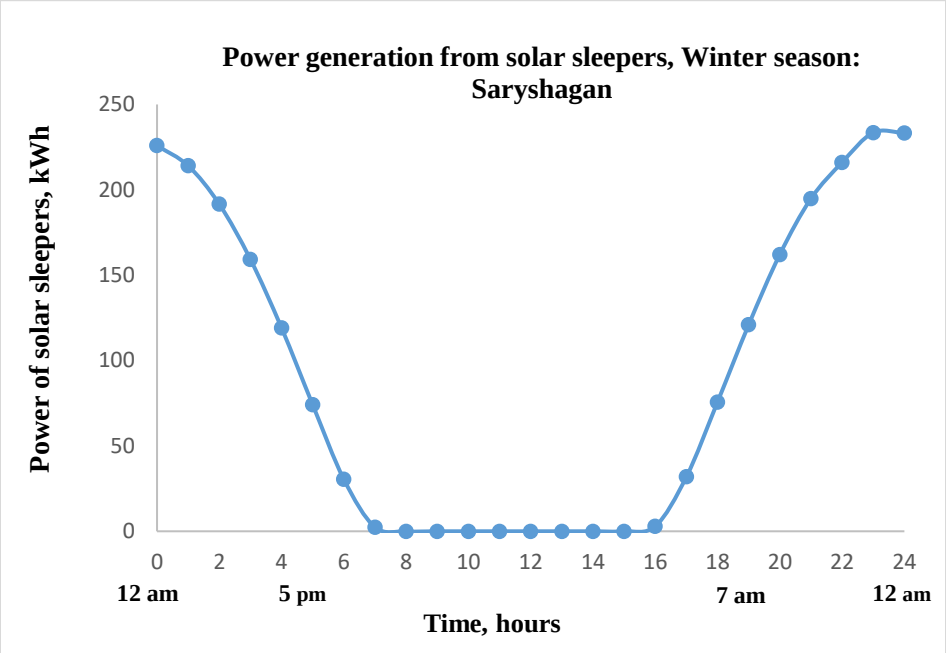

Figure B.30. The power of solar sleepers (kWh), winter season: Saryshagan

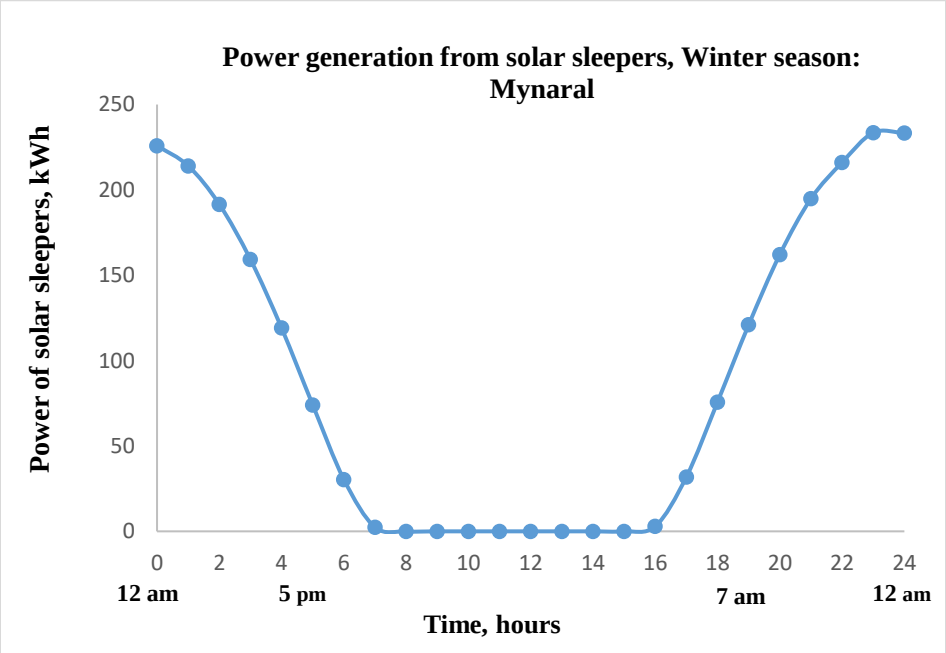

Figure B.31. The power of solar sleepers (kWh), winter season: Mynaral

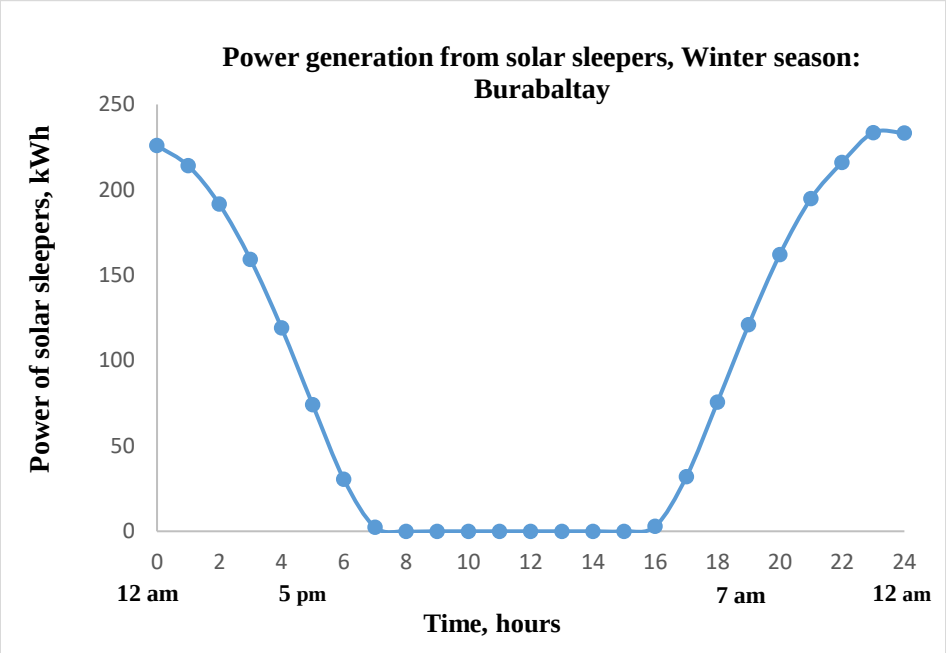

Figure B.32. The power of solar sleepers (kWh), winter season: Buraybaltay

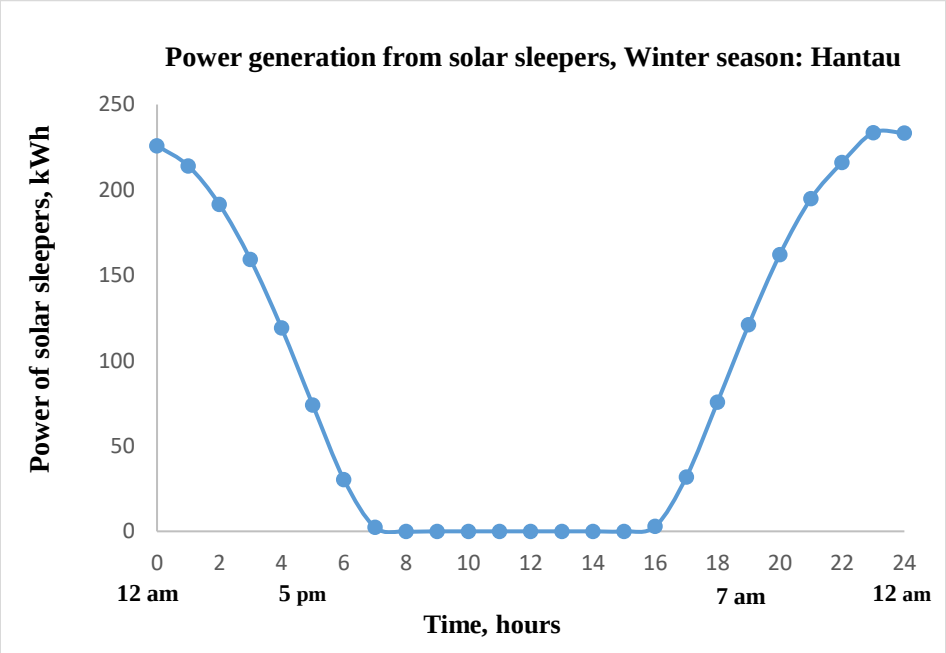

Figure B.33. The power of solar sleepers (kWh), winter season: Hantau

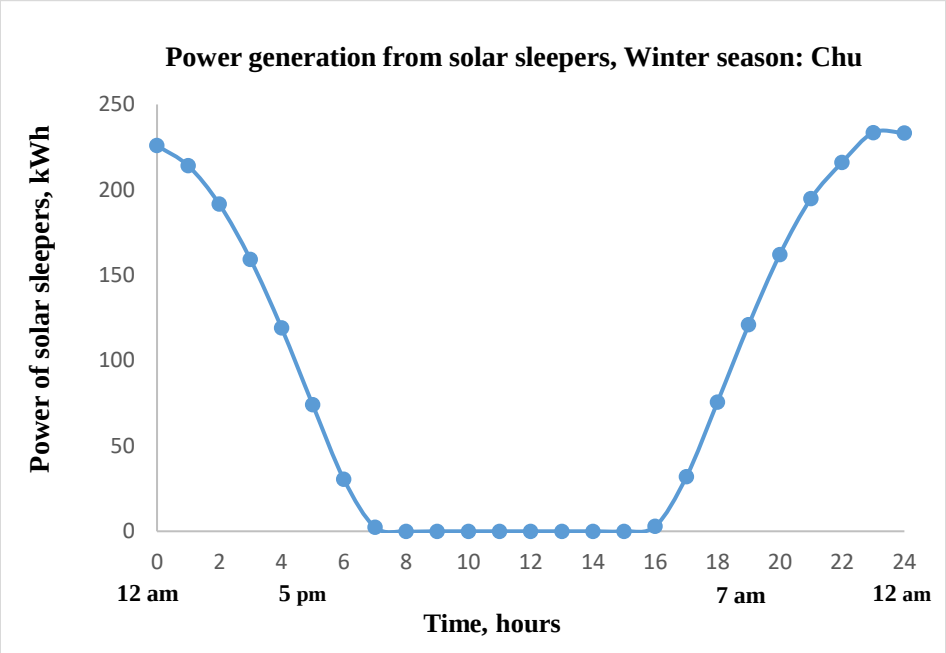

Figure B.34. The power of solar sleepers (kWh), winter season: Chu

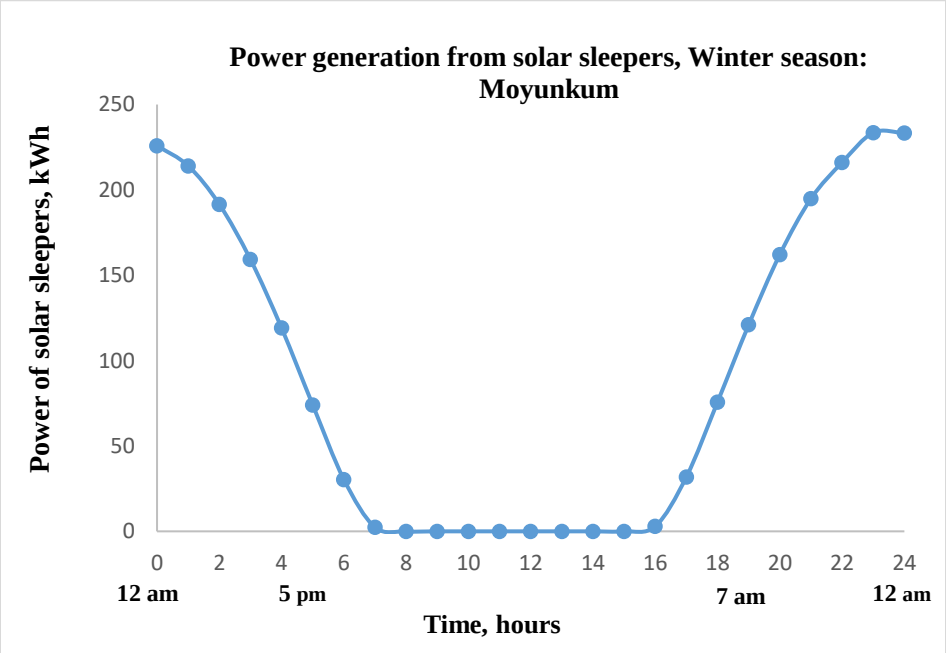

Figure B.35. The power of solar sleepers (kWh), winter season: Moyunkum

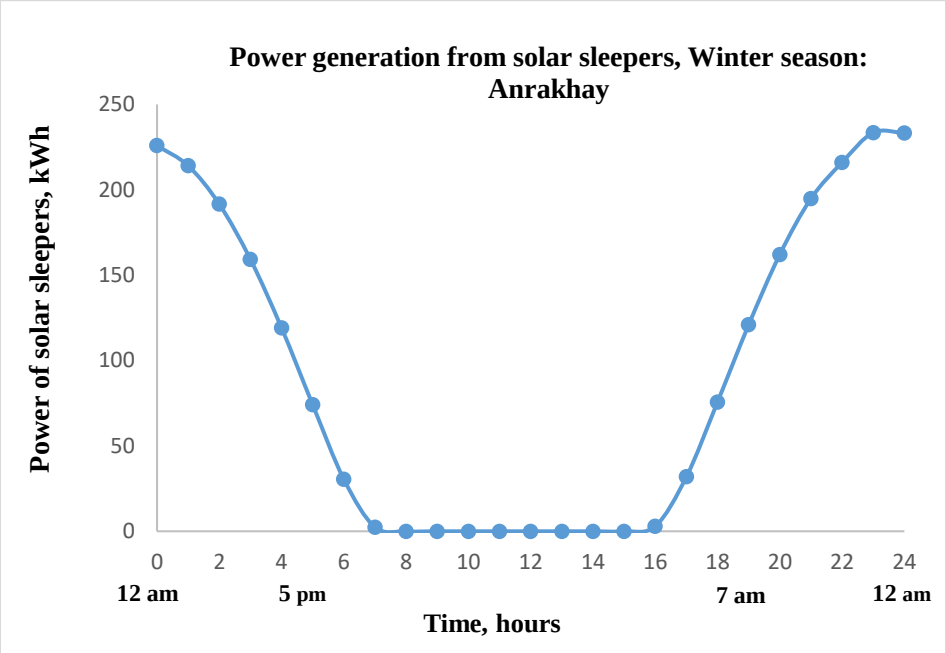

Figure B.36. The power of solar sleepers (kWh), winter season: Anrakhay

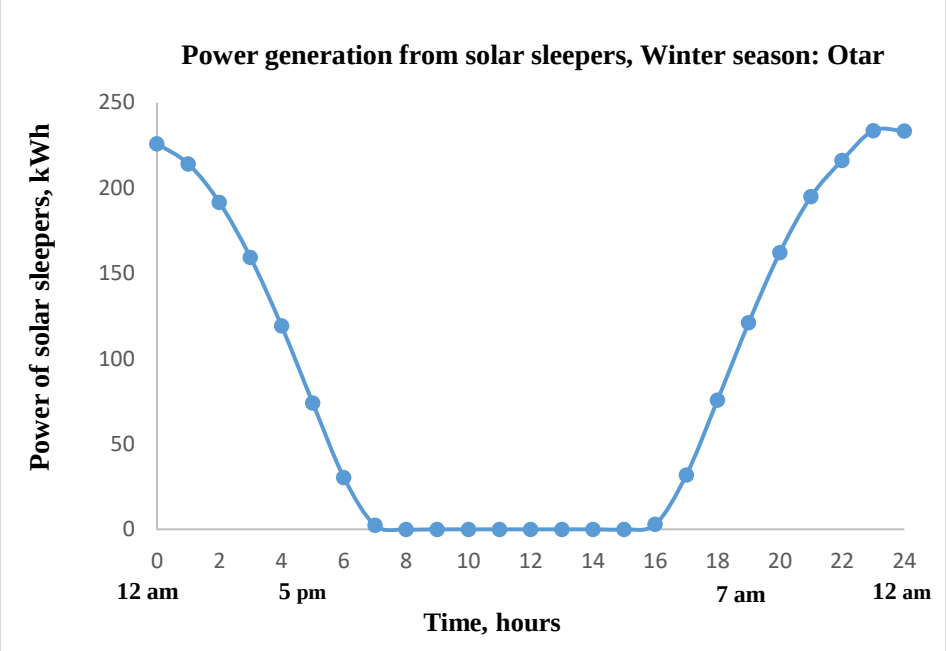

Figure B.37. The power of solar sleepers (kWh), winter season: Otar

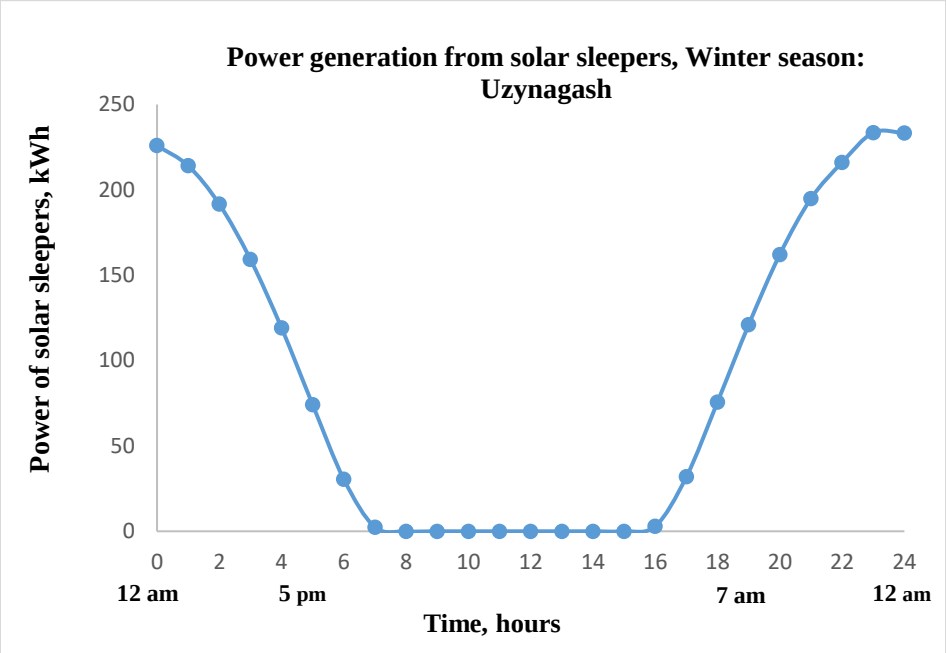

Figure B.38. The power of solar sleepers (kWh), winter season: Uzynagash

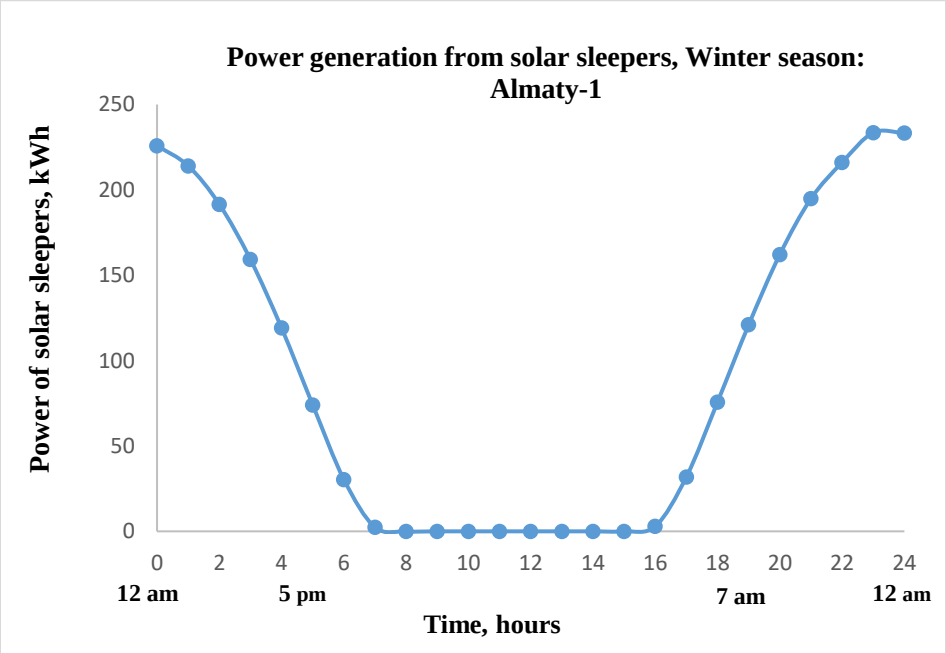

Figure B.39. The power of solar sleepers (kWh), winter season: Almaty-1

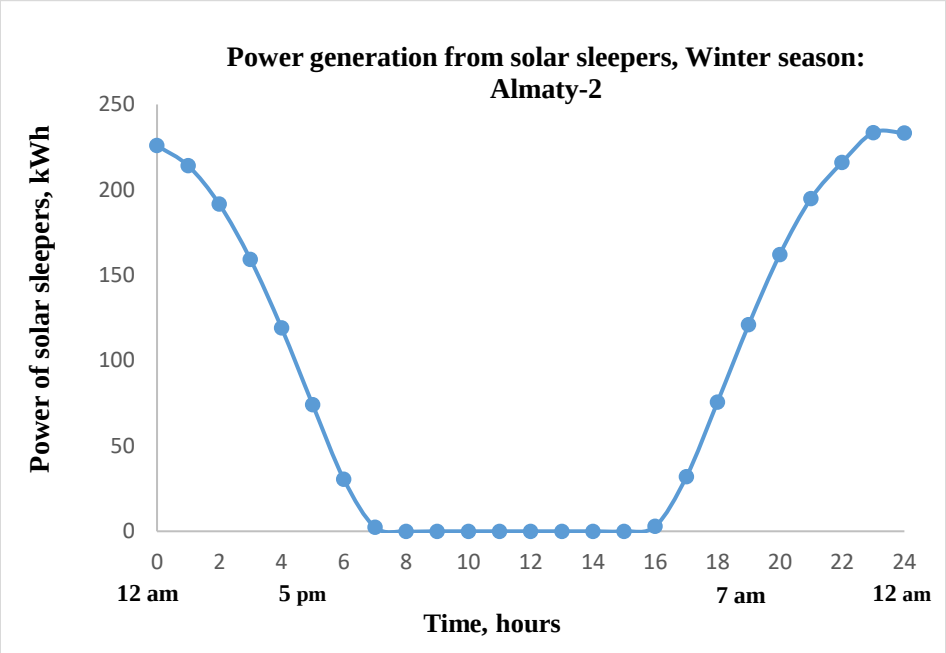

Figure B.40. The power of solar sleepers (kWh), winter season: Almaty-2

B.3. Spring season, May

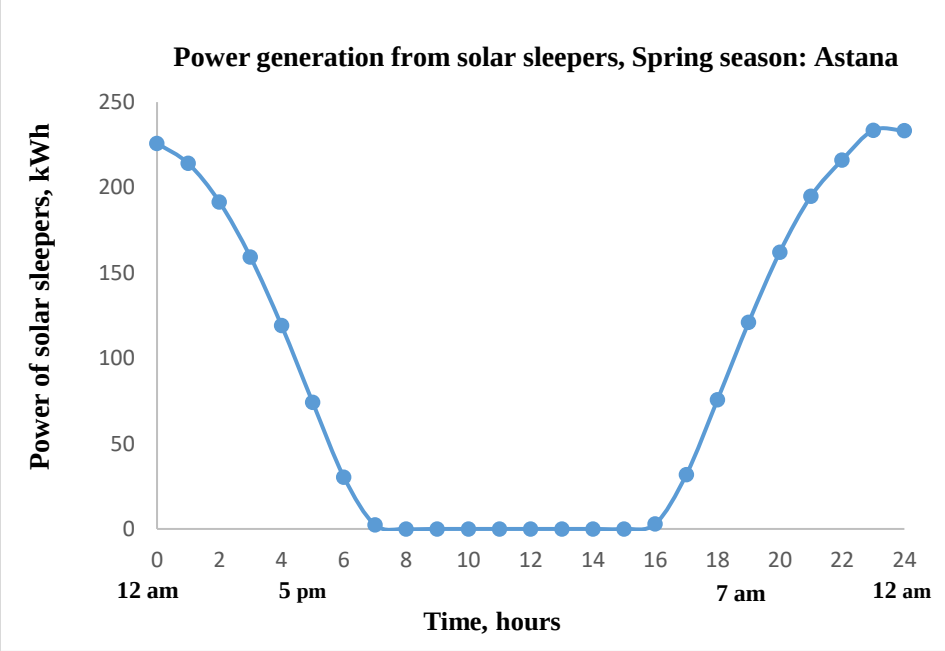

Figure B.41. The power of solar sleepers (kWh), spring season: Astana

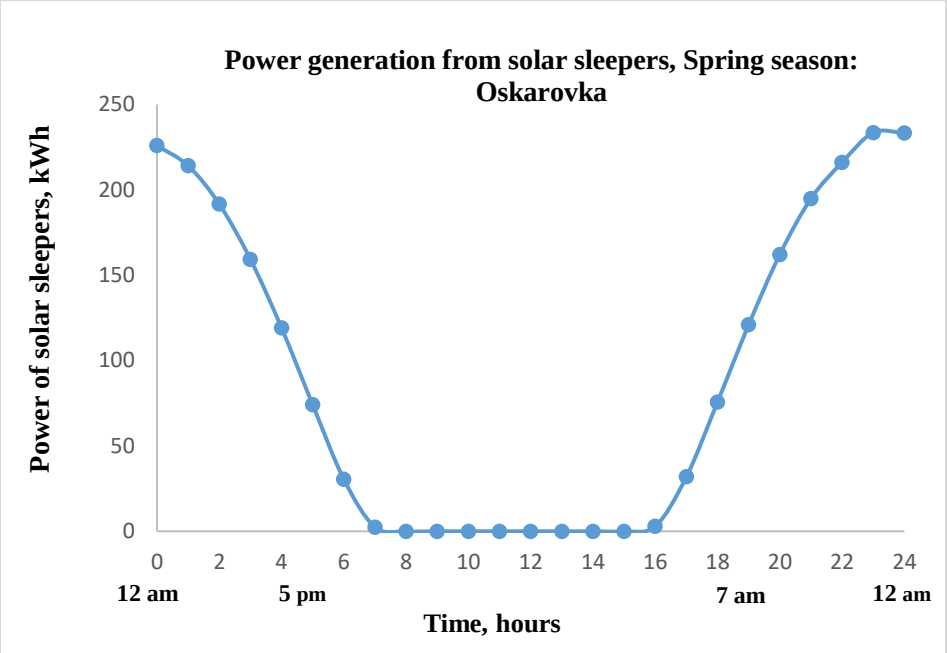

Figure B.42. The power of solar sleepers (kWh), spring season: Oskarovka

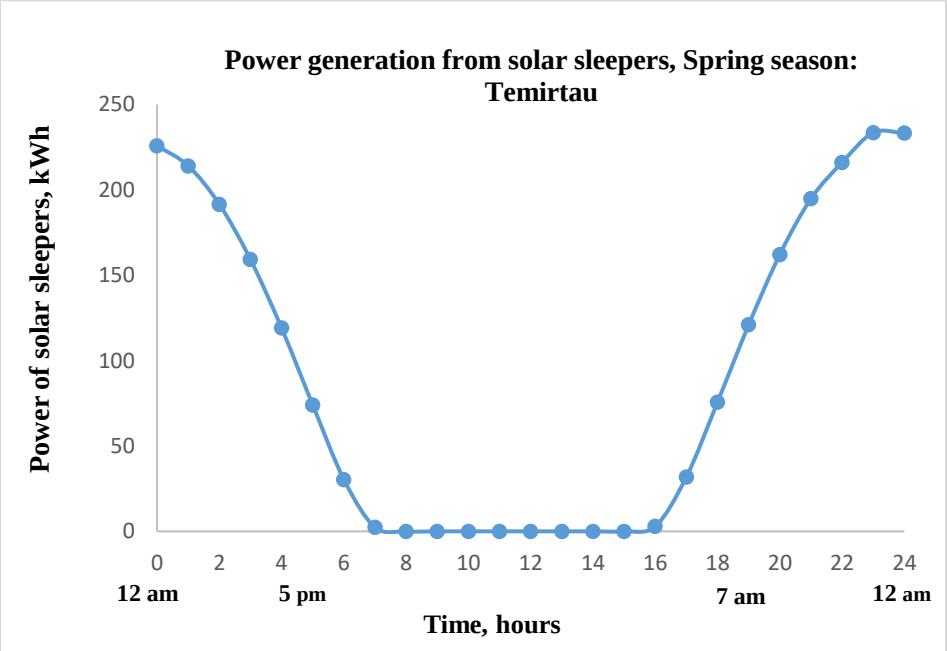

Figure B.43. The power of solar sleepers (kWh), spring season: Temirtau

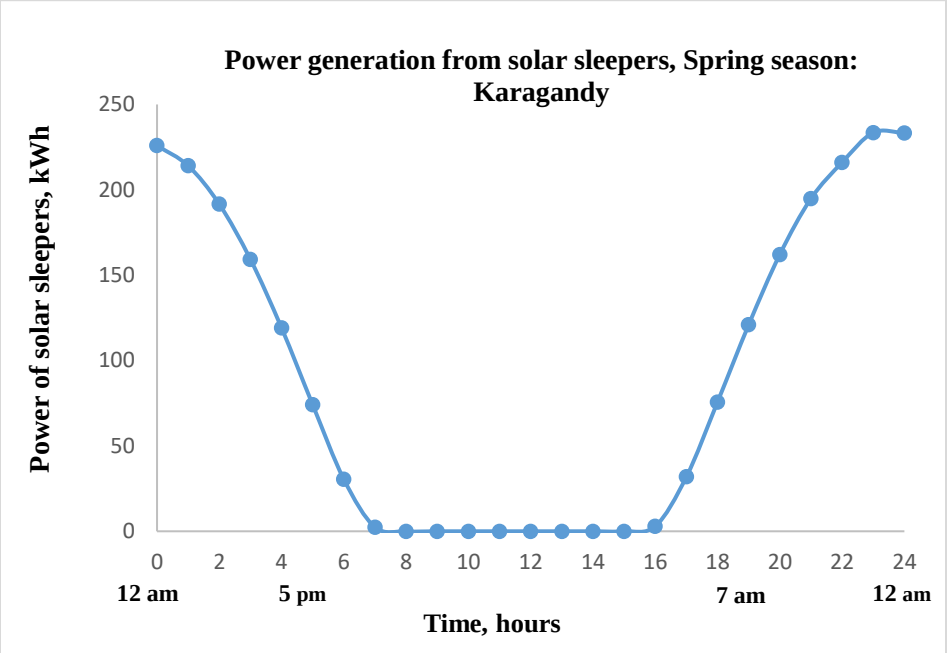

Figure B.44. The power of solar sleepers (kWh), spring season: Karagandy

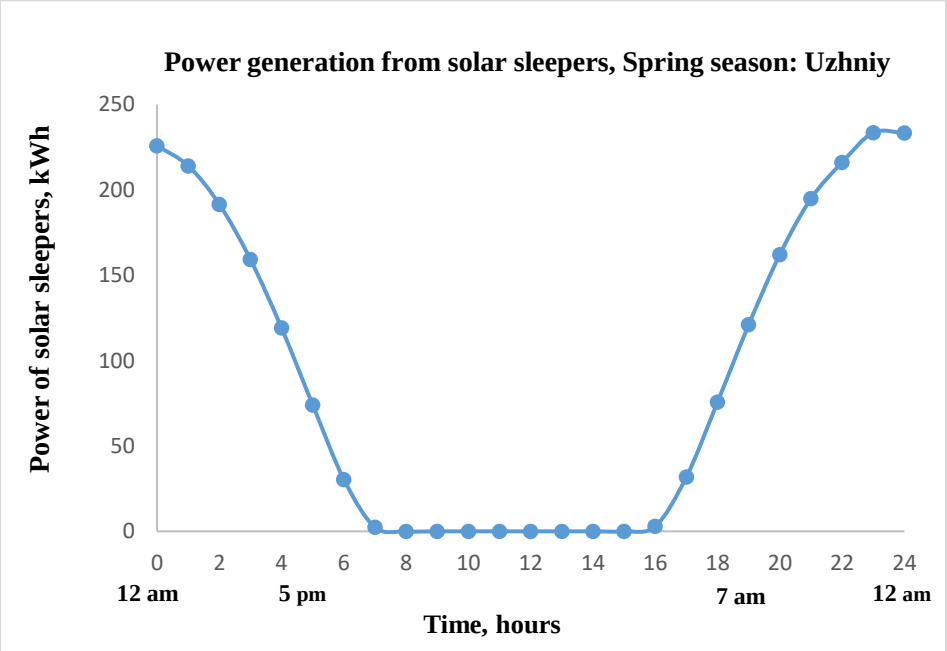

Figure B.45. The power of solar sleepers (kWh), spring season: Uzhniy

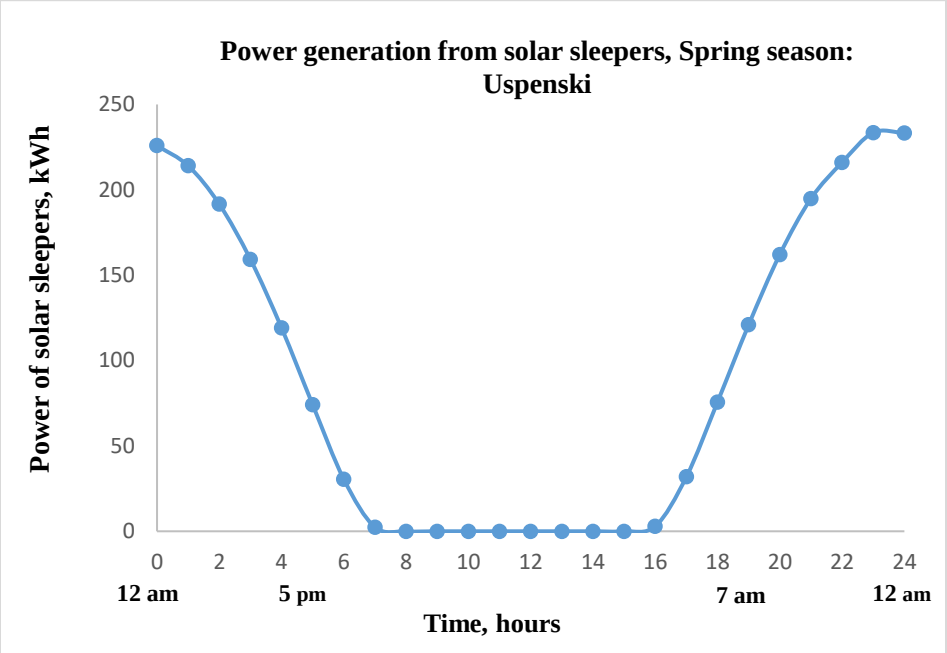

Figure B.46. The power of solar sleepers (kWh), spring season: Uspenski

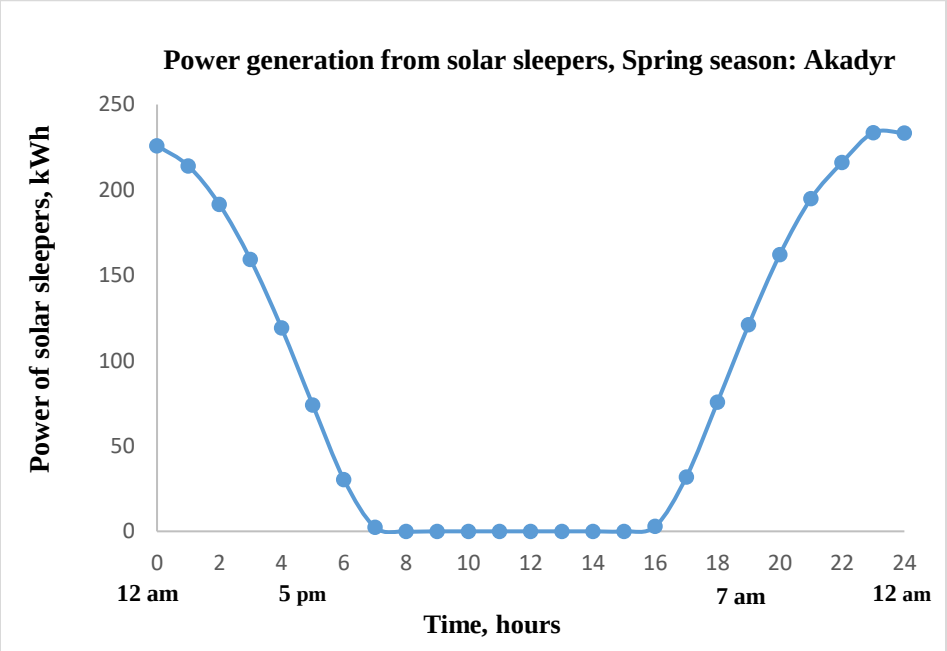

Figure B.47. The power of solar sleepers (kWh), spring season: Akadyr

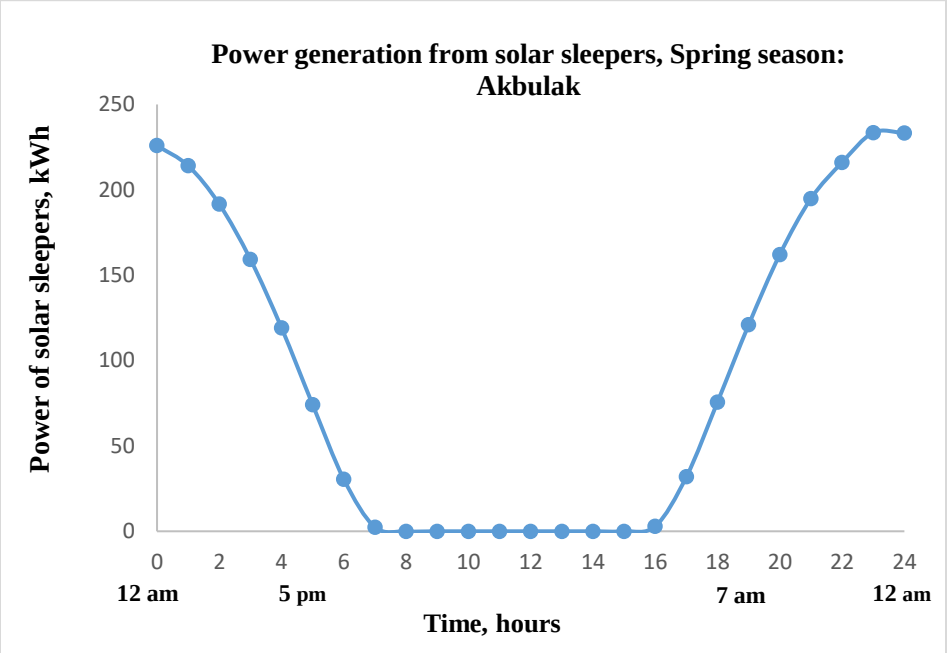

Figure B.48. The power of solar sleepers (kWh), spring season: Akbulak

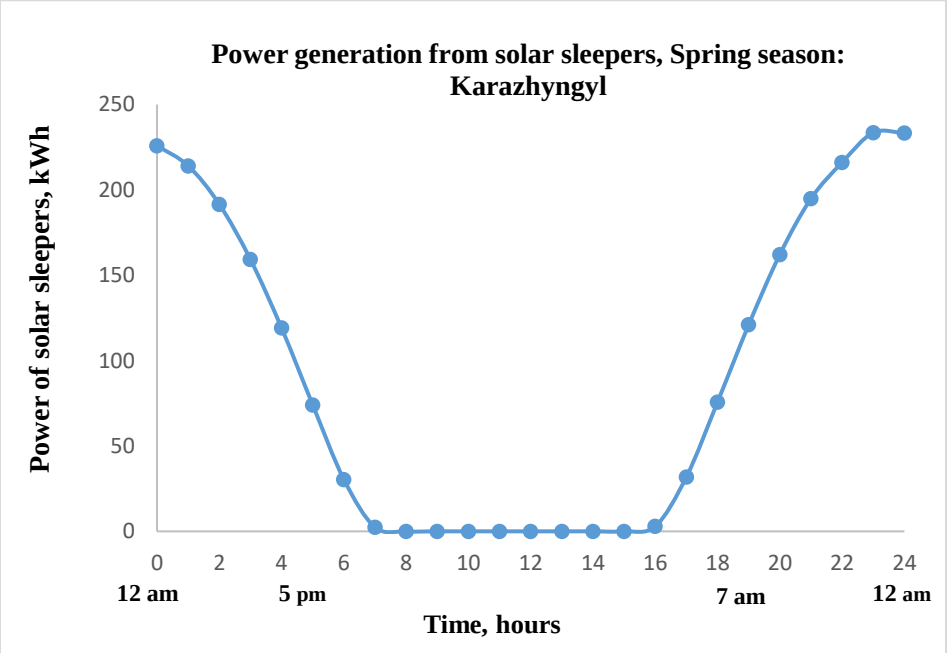

Figure B.49. The power of solar sleepers (kWh), spring season: Karazhyngyl

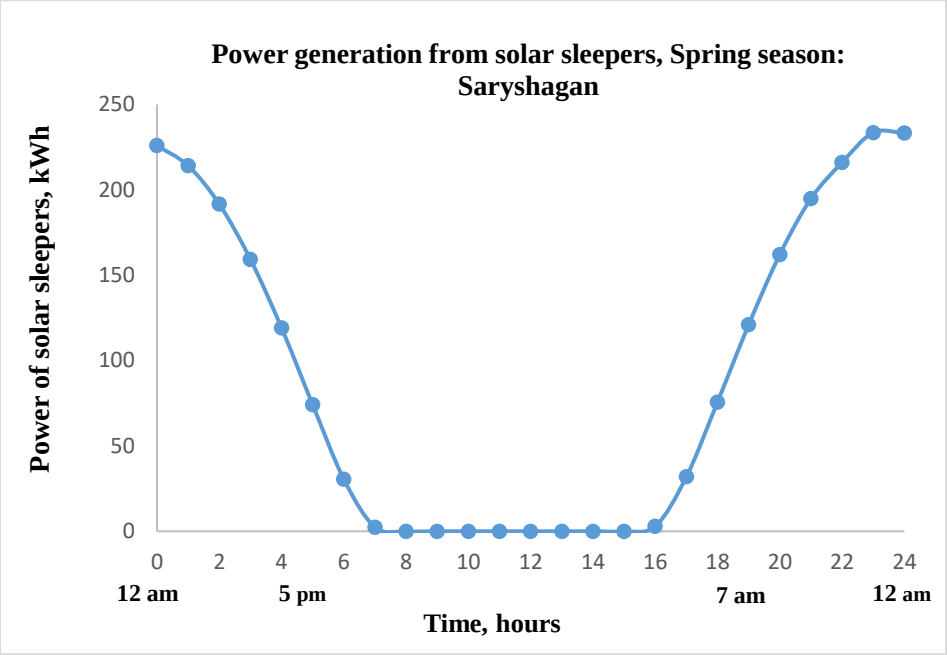

Figure B.50. The power of solar sleepers (kWh), spring season: Saryshagan

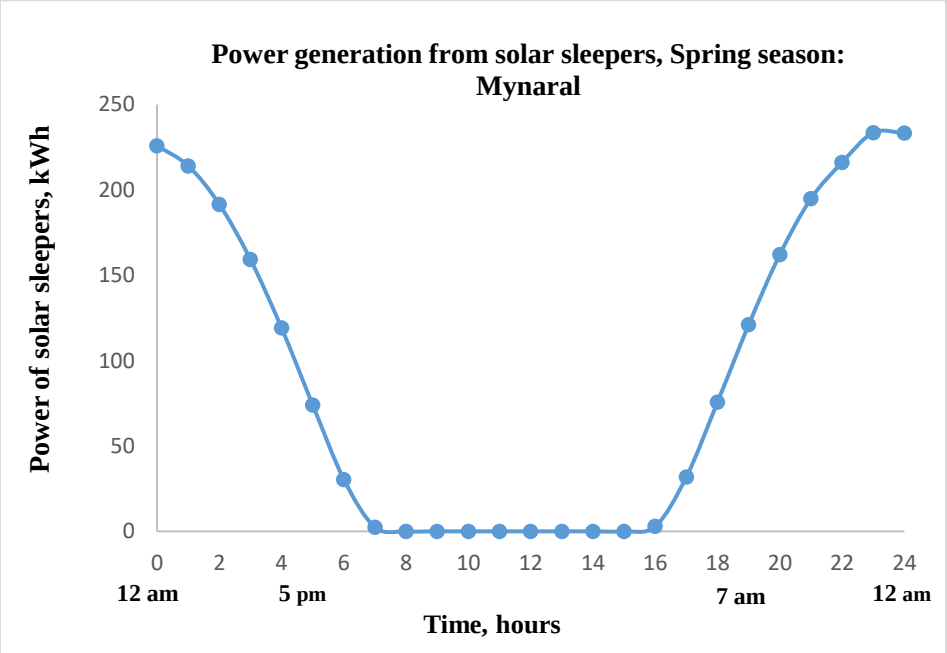

Figure B.51. The power of solar sleepers (kWh), spring season: Mynaral

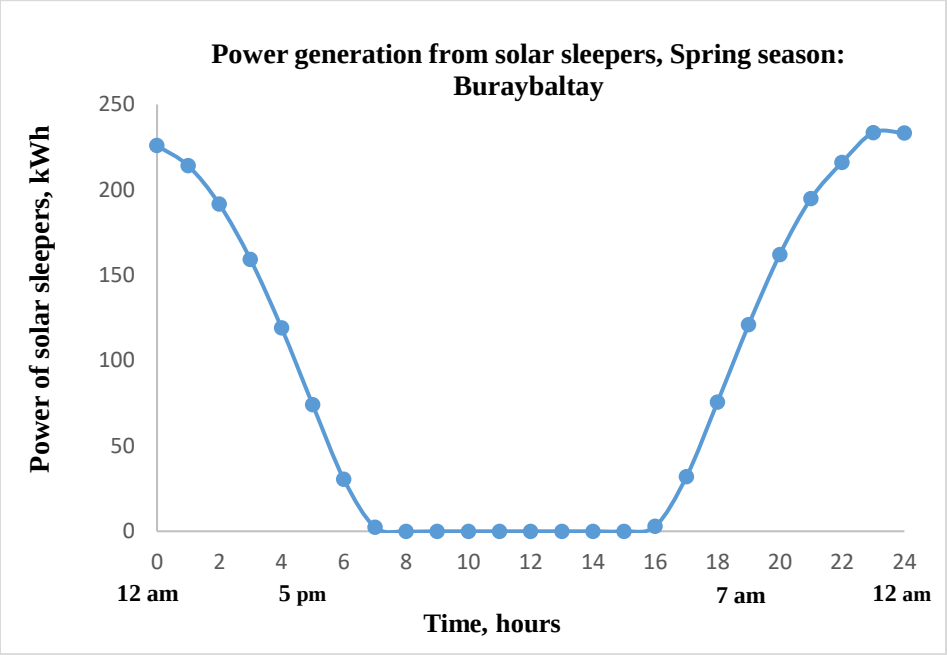

Figure B.52. The power of solar sleepers (kWh), spring season: Buraybaltay

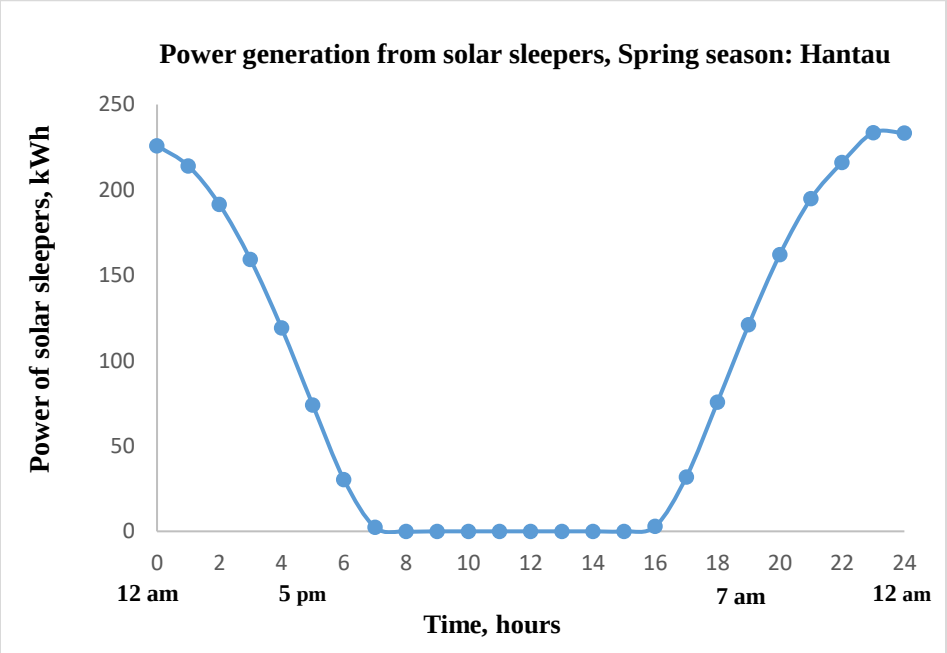

Figure B.53. The power of solar sleepers (kWh), spring season: Hantau

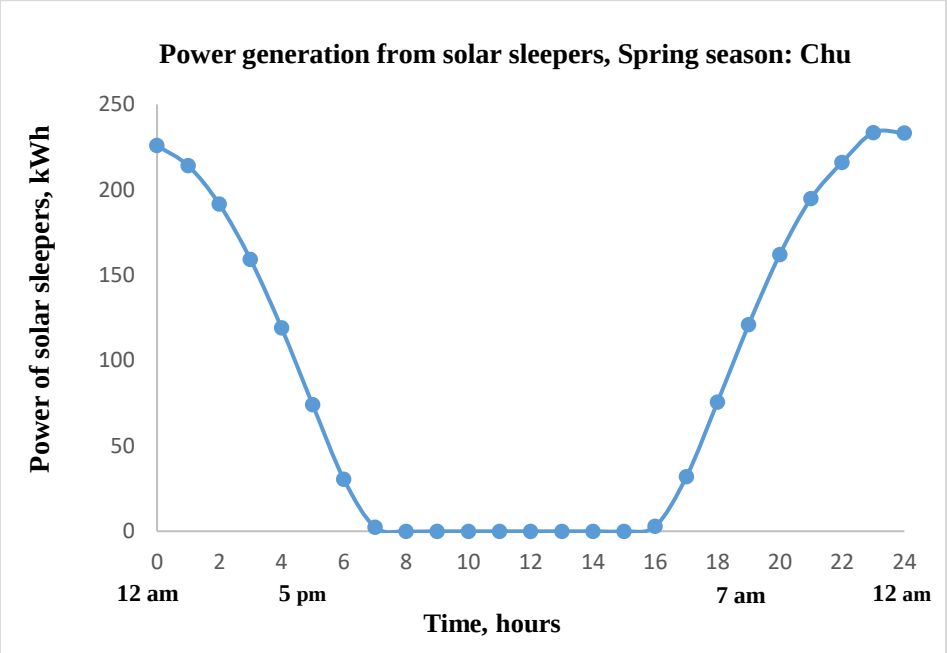

Figure B.54. The power of solar sleepers (kWh), spring season: Chu

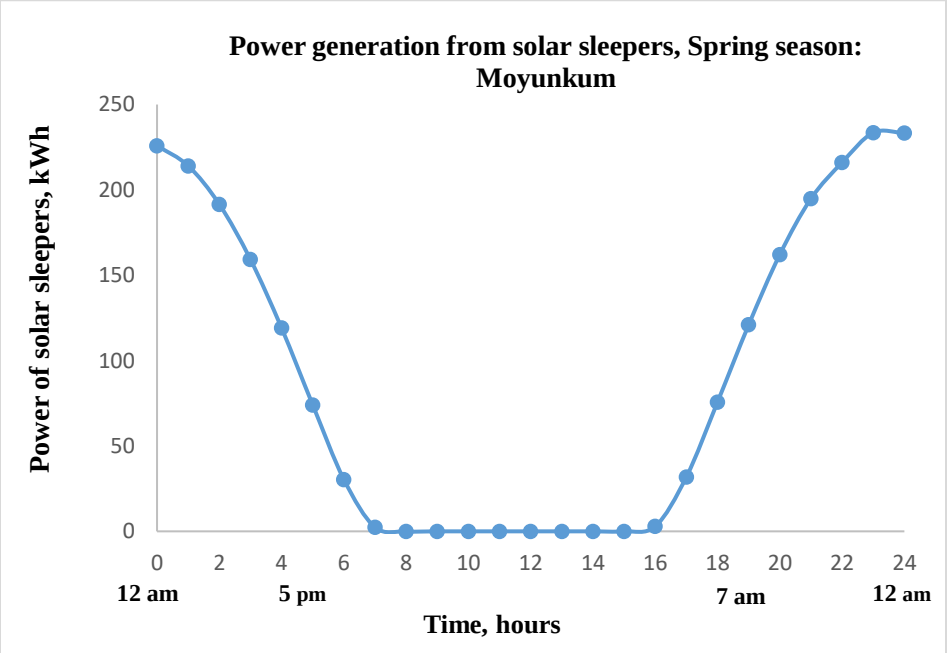

Figure B.55. The power of solar sleepers (kWh), spring season: Moyunkum

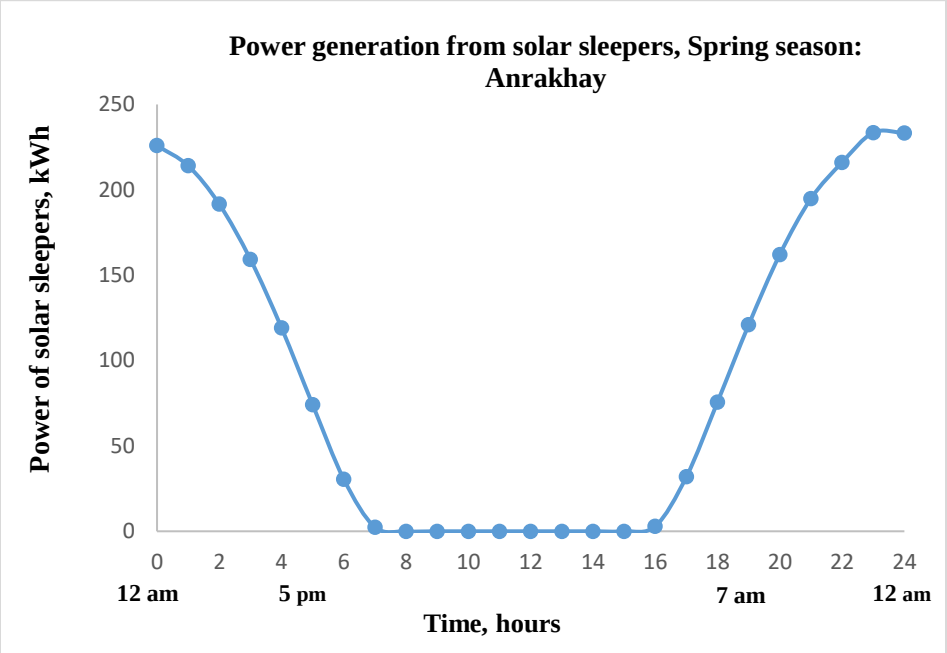

Figure B.56. The power of solar sleepers (kWh), spring season: Anrakhay

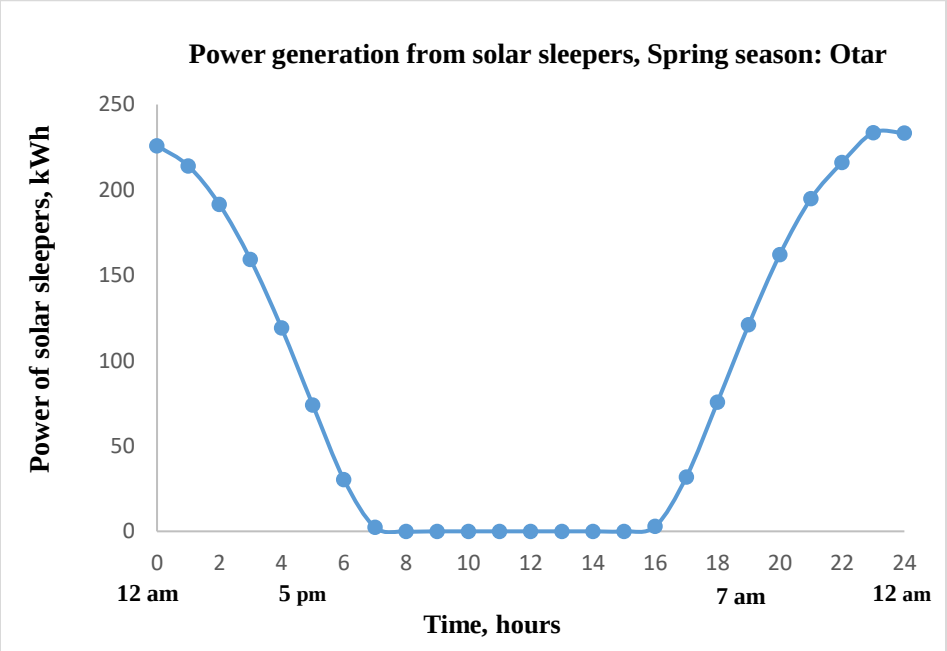

Figure B.57. The power of solar sleepers (kWh), spring season: Otar

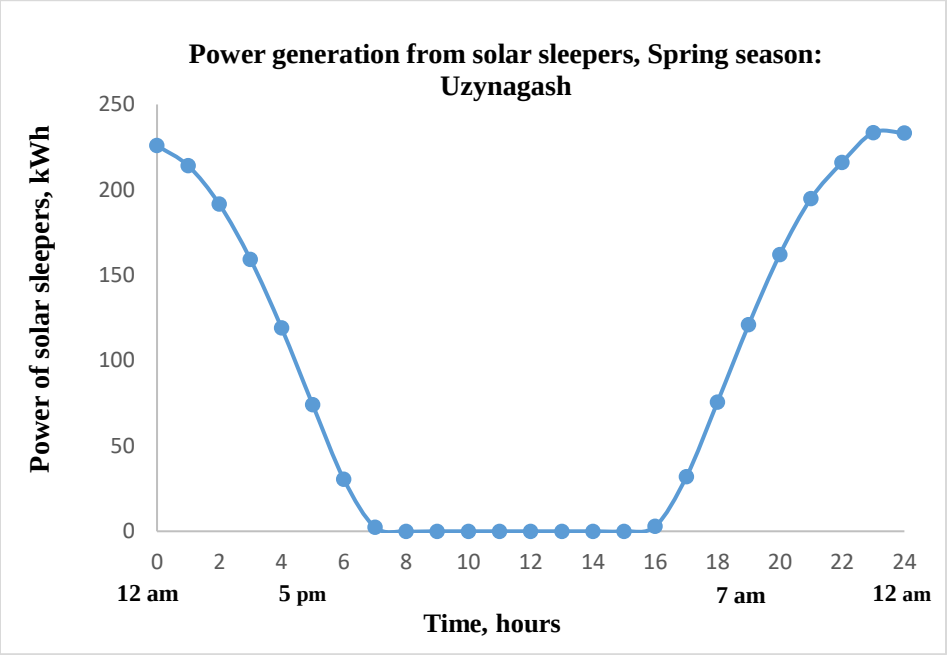

Figure B.58. The power of solar sleepers (kWh), spring season: Uzynagash

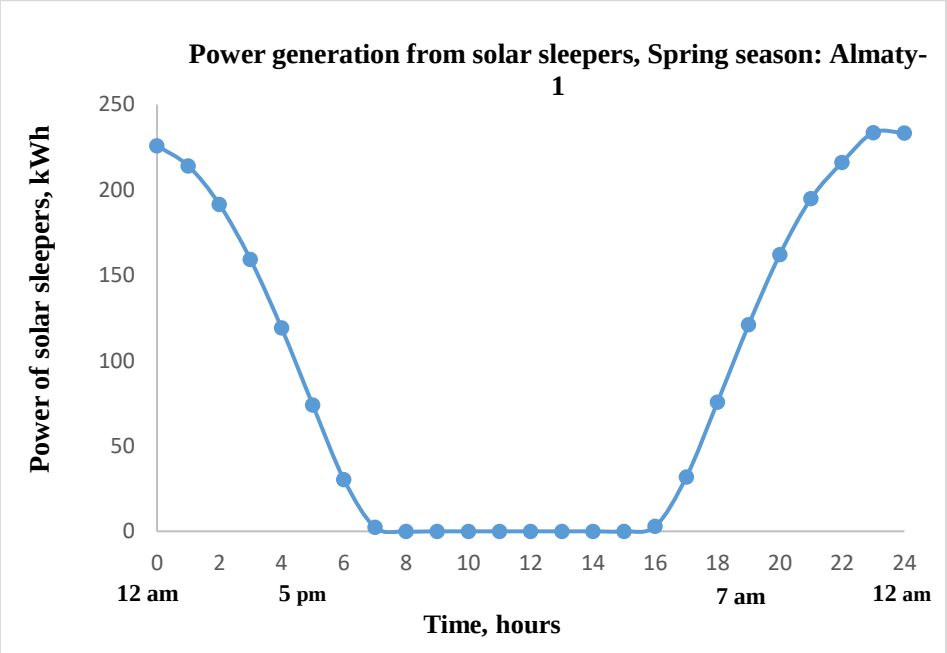

Figure B.59. The power of solar sleepers (kWh), spring season: Almaty-1

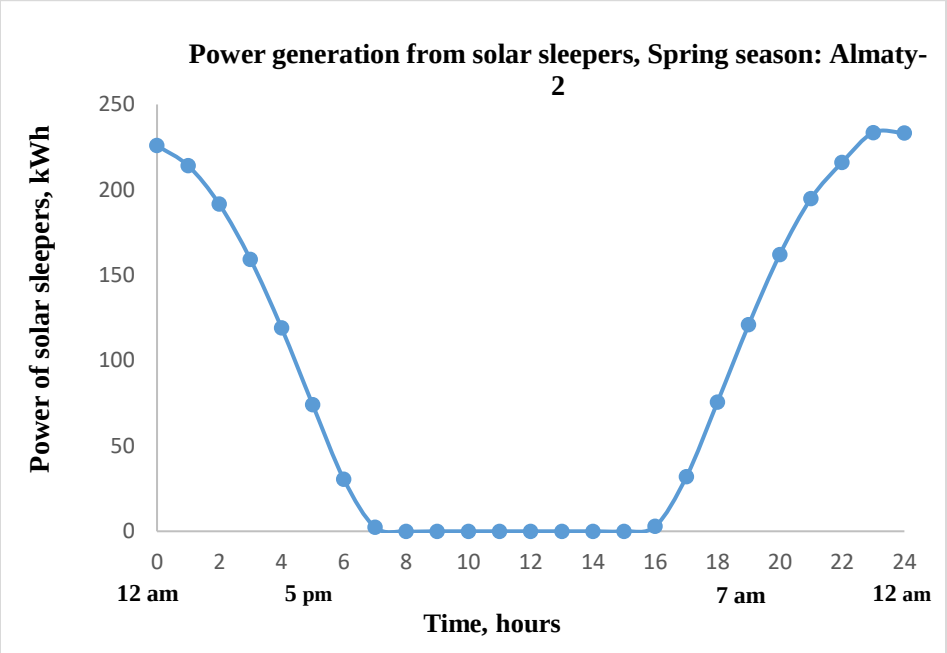

Figure B.60. The power of solar sleepers (kWh), spring season: Almaty-2

B.4. Summer season, July

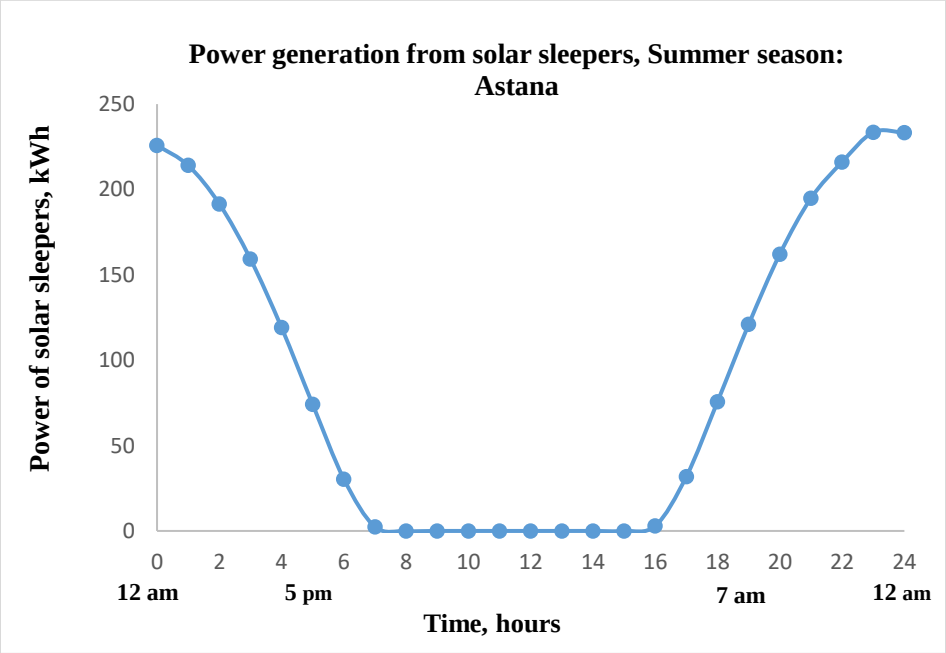

Figure B.61. The power of solar sleepers (kWh), summer season: Astana

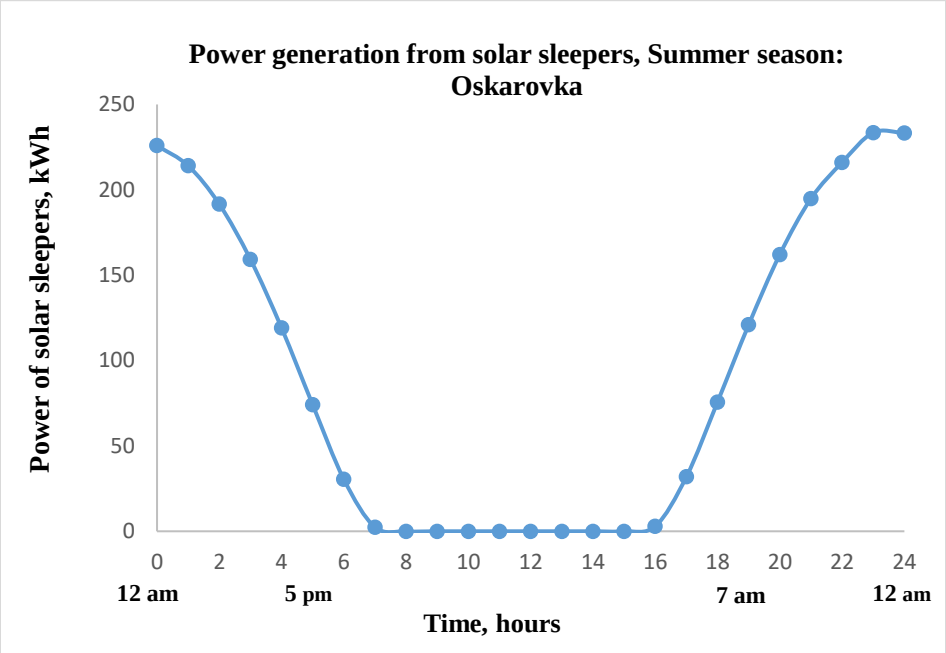

Figure B.62. The power of solar sleepers (kWh), summer season: Oskarovka

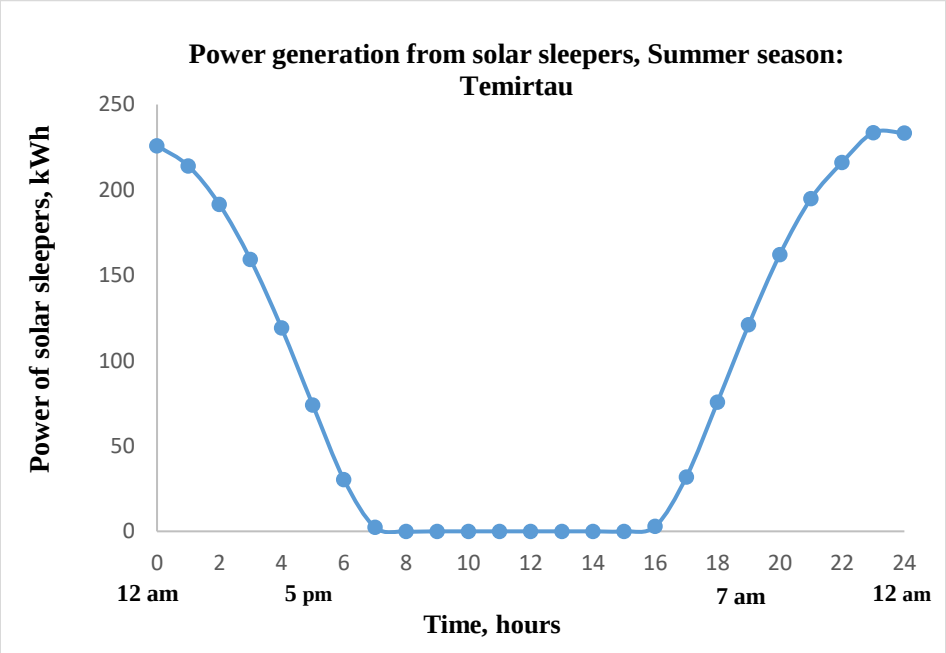

Figure B.63. The power of solar sleepers (kWh), summer season: Temirtau

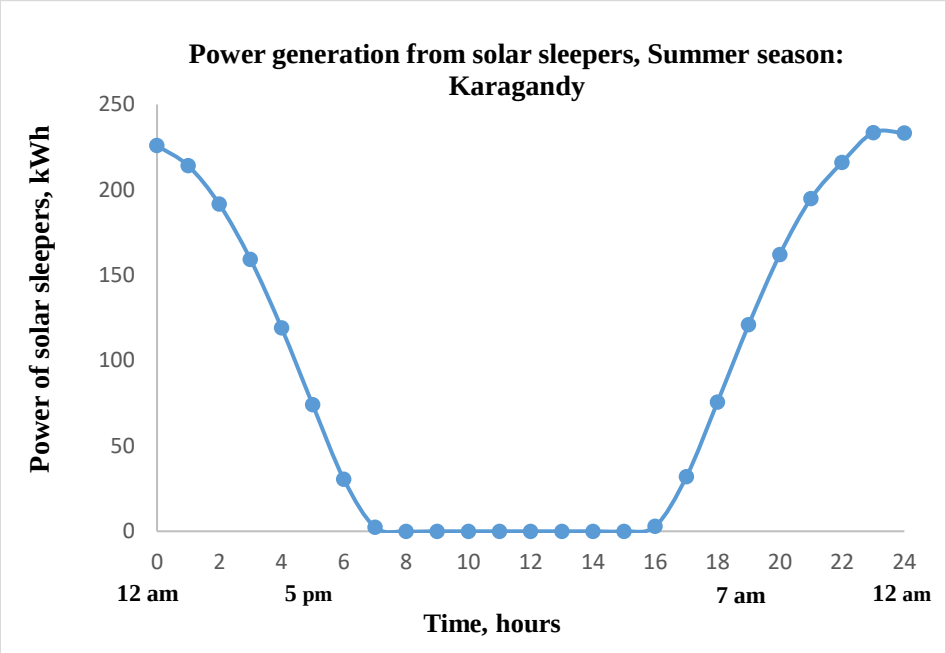

Figure B.64. The power of solar sleepers (kWh), summer season: Karagandy

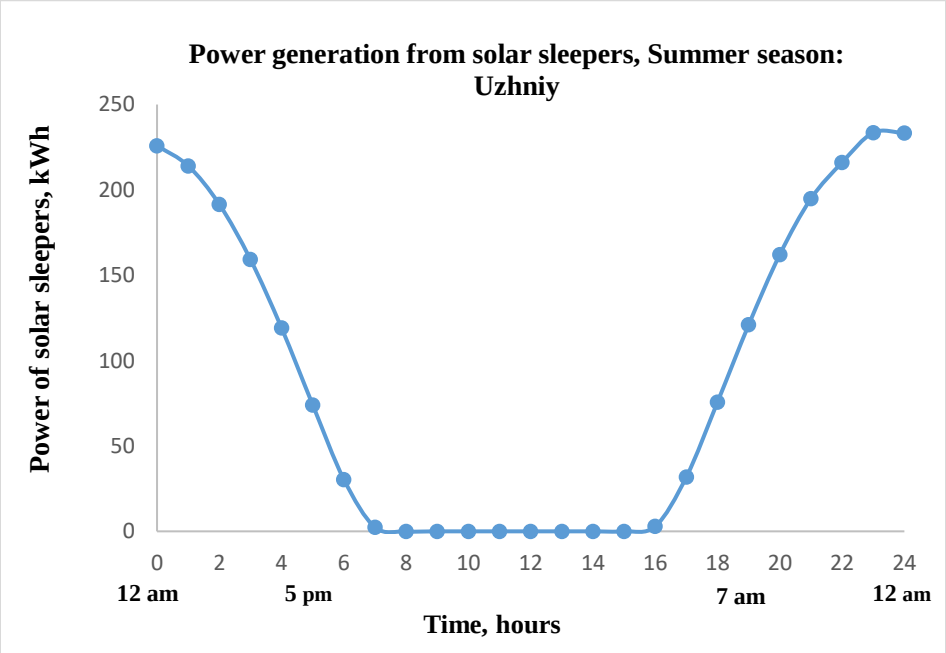

Figure B.65. The power of solar sleepers (kWh), summer season: Uzhniy

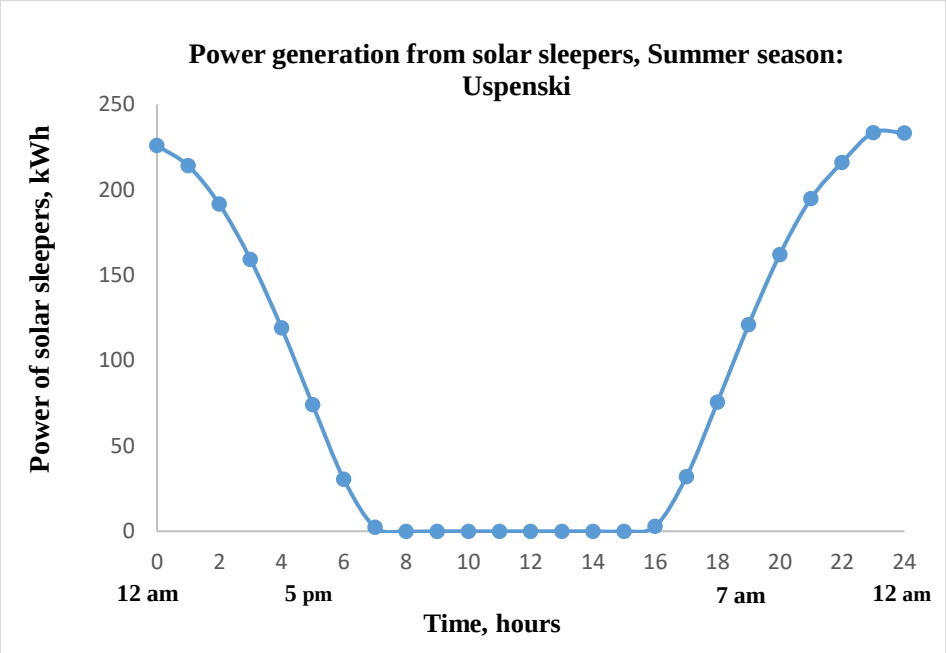

Figure B.66. The power of solar sleepers (kWh), summer season: Uspenski

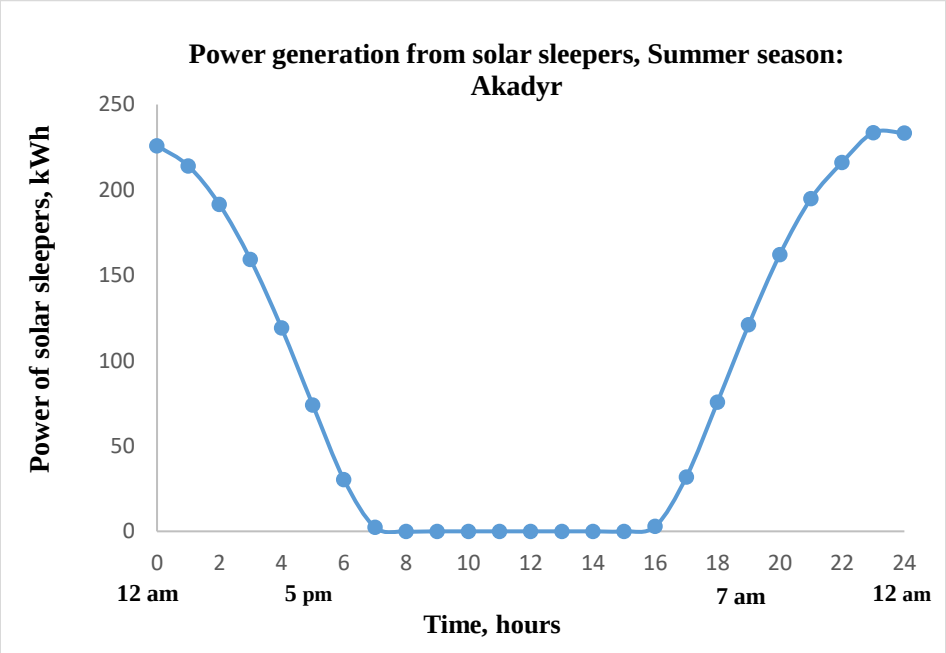

Figure B.67. The power of solar sleepers (kWh), summer season: Akadyr

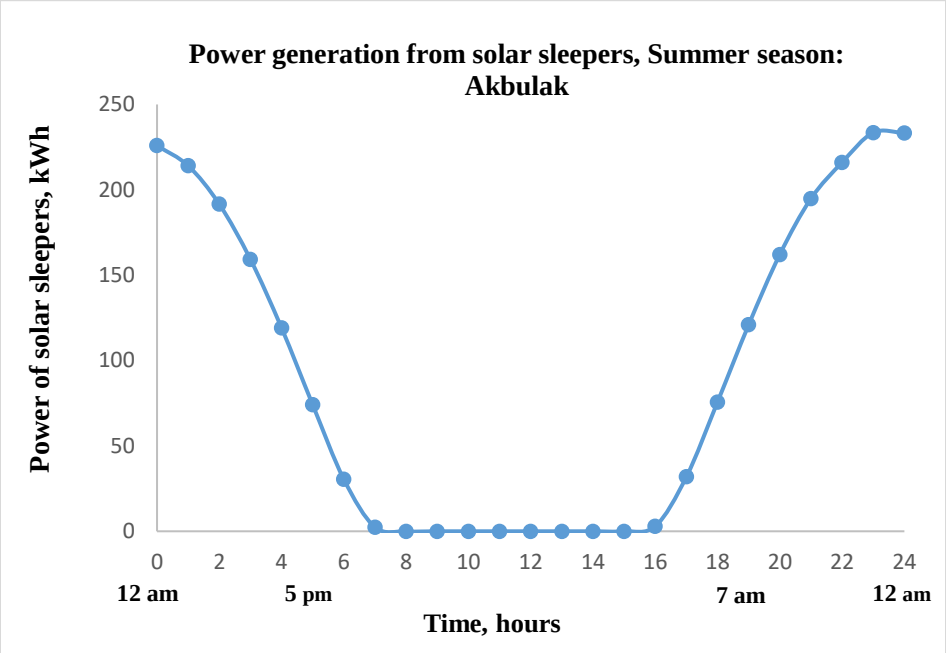

Figure B.68. The power of solar sleepers (kWh), summer season: Akbulak

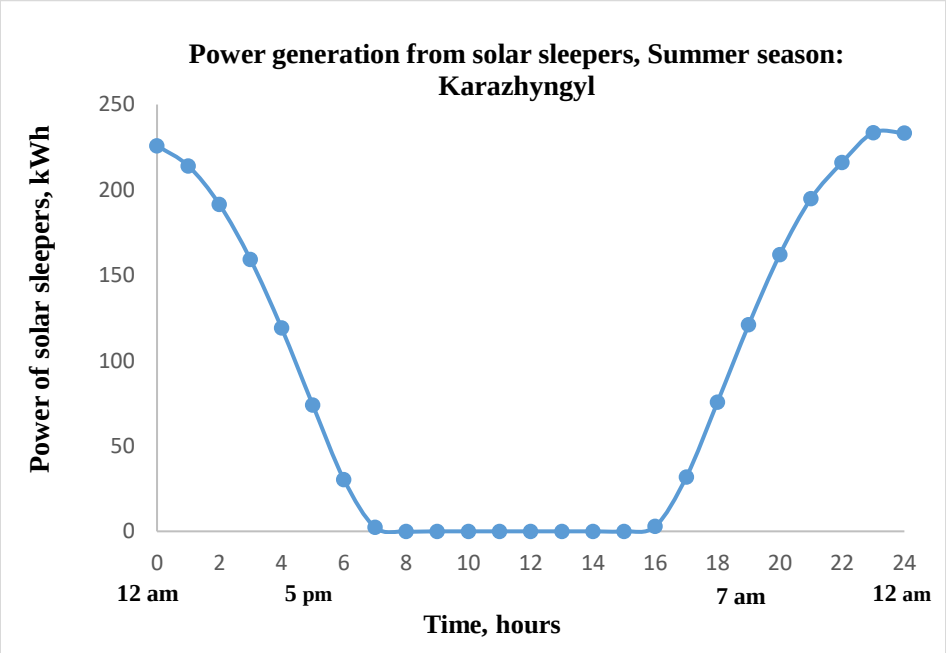

Figure B.69. The power of solar sleepers (kWh), summer season: Karazhyngyl

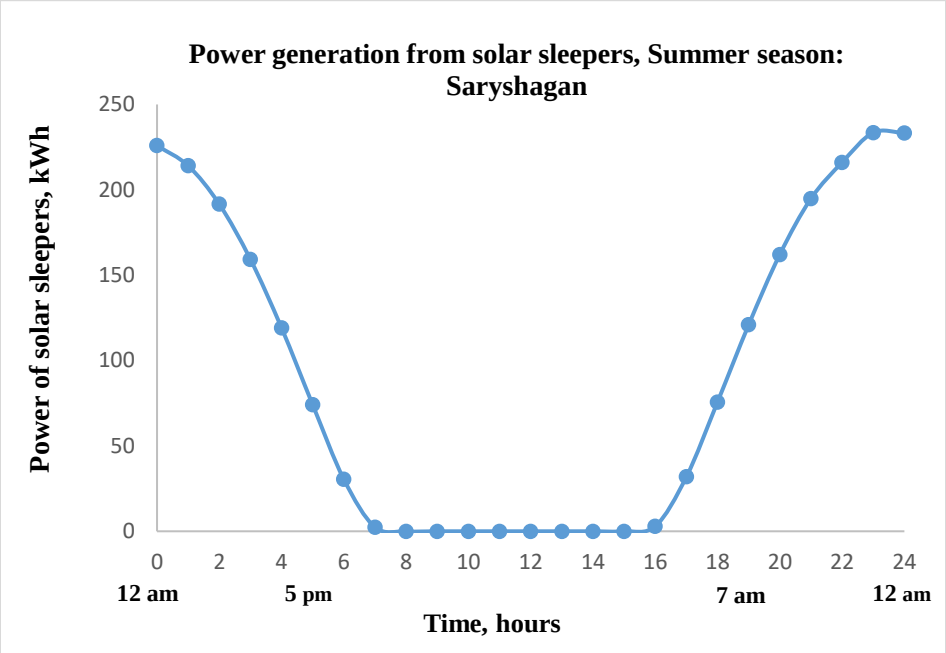

Figure B.70. The power of solar sleepers (kWh), summer season: Saryshagan

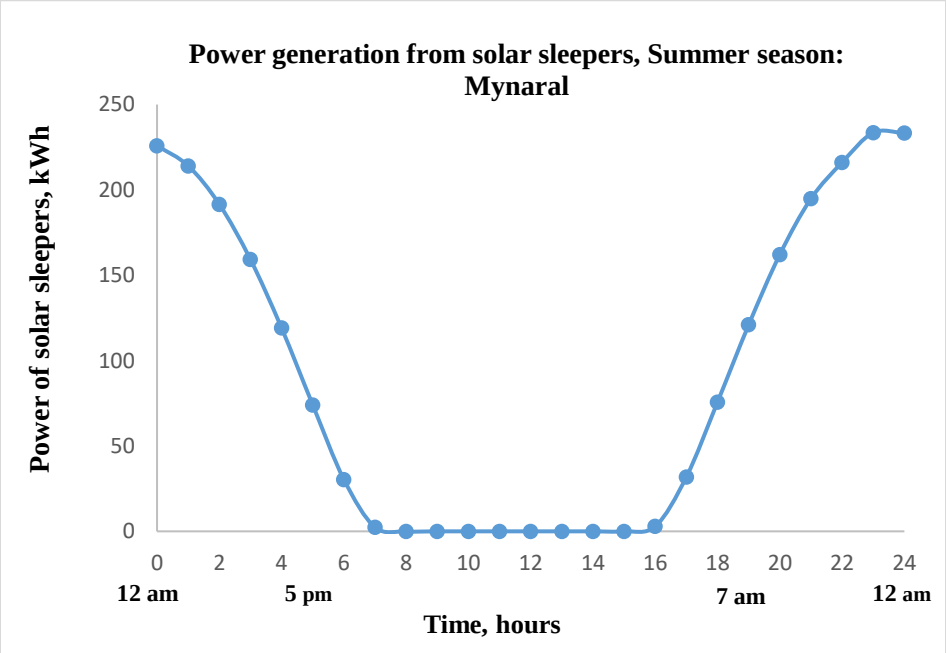

Figure B.71. The power of solar sleepers (kWh), summer season: Mynaral

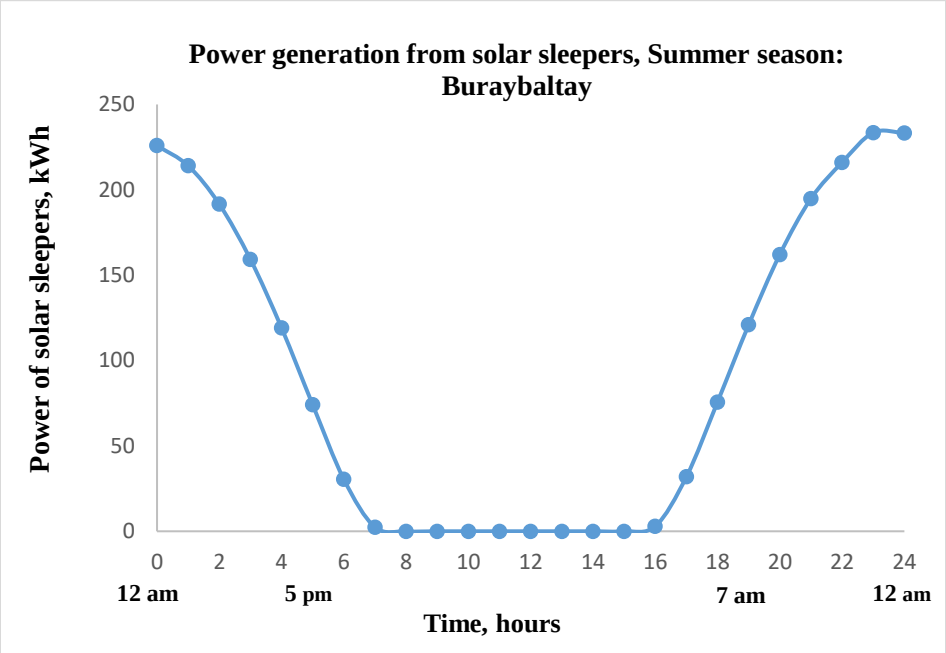

Figure B.72. The power of solar sleepers (kWh), summer season: Buraybaltay

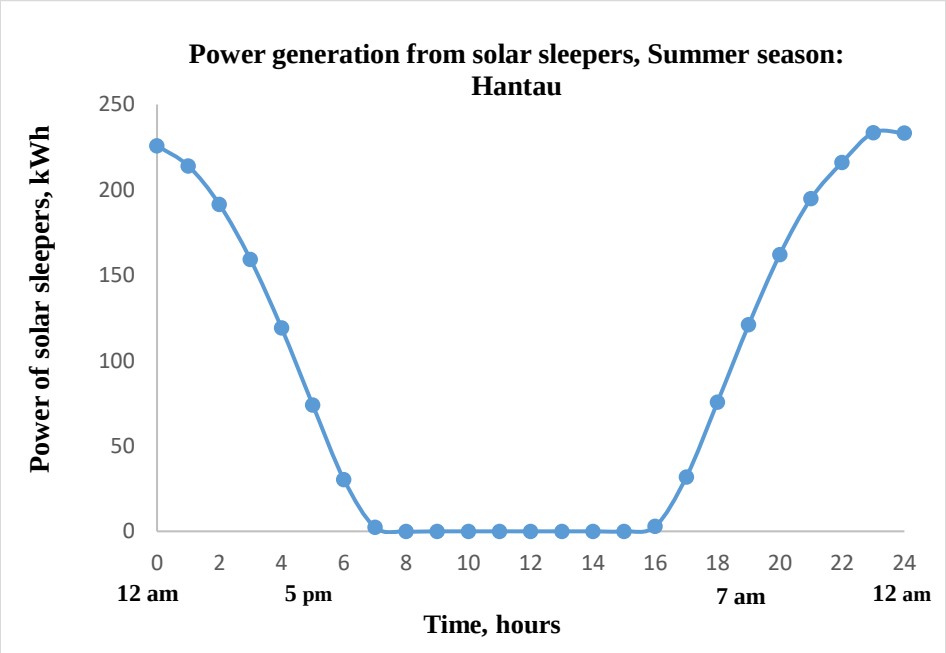

Figure B.73. The power of solar sleepers (kWh), summer season: Hantau

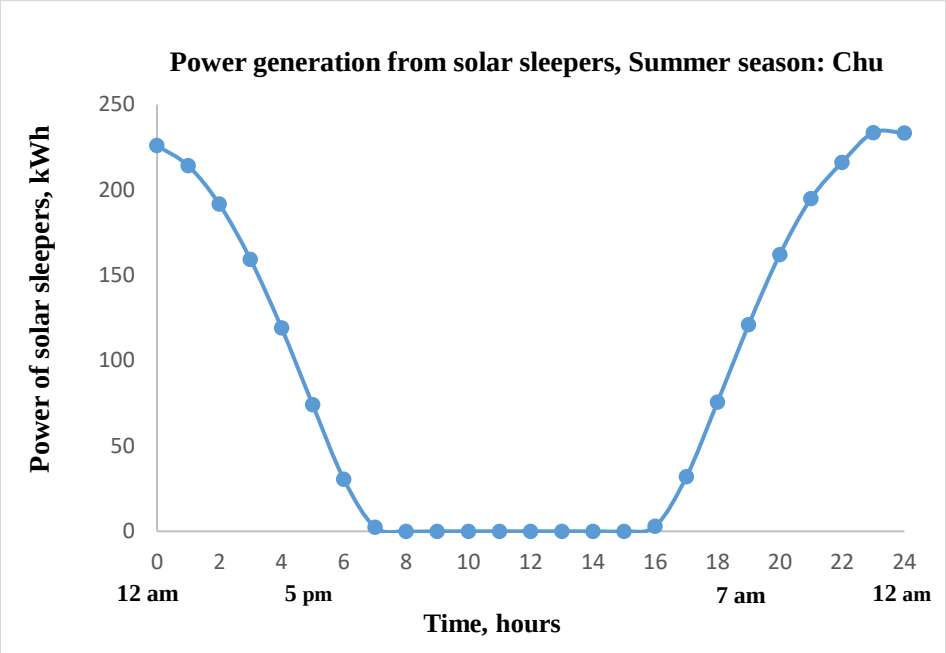

Figure B.74. The power of solar sleepers (kWh), summer season: Chu

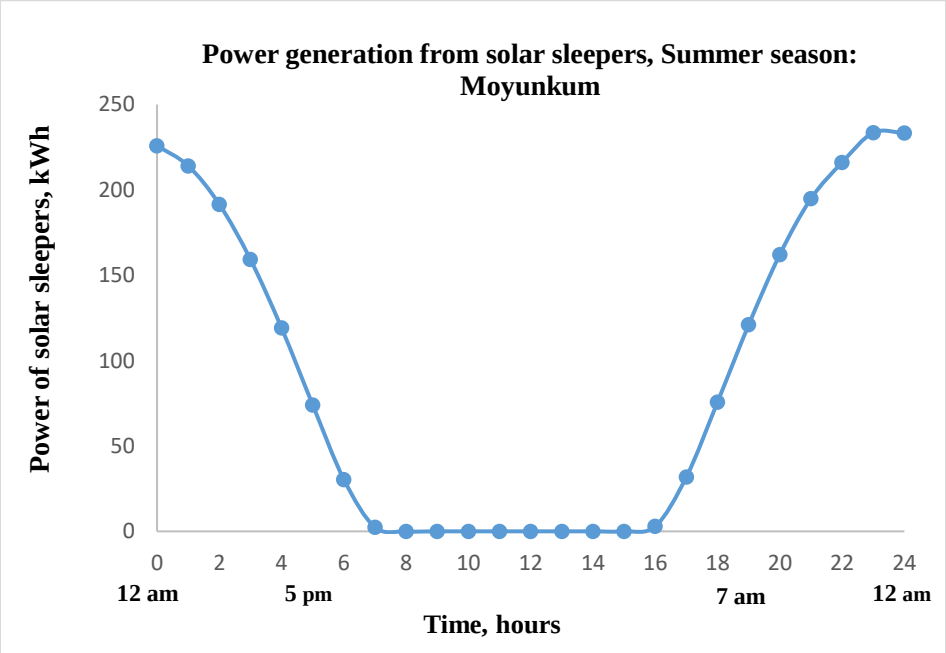

Figure B.75. The power of solar sleepers (kWh), summer season: Moyunkum

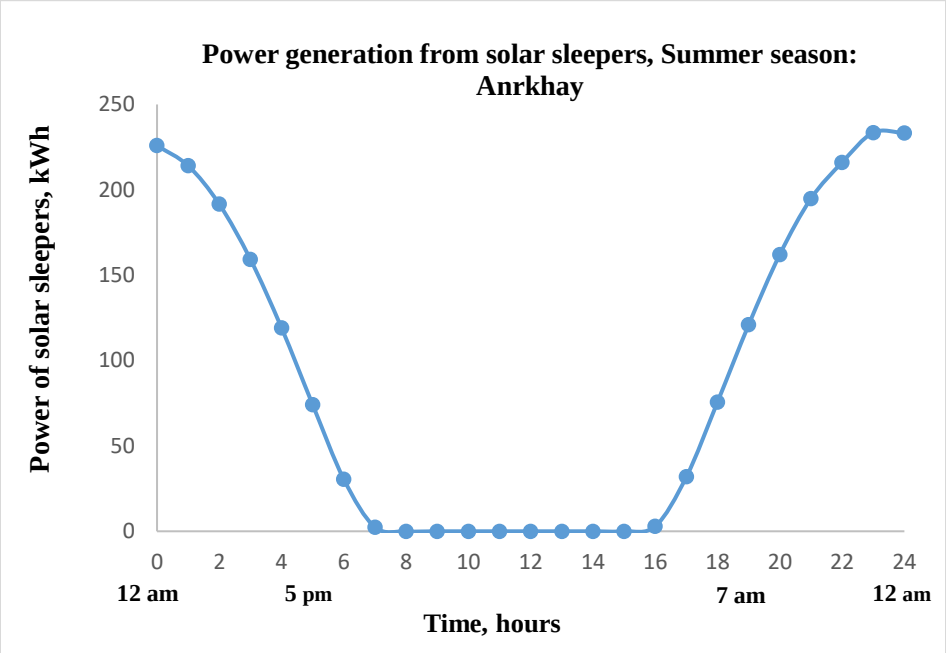

Figure B.76. The power of solar sleepers (kWh), summer season: Anrakhay

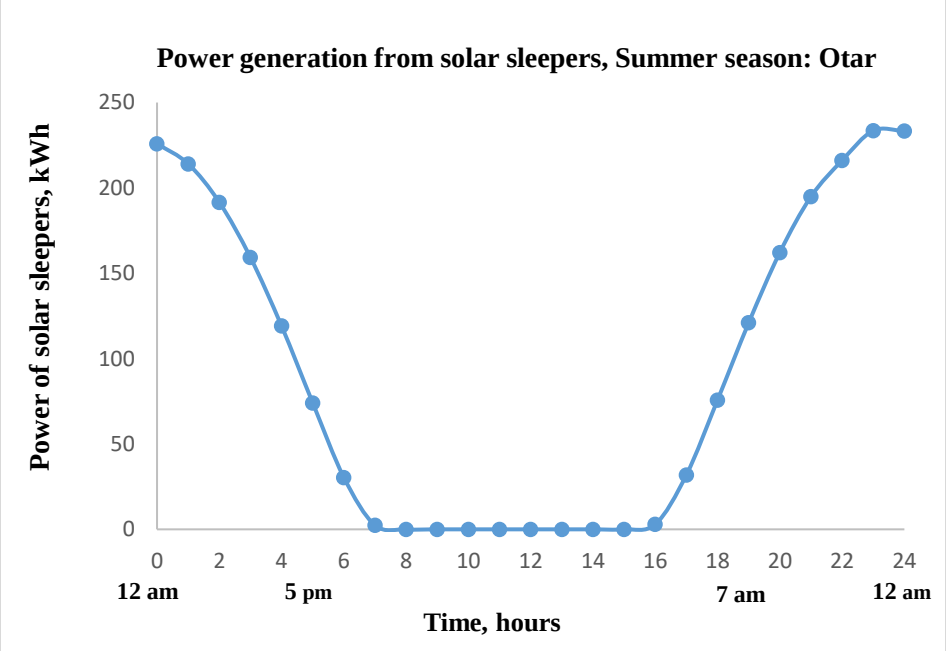

Figure B.77. The power of solar sleepers (kWh), summer season: Otar

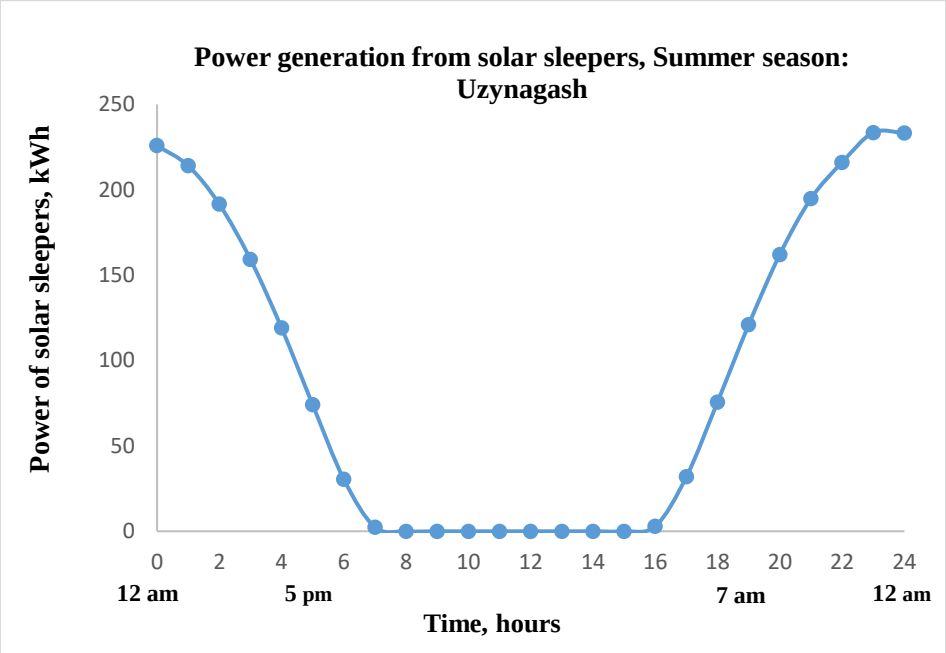

Figure B.78. The power of solar sleepers (kWh), summer season: Uzynagash

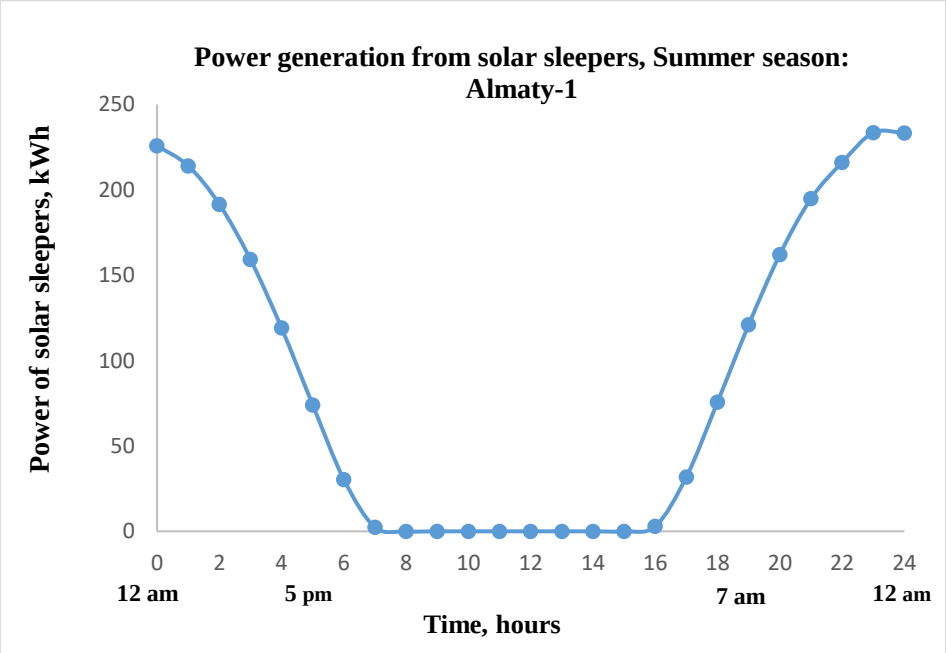

Figure B.79. The power of solar sleepers (kWh), summer season: Almaty-1

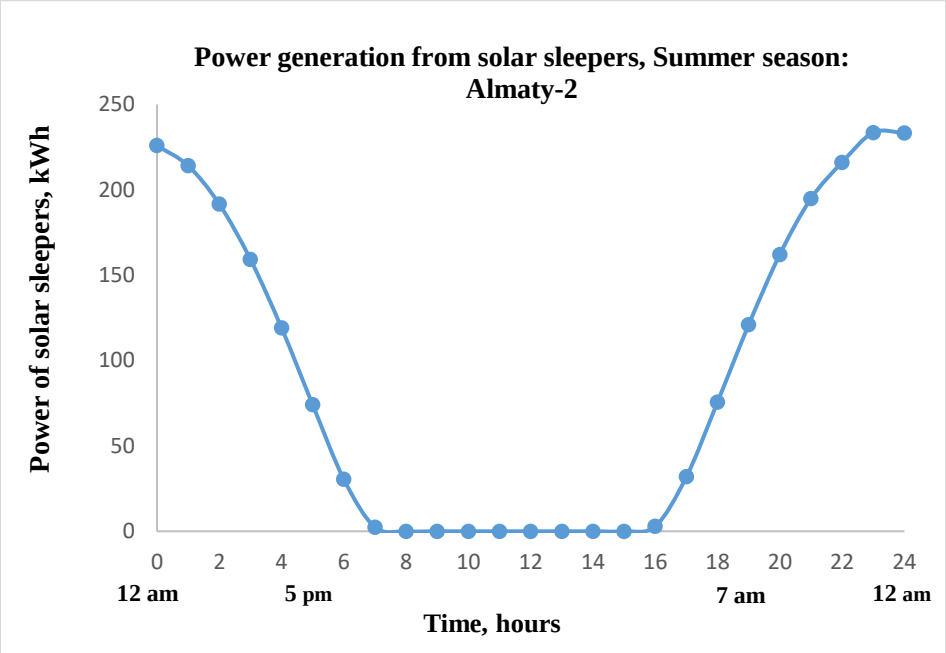

Figure B.80. The power of solar sleepers (kWh), summer season: Almaty-2

Appendix C

The code implemented in case study 1 is given below:

```
>>
% Read CSV file
data = readtable('Train C Summer.csv');
% Extract input and output labels from the first row
input_labels = data.Properties.VariableNames(1:3);
output_labels = data.Properties.VariableNames(7:end);
% Extract data into separate arrays
time = data.Time;
PV = data.PV;
Wind = data.Wind;
Train =data.Load;
for t=1:1440
% Objective function
objective_function = @(variables) sum(PV + Wind - Train);
% Particle Swarm Optimization
lb = [0, 0];  % Lower bounds for PV, Wind
ub = [42, 1000];  % Upper bounds for PV, Wind
initial_P_PV= 10;
initial_P_Wind=15;
initial_guess = [initial_P_PV, initial_P_Wind];
options = optimoptions(@particleswarm, 'SwarmSize', 100, 'MaxIterations',
100);
optimized_variables = particleswarm(objective_function, 2, lb, ub, options);
% Display optimized variables
disp('Optimized Variables:');
disp(optimized_variables);
% Calculate power values using optimized variables
```

```
optimized_P_PV = optimized_variables(1);
optimized_P_Wind = optimized_variables(2);
optimized_P_Total = optimized_P_PV + optimized_P_Wind - Train;
% Calculate available energy from solar and battery
renewable_energy(t) = PV(t)+ Wind(t);
Load(t) = Train(t);
%remaining_power = renewable_energy - load_demand(t);
if renewable_energy(t)<Load(t)
   Take_from_grid(t) = Load(t) - renewable_energy(t);
else
   Return_to_Grid(t) = Load(t) - renewable_energy(t);
end
end
% Convert minutes to hours for display purposes
time_hours = time / 60;
% Total Energy Generated by Renewables (PV + Wind)
total_energy_generated = sum(PV + Wind); % in kW
% Excess Energy Calculation
excess_energy = sum(max(0, (PV + Wind) - Train)); % in kW
% Total Solar and Wind Generation
total_solar_generation = sum(PV); % in kW
total_wind_generation = sum(Wind); % in kW
% Energy Savings (in percent)
grid_energy_without_renewables = sum(Train); % Assuming grid meets all demand
without renewables
grid_energy_with_renewables = sum(max(0, Train - (PV + Wind))); % Energy from
grid with renewables
energy_savings_percentage = ((grid_energy_without_renewables -
grid_energy_with_renewables) / grid_energy_without_renewables) * 100;
% Display the results
fprintf('Total Energy Generated by Renewable energy sources: %.2f kWh\n',
total_energy_generated / 60);
fprintf('Excess Energy: %.2f kWh\n', excess_energy / 60);
fprintf('Total Solar Generation: %.2f kWh\n', total_solar_generation / 60);
fprintf('Total Wind Generation: %.2f kWh\n', total_wind_generation / 60);
fprintf('Energy Savings: %.2f%%\n', energy_savings_percentage);
% Visualize Results
figure;
plot(time, PV, 'LineWidth', 1.5, 'DisplayName', 'PV');
hold on;
plot(time, Wind, 'LineWidth', 1.5, 'DisplayName', 'Wind');
hold on;
plot(time, Train, 'LineWidth', 1.5, 'DisplayName', 'Train');
plot(time, Take_from_grid, 'LineWidth', 1.5, 'DisplayName',
'Take_from_grid');
plot(time, Return_to_Grid, 'LineWidth', 1.5, 'DisplayName',
'Return_to_Grid');
xlabel('Time');
ylabel('Power (kW)');
title('Energy Management System Results - Case 1');
legend('Location', 'northwest');
grid on;
hold off;
```

Appendix D

The implemented code for case study 2 is given below:

```
>>
% Load the CSV file with renewable energy generation, load, and BESS data
data = readtable('Train C Spring.csv');
% Extract necessary data
time = data.Time;
PV = data.PV; % PV generation data
Wind = data.Wind; % Wind generation data
Load = data.Load; % Train energy consumption
SOC_BESS_initial = data.SOC_BESS(1); % Initial SOC of BESS
% System Parameters
SOC_BESS_min = 20; % Minimum SOC percentage
SOC_BESS_max = 85; % Maximum SOC percentage
BESS_capacity = 63.88; % BESS capacity in kWh
% Adjust num_time_steps to match the available data length
num_time_steps = min([height(PV), height(Wind), height(Load)]);
% Define lower and upper bounds for charging and discharging decisions
lb = zeros(2 * num_time_steps, 1); % Lower bounds for each decision variable
ub = repmat([BESS_capacity; BESS_capacity], num_time_steps, 1); % Upper
bounds
% Objective function setup for PSO
objectiveFcn = @(decisions) objectiveFunction(decisions, data, SOC_BESS_min,
SOC_BESS_max, BESS_capacity, num_time_steps);
% PSO options
options = optimoptions(@particleswarm, 'SwarmSize', 50, 'MaxIterations', 200,
'Display', 'iter');
% Execute PSO
[optimized_decisions, objective_val] = particleswarm(objectiveFcn, 2 *
num_time_steps, lb, ub, options);
% Apply the optimized decisions to simulate the system's behavior
[SOC_BESS, grid_interaction, renewable_usage] =
applyDecisions(optimized_decisions, data, SOC_BESS_min, SOC_BESS_max,
BESS_capacity, num_time_steps);
% Assuming the first half of optimized_decisions corresponds to charging
% and the second half to discharging
Charge_Decisions = optimized_decisions(1:num_time_steps); % This should be
defined based on your optimization output
Discharge_Decisions = optimized_decisions(num_time_steps + 1:end); % This
should be defined based on your optimization output
% Calculate net BESS power (positive for charging, negative for discharging)
BESS_Power = Charge_Decisions - Discharge_Decisions;
% Define the span for the moving average (this is the number of points used
in the smoothing)
span = 10;  % Span should be chosen based on the level of smoothing desired
% Compute the moving average using the "smoothdata" function
smoothed_SOC_BESS = smoothdata(SOC_BESS, 'movmean', span);
% Create a time vector for the x-axis
Time = 1:num_time_steps;
% Plot the smoothed SOC data
figure; % Creates a new figure for plotting
plot(Time, smoothed_SOC_BESS, 'LineWidth', 2);
title('Smoothed State of Charge (SOC) of BESS Over Time');
```

```
xlabel('Time (minutes)');
ylabel('SOC (%)');
grid on; % Adds grid lines to the plot for better readability
windowSize = 10; % Size of the moving average window
smoothed_BESS_Power = movmean(BESS_Power, windowSize);
figure;
plot(Time, smoothed_BESS_Power, 'LineWidth', 2);
title('Smoothed BESS Power Over Time');
xlabel('Time (minutes)');
ylabel('Power (kW)');
grid on;
% Plotting results for system behavior analysis
plotResults(num_time_steps, renewable_usage, grid_interaction, Load,
SOC_BESS);
% Assuming grid_interaction contains negative values for drawing from the
grid
% and positive values for supplying back to the grid
% Filter out only the negative values which represent grid energy usage
grid_energy_usage = grid_interaction(grid_interaction > 0);
% Sum the negative values and convert from kW to kWh since each timestep is 1
minute
total_grid_energy_usage_kWh = sum(grid_energy_usage) / 60;
% Display the total grid energy usage
disp(['Total Grid Energy Usage: ', num2str(total_grid_energy_usage_kWh), '
kWh']);
% Energy Savings (in percent)
grid_energy_without_renewables = sum(Load); % Assuming grid meets all demand
without renewables
grid_energy_with_renewables = sum(max(0, Load - (PV + Wind))); % Energy from
grid with renewables
energy_savings_percentage = ((grid_energy_without_renewables -
grid_energy_with_renewables) / grid_energy_without_renewables) * 100;
% Convert minutes to hours for display purposes
time_hours = time / 60;
% Total Energy Generated by Renewables (PV + Wind)
total_energy_generated = sum(PV + Wind); % in kW
% Excess Energy Calculation
excess_energy = sum(max(0, (PV + Wind) - Load)); % in kW
% Total Solar and Wind Generation
total_solar_generation = sum(PV); % in kW
total_wind_generation = sum(Wind); % in kW
% Display the results
fprintf('Total Energy Generated by Renewable energy sources: %.2f kWh\n',
total_energy_generated / 60);
fprintf('Excess Energy: %.2f kWh\n', excess_energy / 60);
fprintf('Total Solar Generation: %.2f kWh\n', total_solar_generation / 60);
fprintf('Total Wind Generation: %.2f kWh\n', total_wind_generation / 60);
fprintf('Energy Savings: %.2f%%\n', energy_savings_percentage);
% Total Battery Energy Storage (kWh) - Net BESS energy
total_BESS_energy_kWh = (sum(Charge_Decisions) - sum(Discharge_Decisions)) /
60;
disp(['Total BESS energy storage: ', num2str(total_BESS_energy_kWh), '
kWh']);
% Objective Function definition
function cost = objectiveFunction(decisions, data, SOC_BESS_min,
SOC_BESS_max, BESS_capacity, num_time_steps)
```

```
    PV = data.PV;
    Wind = data.Wind;
    Load = data.Load;
    SOC_BESS = zeros(num_time_steps, 1);
    SOC_BESS(1) = data.SOC_BESS(1); % Initial SOC of BESS
    cost = 0;
    for t = 1:num_time_steps
        Charge_Decision = decisions(t);
        Discharge_Decision = decisions(num_time_steps + t);
        SOC_BESS(t) = SOC_BESS(t) + Charge_Decision - Discharge_Decision;
        if SOC_BESS(t) > SOC_BESS_max || SOC_BESS(t) < SOC_BESS_min
            cost = cost + 10000; % Penalty for SOC outside limits
        end
        net_energy = PV(t) + Wind(t) - Load(t) + Charge_Decision -
Discharge_Decision;
        if net_energy < 0 % Penalty for using grid energy
            cost = cost - net_energy;
        end
        if t < num_time_steps
            SOC_BESS(t+1) = SOC_BESS(t); % Update SOC for next time step
        end
    end
end
% Apply Decisions function definition
function [SOC_BESS, grid_interaction, renewable_usage] =
applyDecisions(optimized_decisions, data, SOC_BESS_min, SOC_BESS_max,
BESS_capacity, num_time_steps)
    PV = data.PV;
    Wind = data.Wind;
    Load = data.Load;
    SOC_BESS = zeros(num_time_steps, 1);
    SOC_BESS(1) = data.SOC_BESS(1);
    grid_interaction = zeros(num_time_steps, 1);
    renewable_usage = zeros(num_time_steps, 1);
    for t = 1:num_time_steps
        Charge_Decision = optimized_decisions(t);
        Discharge_Decision = optimized_decisions(num_time_steps + t);

        % Net BESS contribution: positive for discharging, negative for
charging
        BESS_Contribution = Discharge_Decision - Charge_Decision;
        renewable_energy = PV(t) + Wind(t);
        renewable_usage(t) = max(renewable_energy, renewable_energy +
BESS_Contribution);
        renewable_usage(t) = min(renewable_energy, Load(t));
        SOC_BESS(t) = SOC_BESS(t) + Charge_Decision - Discharge_Decision;
        SOC_BESS(t) = max(SOC_BESS_min, min(SOC_BESS(t), SOC_BESS_max));
        net_energy = renewable_energy - Load(t) + Charge_Decision -
Discharge_Decision;
        grid_interaction(t) = -net_energy; % Negative for drawing from grid,
positive for supplying to grid
        if t < num_time_steps
            SOC_BESS(t+1) = SOC_BESS(t);
        end
    end
end
```

```
% Plot Results function definition
function plotResults(num_time_steps, renewable_usage, grid_interaction, Load,
SOC_BESS)
   % Visualization of system behavior over time, including PV and Wind
generation, renewable usage, grid interaction, Load, and BESS SOC
   % Implementation includes creating plots for the mentioned variables
   % Example plot for BESS SOC over time:
figure;
plot(1:1441, renewable_usage, 'LineWidth', 1.5, 'DisplayName','Renewable
Usage');
hold on;
plot(1:1441, grid_interaction, 'LineWidth', 1.5, 'DisplayName','Grid');
hold on;
plot(1:1441, Load, 'LineWidth', 1.5, 'DisplayName', 'Train');
xlabel('Time');
ylabel('Power (kW)');
title('Energy Management System Results (Optimized)');
legend('Location', 'northwest');
grid on;
hold off;
xlabel('Time');
ylabel('Power (kW)');
title('Energy Management System Results - Case 2');
legend('Location', 'northwest');
grid on;
hold off;
figure; plot(1:num_time_steps, SOC_BESS, 'LineWidth', 2);
   title('State of Charge (SOC) of BESS Over Time');
   xlabel('Time (minutes)');
   ylabel('SOC (%)');
   grid on;
end
```

Appendix E

The code implemented in case study 3 is given below:

```
>>
% Load the CSV file with renewable energy generation, load, and BESS data
data = readtable('Train C Winter.csv');
% Extract necessary data
time = data.Time;
PV = data.PV; % PV generation data
Wind = data.Wind; % Wind generation data
Sleeper = data.Solar_Sleeper;
Load = data.Load; % Train energy consumption
SOC_BESS_initial = data.SOC_BESS(1); % Initial SOC of BESS
% System Parameters
SOC_BESS_min = 20; % Minimum SOC percentage
SOC_BESS_max = 85; % Maximum SOC percentage
BESS_capacity = 63.88; % BESS capacity in kWh
% Adjust num_time_steps to match the available data length
num_time_steps = min([height(PV), height(Wind), height(Sleeper),
height(Load)]);
% Define lower and upper bounds for charging and discharging decisions
lb = zeros(2 * num_time_steps, 1); % Lower bounds for each decision variable
```

```
ub = repmat([BESS_capacity; BESS_capacity], num_time_steps, 1); % Upper
bounds
% Objective function setup for PSO
objectiveFcn = @(decisions) objectiveFunction(decisions, data, SOC_BESS_min,
SOC_BESS_max, BESS_capacity, num_time_steps);
% PSO options
options = optimoptions(@particleswarm, 'SwarmSize', 50, 'MaxIterations', 200,
'Display', 'iter');
% Execute PSO
[optimized_decisions, objective_val] = particleswarm(objectiveFcn, 2 *
num_time_steps, lb, ub, options);
% Apply the optimized decisions to simulate the system's behavior
[SOC_BESS, grid_interaction, renewable_usage] =
applyDecisions(optimized_decisions, data, SOC_BESS_min, SOC_BESS_max,
BESS_capacity, num_time_steps);
% Assuming the first half of optimized_decisions corresponds to charging
% and the second half to discharging
Charge_Decisions = optimized_decisions(1:num_time_steps); % This should be
defined based on your optimization output
Discharge_Decisions = optimized_decisions(num_time_steps + 1:end); % This
should be defined based on your optimization output
% Calculate net BESS power (positive for charging, negative for discharging)
BESS_Power = Charge_Decisions - Discharge_Decisions;
% Define the span for the moving average (this is the number of points used
in the smoothing)
span = 10;  % Span should be chosen based on the level of smoothing desired
% Compute the moving average using the "smoothdata" function
smoothed_SOC_BESS = smoothdata(SOC_BESS, 'movmean', span);
% Create a time vector for the x-axis
Time = 1:num_time_steps;
figure; % Creates a new figure for plotting
plot(Time, SOC_BESS, 'LineWidth', 2);  % Plotting raw SOC_BESS values
title('State of Charge (SOC) of BESS Over Time');
xlabel('Time (minutes)');
ylabel('SOC (%)');
grid on;  % Adds grid lines to the plot for better readability
% Plot the smoothed SOC data
figure; % Creates a new figure for plotting
plot(Time, smoothed_SOC_BESS, 'LineWidth', 2);
title('Smoothed State of Charge (SOC) of BESS Over Time');
xlabel('Time (minutes)');
ylabel('SOC (%)');
grid on; % Adds grid lines to the plot for better readability
windowSize = 10; % Size of the moving average window
smoothed_BESS_Power = movmean(BESS_Power, windowSize);
figure;
plot(Time, smoothed_BESS_Power, 'LineWidth', 2);
title('Smoothed BESS Power Over Time');
xlabel('Time (minutes)');
ylabel('Power (kW)');
grid on;
% Plotting results for system behavior analysis
plotResults(Sleeper, renewable_usage, grid_interaction, Load);
% Assuming grid_interaction contains negative values for drawing from the
grid
% and positive values for supplying back to the grid
```

```
% Filter out only the negative values which represent grid energy usage
grid_energy_usage = grid_interaction(grid_interaction > 0);
% Sum the negative values and convert from kW to kWh since each timestep is 1
minute
total_grid_energy_usage_kWh = sum(grid_energy_usage) / 60;
% Display the total grid energy usage
disp(['Total Grid Energy Usage: ', num2str(total_grid_energy_usage_kWh), '
kWh']);
% Energy Savings (in percent)
grid_energy_without_renewables = sum(Load); % Assuming grid meets all demand
without renewables
grid_energy_with_renewables = sum(max(0, Load - (PV + Wind + Sleeper))); %
Energy from grid with renewables
energy_savings_percentage = ((grid_energy_without_renewables -
grid_energy_with_renewables) / grid_energy_without_renewables) * 100;
% Convert minutes to hours for display purposes
time_hours = time / 60;
% Total Energy Generated by Renewables (PV + Wind)
total_energy_generated = sum(PV + Wind + Sleeper); % in kW
% Excess Energy Calculation
excess_energy = sum(max(0, (PV + Wind + Sleeper) - Load)); % in kW
% Total Solar and Wind Generation
total_solar_generation = sum(PV); % in kW
total_wind_generation = sum(Wind); % in kW
% Display the results
fprintf('Total Energy Generated by Renewable energy sources: %.2f kWh\n',
total_energy_generated / 60);
fprintf('Excess Energy: %.2f kWh\n', excess_energy / 60);
fprintf('Total Solar Generation: %.2f kWh\n', total_solar_generation / 60);
fprintf('Total Wind Generation: %.2f kWh\n', total_wind_generation / 60);
fprintf('Energy Savings: %.2f%%\n', energy_savings_percentage);
% Total Battery Energy Storage (kWh) - Net BESS energy
total_BESS_energy_kWh = (sum(Charge_Decisions) - sum(Discharge_Decisions)) /
60;
disp(['Total BESS energy storage: ', num2str(total_BESS_energy_kWh), '
kWh']);
% Objective Function definition
function cost = objectiveFunction(decisions, data, SOC_BESS_min,
SOC_BESS_max, BESS_capacity, num_time_steps)
   PV = data.PV;
   Wind = data.Wind;
   Sleeper = data.Solar_Sleeper;
   Load = data.Load;
   SOC_BESS = zeros(num_time_steps, 1);
   SOC_BESS(1) = data.SOC_BESS(1); % Initial SOC of BESS
   cost = 0;
   for t = 1:num_time_steps
       Charge_Decision = decisions(t);
       Discharge_Decision = decisions(num_time_steps + t);
       SOC_BESS(t) = SOC_BESS(t) + Charge_Decision - Discharge_Decision;
       if SOC_BESS(t) > SOC_BESS_max || SOC_BESS(t) < SOC_BESS_min
           cost = cost + 10000; % Penalty for SOC outside limits
       end
       net_energy = PV(t) + Wind(t) + Sleeper(t) - Load(t) + Charge_Decision
- Discharge_Decision;
       if net_energy < 0 % Penalty for using grid energy
```

```
            cost = cost - net_energy;
        end
        if t < num_time_steps
            SOC_BESS(t+1) = SOC_BESS(t); % Update SOC for next time step
        end
    end
end
function [SOC_BESS, grid_interaction, renewable_usage] =
applyDecisions(optimized_decisions, data, SOC_BESS_min, SOC_BESS_max,
BESS_capacity, num_time_steps)
    PV = data.PV;
    Wind = data.Wind;
    Sleeper = data.Solar_Sleeper; % Solar Sleeper generation data
    Load = data.Load;
    SOC_BESS = zeros(num_time_steps, 1);
    SOC_BESS(1) = data.SOC_BESS(1); % Initial SOC of BESS
    grid_interaction = zeros(num_time_steps, 1);
    renewable_usage = zeros(num_time_steps, 1);
    for t = 1:num_time_steps
        Charge_Decision = optimized_decisions(t); % Charging decision at time
t
        Discharge_Decision = optimized_decisions(num_time_steps + t); %
Discharging decision at time t
        % Renewable energy generated at time t
        renewable_energy = PV(t) + Wind(t) + Sleeper(t);
        % Update SOC_BESS based on Charge and Discharge decisions
        % Charging increases SOC, discharging decreases SOC
        % Conversion from power to energy (kWh), considering each time step
represents 1 minute
        SOC_BESS(t) = SOC_BESS(t) + ((Charge_Decision - Discharge_Decision) /
60.0) / BESS_capacity * 100;

        % Ensure SOC is within the specified limits
        SOC_BESS(t) = max(SOC_BESS_min, min(SOC_BESS(t), SOC_BESS_max));

        % Calculate the renewable usage
        renewable_usage(t) = renewable_energy;

        % Grid interaction calculation
        if renewable_energy + Discharge_Decision - Charge_Decision >= Load(t)
            % Excess energy scenario, either feed into grid or wasted
            grid_interaction(t) = -(renewable_energy + Discharge_Decision -
Charge_Decision - Load(t));
        else
            % Deficit scenario, drawing from the grid
            grid_interaction(t) = Load(t) - (renewable_energy +
Discharge_Decision - Charge_Decision);
        end

        % Prepare SOC for the next time step, if not the last step
        if t < num_time_steps
            SOC_BESS(t+1) = SOC_BESS(t);
        end
    end
end
% Plot Results function definition
```

```
function plotResults(Sleeper, renewable_usage, grid_interaction, Load)
   % Visualization of system behavior over time, including PV and Wind
generation, renewable usage, grid interaction, Load, and BESS SOC
   % Implementation includes creating plots for the mentioned variables
   % Example plot for BESS SOC over time:
figure;
plot(1:1441, Sleeper, 'LineWidth', 1.5, 'DisplayName','Sleepers');
hold on;
plot(1:1441, renewable_usage, 'LineWidth', 1.5, 'DisplayName','Renewable
Usage');
hold on;
plot(1:1441, grid_interaction, 'LineWidth', 1.5, 'DisplayName','Grid');
hold on;
plot(1:1441, Load, 'LineWidth', 1.5, 'DisplayName', 'Train');
xlabel('Time');
ylabel('Power (kW)');
title('Energy Management System Results (Optimized)');
legend('Location', 'northwest');
grid on;
hold off;
xlabel('Time');
ylabel('Power (kW)');
title('Energy Management System Results - Case 3');
legend('Location', 'northwest');
grid on;
hold off;
end
```